CONTROL OF FLOWERING TIME AND VERNALIZATION IN *ARABIDOPSIS THALIANA* BY THE N-END RULE PATHWAY

By

HANNAH MARY TEDDS

Supervised by Dr Daniel J. Gibbs

A Thesis submitted to the

The University of Birmingham

For the degree of

DOCTOR OF PHILOSOPHY

School of Biosciences
The University of Birmingham
October 2018

Abstract

The N-end rule pathway of proteolysis targets proteins for destruction based on the nature of their N-terminus. I have shown that the N-end rule pathway in *Arabidopsis* regulates the 'Methionine-Cysteine (MC)-initiating' protein VERNALIZATION2 (VRN2). VRN2 functions to coordinate cold-responsive flowering and has several other key developmental roles. VRN2 is one of three plant homologues of the *Drosophila* protein SUPPRESSOR OF ZESTE12 (Su(z)12), which functions as part of the polycomb repressive complex2 (PRC2), a conserved eukaryotic complex that regulates the epigenetic silencing of genes through depositing the Histone 3 Lysine 27 tri-methylation (H3K27me3) repressive mark to chromatin. Here I provide *in vitro* and *in vivo* evidence that VRN2 is a physiological substrate of the N-end rule pathway. VRN2 is stabilised under hypoxia and NO-limited conditions and post-translational accumulation of VRN2 during vernalization is linked to its regulation by the N-end rule. One hypothesis to explain VRN2 stabilisation is that cold-induced VERNALIZATION INSENSITIVE3 (VIN3) shields the MC terminus to prevent it being targeted for degradation by the E3 ligase PROTEOLYSIS6 (PRT6). However, *in vitro* and via inducible *VIN3* transgenic lines VRN2 is still degraded in the presence of VIN3. Additionally, this project demonstrates that the destabilising N-terminus of VRN2 likely arose following gene duplication and N-terminal truncation of an ancient homologue of EMBRYONIC FLOWER2 (EMF2), providing new insight into how proteins can become co-opted to the N-end rule pathway during evolution to provide new functions. Finally, I have found that EMF2c in Barley is also a substrate of the N-end rule pathway and may represent a functional homologue of VRN2.

Acknowledgements

Firstly, I would like to thank my supervisor Daniel Gibbs for taking me on as his first PhD student and providing me with support and guidance throughout the project. I would like to thank other members of the Gibbs' lab who have supported me during the ups and downs of my project. In particular, I would like to express my thanks to Mark Bailey for all his advice, encouragement and help. Thanks also to Adrienne Payne who helped me in the early part of my project and to Colleeen Sprigg and Rory Osborne who helped me with cloning and with all the genotyping!

Thank you to all of the other friends and colleagues I have met from the department of Plant Science at the University of Birmingham who have made the laboratory and office a more enjoyable place to be. Thanks, must also go to the Functional Genomics lab, the people in the glasshouse facilities, stores and central services that have helped provide me with the equipment and facilities I have needed throughout my project.

I would like to acknowledge the MIBTP, BBSRC and the University of Birmingham for funding my PhD studentship.

I would like to thank all of my friends for listening to me and providing fun and relaxation along the way.

Finally, I would like to thank my mum, nan, sister and fiancé Andrew for their love and support.

Table of Contents

List of Figures

List of Tables

Chapter 1

Introduction

1.1 Project Introduction

Regulation of cellular protein levels is essential for all organisms in order to control their development in response to environmental stimuli. Targeted protein degradation (proteolysis), autophagy and the endosomal system are mechanisms that have evolved to allow cells to alter regulatory protein levels, rapidly respond to change via protein signaling and also to break down mis-folded or damaged proteins (Schrader et al., 2009). AAA proteases are a conserved class of ATP-dependent proteases that mediate the degradation of membrane proteins in bacteria, mitochondria and chloroplasts (Langer, 2000). One method of targeted protein degradation in eukaryotes is the ubiquitin proteasome system (UPS). This project will look in detail at one particular branch of the UPS, the N-end rule pathway (Varshavsky, 2011).

The N-end rule pathway is a specific branch of the UPS that is directed by which amino acid is present at the N-terminus (Gibbs et al., 2014a). It is a proteolytic system whereby proteins undergo post-translational modifications. There is more than one route to the pathway (discussed in section 1.3) but this project will focus on the arginylation part of the N-end rule pathway. The N-end rule is responsible for the plant response to hypoxia where cysteine is the destabilizing N-terminal residue called the N-degron (Gibbs et al., 2011). Known targets of the N-end rule pathway in plants include the Met-Cys initiating proteins called Group 7 ethylene response factors (ERFVII transcription factors) involved in oxygen and nitric oxide sensing ((Gibbs et al.,

2011, Licausi et al., 2011, Gibbs et al., 2014b). Direct transcriptional response to O_2/NO is mediated by the proteolytic control of ERFVIIs by the N-end rule pathway. Proteins are targeted for destruction based on the distinctive N-degron Met-Cys- (MC-) and in the presence of O_2/NO the proteins are degraded. If O_2/NO availability is reduced then the proteins accumulate and subsequently their downstream genes are activated (Gibbs et al., 2014b). This is a direct mechanism for perceiving and transducing gaseous signals found in plants. Recent work in the Gibbs lab (Gibbs et al., 2018) has found that VRN2 is an MC-initiating protein that is an O_2/NO regulated substrate of the N-end rule pathway but instead of acting as a transcription factor, it is known to act as part of the polycomb repressive complex 2 (PRC2), a chromatin modifying complex that regulates the epigenetic repression of gene expression. When O_2/NO levels are low VRN2 accumulates and therefore may act within the PRC2 complex to conditionally catalyzes the deposition of the repressive H3K27me3 mark to chromatin.

This project will focus on the hypothesis that VRN2 is a novel gas regulated target of the N-end rule pathway that links O_2/NO perception to global chromatin dynamics to control downstream developmental and environmental responses. The project aims to advance our understanding of signal perception and integration in plants and with potential to identify new targets for the development of improved crops. The following sections of this introduction will describe in detail the N-end rule pathway, VRN2 and the process of vernalization, PCR2 complexes, what might affect the stability of VRN2 and how VRN2 may have evolved.

1.2 Targeted protein degradation

Cellular regulation of growth and development in all organisms is dependent on the regulation of protein abundance and function. This can be at the transcriptional level where genes are expressed or suppressed according to cell signaling mechanisms or epigenetic responses. It can be at the translational level where mRNA can be modified and splice variants of proteins can be created. It can also be at the post-translational level where proteins can be modified and various tags added to them to control protein activity and stability. All eukaryotes use the ubiquitin/26S proteasome pathway as a way of degrading specific proteins when signals determine that it is required. Plants have a large proportion of their genes that encode proteins that are components of this regulatory pathway (Hellmann and Estelle, 2002, Sadanandom et al., 2012). Targeted protein degradation enables tight control of cell signaling and protein levels.

1.2.1 Ubiquitylation

Ubiquitin is a highly conserved 76 amino acid adapter protein found in eukaryotes. Ubiquitylation is a type of post-translational modification where ubiquitin is conjugated to specific Lysine (Lys) residues in a selected protein to form chains of one or more ubiquitin subunits. Ubiquitin conjugation not only controls protein degradation but also affects protein sorting, enzymatic activity and protein-protein interactions. (Hershko and Ciechanover, 1998). Three classes of enzyme are involved in a cascade in order for ubiquitylation

to occur; the ubiquitin-activating (E1), the ubiquitin-conjugating (E2) and the substrate specific ubiquitin-protein ligase (E3) enzymes (Ciechanover, 1998, Komander and Rape, 2012). An additional conjugation factor (E4) has been shown to be involved in ubiquitin chain assembly in yeast and humans (Koegl et al 1999). ATP is required to first form a bond between a ubiquitin monomer and an E1 ligase (FIGURE 1.1). The ubiquitin is then transferred to an E2 by trans-esterification. At the same time an E3 will bind to a specific protein substrate and the E3 mediates the transfer of the ubiquitin from the E2 to the protein substrate. An isopeptide bond is catalyzed between the C-terminal carboxyl group of ubiquitin to a Lys within the protein substrate (Zimmerman et al., 2010). Mono-ubiquitylation can regulate gene expression and membrane trafficking (Hicke, 2001). Multi-ubiquilylation is where ubiquitin is added to a protein at multiple Lys sites and is related to DNA repair and endocytosis. Repeated ubiquitylation is called poly-ubiquitylation and occurs when ubiquitin monomers are added first to the substrate and then to each other to form a branched or single poly-ubiquitin chain. Single poly-ubiquitin chains can act as a signal for the protein to be degraded by the proteasome (Gibbs et al., 2014a, Gibbs et al., 2016).

1.2.2 E3 ubiquitin ligases

E3 Ubiquitin ligases can be classified into single or multi subunit enzymes. Single subunit E3s can be further divided into HECT (Homology to E6-AP C-terminus) domain proteins and RING (Really interesting New Gene)/U-box proteins (Pickart, 2001). These are examples of single subunit E3s and bind

to both the E2 and the target substrate. HECT E3s bind to the E2 and the ubiquitin binds directly to the E3 before transferring to the protein substrate. RING single-subunit E3s bind to both the E2 and substrate and catalyze the ubiquitin transfer directly from the E2 to the substrate without binding to ubiquitin itself (Jackson et al., 2000). The multi subunit E3s are often referred to as CULLIN-RING ligases as they comprised of a CULLIN protein and a RING protein (Zimmerman et al., 2010). The number of subunits and the type of CULLIN they associate with can vary (Petroski and Deshaies, 2005a). The anaphase promoting complex (APC), essential for mitotic progression in eukaryotic cells (Peters, 2002), and SKP1-CULLIN1-F-box (SCF), involved in phosphorylation-mediated proteolysis of developmental proteins (Deshaies, 1999, Petroski and Deshaies, 2005b), are other examples of multi-subunit E3 ubiquitin ligases.

In Eukaryotes some E3 ubiquitin-ligase enzymes act as an N-recognins. N-recognins are specific binding proteins that contain specialized binding sites for recognition of Type I and Type II primary destabilizing residues in substrates targeted for degradation by the N-end rule pathway. Some E3 ligases interact with other proteins via internal domains, whereas the N-recognin selectively interacts with the N-terminus of the target protein via specific recognition domains and provides specificity to the N-end rule pathway of proteolysis. The N-recognin is typically a single subunit enzyme that interacts with an E2 enzyme and specific N-terminal (Nt) - residues of target protein substrates, in contrast to multi-subunit E3 ligases that require interaction with multiple proteins for ubiquitylation (Deshaies and Joazeiro,

2009). Once the ubiquitin has bound to the substrate, the substrate is then degraded by the 26S proteasome.

1.2.3 The 26S Proteasome

The 26S proteasome is an ATP-dependent protease. It is a large complex made of multiple proteins (FIGURE 1.2). The two main components are the 20S core particle (CP) and two 19S regulatory particles (RPs) that are found at either end of the 20S CP as a lid and a base (Gallastegui and Groll, 2010). The lid of the proteasome recognizes proteins with poly-ubiquitin chains. The protein is de-ubiquitylated and then unfolded. The protein travels through the alpha subunits of the 20S that act as a gated channel. The beta subunits of the 20S depend on ATP to cleave the substrate into small fragments. Degradation products are released from the 19S base and the ubiquitin monomers are recycled.

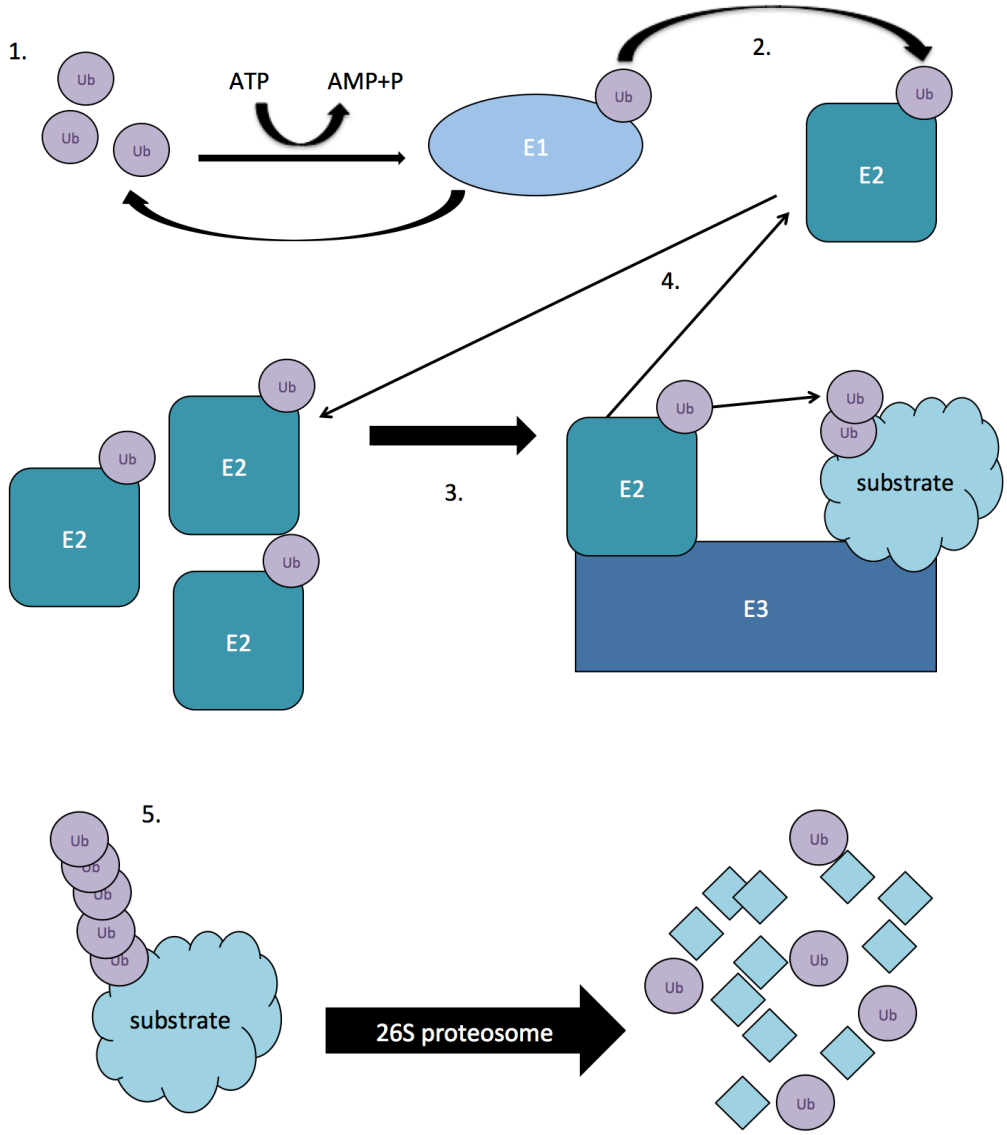

FIGURE 1.1 The polyubiquitin reaction cascade

Ubiquitylation of a protein involves the ubiquitin activating E1, the ubiquitin conjugating E2 and the ubiquitin-protein ligase E3 enzymes (Ciechanover, 1998).
1) ATP is required for the formation of a bond between E1 and a ubiquitin monomer.
2) The activated ubiquitin is then transferred to the E2 by transesterification.
3) E3 catalyzes the conjugation of ubiquitin to the protein substrate.
4) Ubiquitylation of the protein substrate continues in an iterative manner.
5) The polyubiquitylated protein is targeted for destruction by the 26S proteasome.

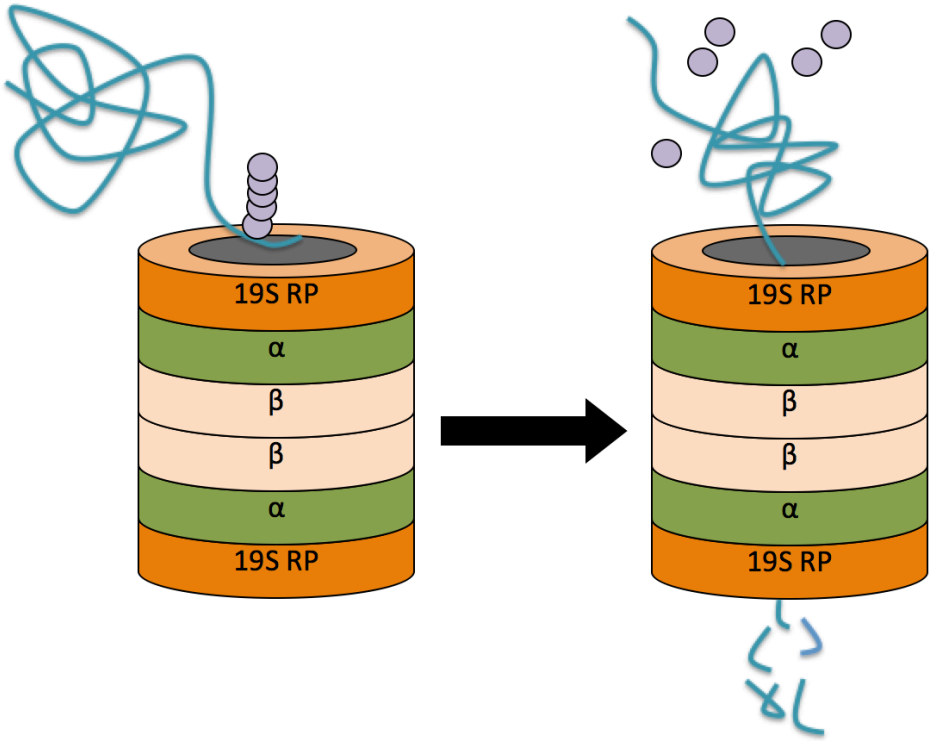

FIGURE 1.2 the 26S proteasome

The 26S proteasome is made of 2 β subunits in the centre and 2 α subunits either side of those. These 4 subunits make the core particle (CP). On each end of the CP are 19S regulatory particles. The RP catalyzes the deubiquitylation and unfolding of protein substrates, directing them through the centre of the CP where they are cleaved to small pieces and released.

1.3 The N-end rule pathway

1.3.1 The N-end rule pathway - Eukaryotes

The N-end rule pathway was first discovered in yeast *Saccharomyces cerevisiae* (Bachmair et al., 1986) where it was observed that the stability of ubiquitin β galactosidase reporter proteins was affected following de-ubiquitylation according to which Nt-residue was exposed (Sriram et al., 2011, Gibbs et al., 2014a). De-ubiquitylating enzymes cleave the ubiquitin at the N-terminus of proteins in yeast. Once cleaved, this exposes a new N-terminus. Proteins are degraded or stabilized according to the amino acid residue present at the n-end of the protein. With arginine at the N-terminus the protein was relatively unstable with a half-life of 2 minutes compared to alanine at the N-terminus where the reporter protein was stable for 20 minutes. As well as being present in yeast, the N-end rule is also found in mammals, plants and bacteria (although it is not ubiquitin related in prokaryotes). Ubiquitylation on a protein induces selective proteolysis by forming part of a degradation signal called a degron. A degron is a region of a protein sufficient to target the protein for destruction by the 26s proteasome (Petroski and Deshaies, 2005a). In the N-end rule pathway the N-terminus of N-end protein substrates have a particular N-terminal amino acid residue that is post-translationally modified and acts as destabilizing N-degron. N-degrons comprise a destabilizing Nt-residue, a Lys site for ubiquitylation and an N-terminal protein structure that exposes the N-terminus on the outside of the protein for interaction with other proteins (Gibbs et al., 2014a). In eukaryotes the poly-ubiquitin chain, when conjugated to a lysine in the N-degron, targets the protein for destruction by the 26s proteasome (Sriram et al., 2011).

1.3.2 The Arg/N-end rule

Nt-residues were first classified as stabilizing or destabilizing (Bachmair et al., 1986) Proteins are synthesized with a methionine at the N-terminus but post-translational modifications usually reveal new Nt-amino acids. Proteins can be cleaved internally by endopeptidases (Piatkov et al., 2014) or the Nt-methionine can be removed co-translationally by methionine amino peptidases (MetAPs) depending on the size of the second residue (Giglione et al., 2004). The newly exposed Nt-residue can be defined as stabilizing or either a primary, secondary or tertiary destabilizing residue. There are now sub-categories of primary destabilizing residue: type I basic residues or type II hydrophobic residues (Tasaki et al., 2012). Type I residues include arginine (R), lysine (K) and histidine (H). Type II residues include leucine (L), isoleucine (I), phenylalanine (F), tryptophan (W) and tyrosine (Y). In plants and animals, under certain conditions, tertiary destabilizing residues are modified to secondary destabilizing residues. One example in plants of a tertiary destabilizing residue is where cysteine (C) is oxidized by plant cysteine oxidases (PCOs). Post-translational cysteine oxidation in animals does occur but via reactive oxygen species (ROSs) from sources such as mitochondria and NADPH oxidases and this oxidation can regulate enzyme activity, metal binding and protein turnover (Reddie and Carroll, 2008). Another example of tertiary destabilizing residues are asparagine (N) and glutamine (Q) which are then modified via Nt-deamidation to secondary destabilizing residues aspartic acid (D) and Glutamic acid (E) respectively (An et al., 2006, Tasaki et al., 2012). Secondary destabilizing residues are then

modified to primary destabilizing residues via Nt-arginylation by arginyl-tRNA transferases (ATEs) (Varshavsky, 1996).

In eukaryotes N-recognins (E3 ubiquitin ligases) recognize the N-degrons and bind directly to primary destabilizing residues, catalyzing the addition of a polyubiquitin chain to a lysine a short distance from the N-terminus, targeting the protein for destruction by the 26S proteasome (Varshavsky, 2011). Gid4, a subunit of the GID ubiquitin ligase in yeast, is a pro/N-recognin that has been found to target gluconeogenic enzymes. (Chen et al., 2017). There is a pro/N-end rule pathway in yeast that targets proteins for destruction through their N-terminal proline (Dougan and Varshavsky, 2018). Yeast has a single N-recognin ubiquitin system recognition component 1 (UBR1) that recognizes both type I and type II primary destabilizing residues in the Arg/N-end rule pathway (Garzon et al., 2007). In mammals several isoforms of this N-recognin are encoded. There are at least four N-recognin proteins UBR1, UBR2, UBR4 and UBR5 shown to bind with N-degrons and one common feature of these is a Cys/His rich domain termed the UBR box (Tasaki et al., 2009). There could potentially be up to seven N-recognins in mammals as UBR3, UBR6 and UBR7 also contain the 70-residue UBR box substrate recognition domain (Tasaki et al., 2005). Of the two N-recognins that have been identified in plants, PROTEOLYSIS1 (PRT1) and PROTEOLYSIS6 (PRT6), only PRT6 contains the UBR box (Holman et al., 2009). PRT1 recognizes type II basic primary residues and PRT6 recognizes type I aromatic primary residues (Potuschak et al., 1998, Stary et al., 2003, Garzon et al., 2007). As this pathway in plants involved the addition of arginine (Arg or

R) to the N-terminus that is recognized by N-recognins, this branch of the N-end rule pathway is known as the Arg/N-end rule (FIGURE 1.3). The deamidases, ATEs and N-recognins are functionally conserved in eukaryotes (Graciet et al., 2010). Where the primary destabilizing residue is cysteine (Cys) this branch of the N-end rule pathway is known as the Cys/Arg N-end rule pathway (FIGURE 1.6) and will be the focus of this project.

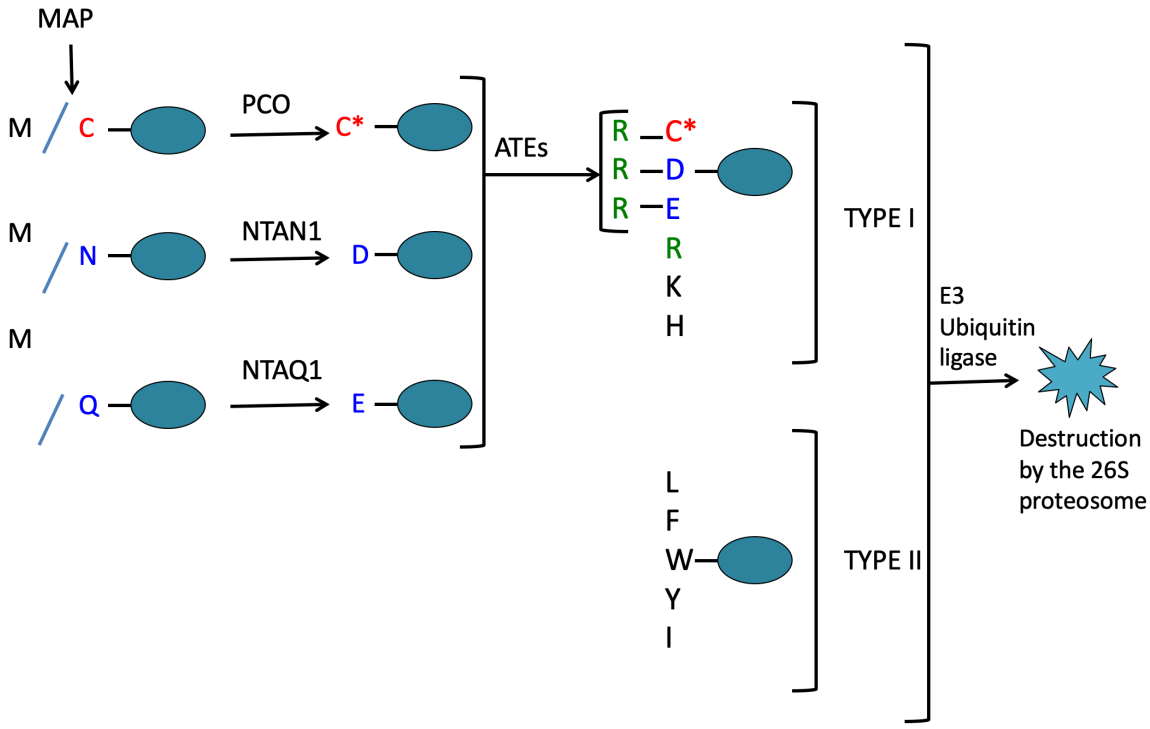

FIGURE 1.3 The Arg/N-end rule pathway

A schematic representation of N-terminal (Nt) processing events leading to degradation of proteins via the Arg(R)/N-end rule pathway: Single letter amino-acid codes are used to represent Nt-residues. Specific N-terminal methionine excision requires methionine amino peptidase (MAP) activity, exposing tertiary Nt-residues: Cys (C), Asn (N) and Gln (Q). Cysteine is oxidized by plant cysteine oxidase (PCO) (denoted in red). N and Q are deamidated to Asp (D) and Glu (E) by N-terminal amidohydrolases (NTAN1 and NTAQ1- denoted in blue). C* indicates oxidized Cys. C*, D and E are secondary residues. An arginyl group (R) is added by the arginyl-tRNA-transferases (ATEs) to the secondary residues. R is a Type-I primary residue as well as Lys (K) and His (H). Leu (L), Phe (F), Trp (W), Tyr (Y) and Ile (I) are type-II primary residues. The E3 ubiquitin-ligases recognize specific proteins via the primary residue as part of the N-degron and catalyze the addition of ubiquitin. The protein is then degraded by the 26S proteasome.

1.3.3 The Ac/N-end rule

Acetylation occurs in the majority of Eukaryotic proteins (Arnesen et al., 2009). The Ac/N-end rule pathway was discovered in yeast and although acetylation has classically been viewed as a stabilizing modification, the Ac/N-end rule pathway uses acetylation to mark proteins for degradation (Hwang et al., 2010). Protein targets of this pathway are modified co-translationally (sometimes post-translationally) and acetylation is believed to be irreversible (Varshavsky, 2011). Nt-acetyltransferases (NATs) associate with ribosomes as proteins are being translated. An acetyl group from acetyl-coenzyme A is transferred to the Nt-amino acid of the protein, catalyzed by a NAT enzyme. The NAT has specificity for which protein to acetylate based on the nature of the Nt. Methionine (M), Alanine (A), Valine (V), Serine (S), Cysteine (C) and Threonine (T) are all residues that are targeted for Nt-acetylation (FIGURE 1.4). The acetylated protein can then, in some cases, be recognized by an N-recognin and is selectively degraded. In yeast there are two confirmed N-recognins of the Ac/N-end rule pathway: degradation of alpha 10 (DOA10) or the negative regulator of transcription 4 (NOT4). Functions of the Ac/N-end rule include regulation of protein stoichiometry and degradation of mis-folded or damaged proteins (Hwang et al., 2010, Shemorry et al., 2013). The NAT enzymes are highly conserved in eukaryotes (Arnesen et al., 2009, Starheim et al., 2012) and homologs of DOA10 and NOT4 exist in animals and plants. Therefore the Ac/N-end rule pathway may be important in multicellular organisms such as plants but further studies are needed to confirm its function and role in proteolysis beyond yeast and animals (Gibbs et al.,

2014a). Some proteins with Nt-Met followed by a hydrophobic residue can be destabilizing if unacetylated. Selective acetylation of these proteins can determine if the protein is degraded by the Ac/ or Arg/N-end rule pathways (Kim et al., 2014). This means that almost all of the possible range of proteins, with their various Nt-residues, can potentially lead to degradation by the N-end rule pathway but this is conditional and dependent on certain environmental cues. There is also evidence to suggest crosstalk between the Ac/ and Arg/N-end rule pathway between each other (Kim and Hwang, 2014). This demonstrates the complexity and significance of the N-end rule pathway in controlling of protein levels in cells.

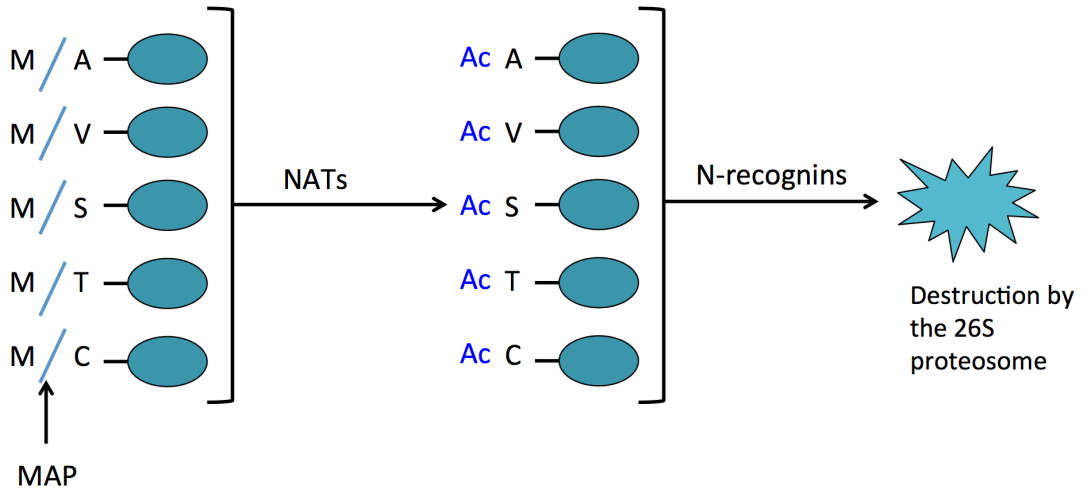

FIGURE 1.4 The Ac/N-end rule pathway

A schematic representation of the Ac/N-end rule pathway. Single letter amino-acid codes are used to represent N-terminal (Nt) residues. Methionine is cleaved by methionine amino peptidase (MAP), exposing Ala (A), Val (V), Ser (S), Thr (T) or Cys (C) residues. The exposed residues are then acetylated by Nt-acetyltransferases (NATs). The acetylated Nt-residue is recognized by an N-recognin, which targets the protein for destruction by the 26S proteasome.

1.3.4 N-end in prokaryotes

Prokaryotes have a variation on the N-end rule pathway that is different to that in eukaryotes, as they lack ubiquitin and the UPS, and they have fewer destabilizing residues (Darwin, 2009). Prokaryotic proteins can have varied amino acids at the Nt due to endopeptidase cleavage exposing residues and protein transferases adding amino acid residues. Lysine (K) and arginine (R) are secondary destabilizing residues. Methionine can also be a destabilizing residue. Many bacterial proteins have formyl-methionine (fMet) at the Nt. In degradation of these bacterial proteins with Nt-fMet, formylation occurs by peptide deformylase. Then methionine this is cleaved to reveal the next amino acid residue at the N-terminus (Frottin et al., 2006). It is thought that MetAP removes the Met in a similar way to eukaryotes, however it may not be the only process in prokaryotes that forms N-degrons due to MetAP specificity (Mogk et al., 2007). Primary destabilizing residues Leucine (L), Phenylalanine (F), Tyrosine (Y) and tryptophan (W) can also be added to Nt-Methionine by tRNA-protein-transferase (Dougan et al., 2010). Proteins with primary destabilizing residues bind to an adapter protein ClpS (caseinolytic protease) (FIGURE 1.5). ClpS is the only N-recognin found in bacteria. Plant chloroplasts have their own n-end rule pathway Clp protease system similar to prokaryotes and ClpS1 is the N-recognin that recognizes substrates in this protein degradation system (Nishimura et al., 2013). In bacteria, one region of the ClpS recognizes N-degrons and another region binds to the ClpAP protease complex where the protein is then degraded (Tobias et al., 1991, Schuenemann et al., 2009). ClpS recognizes the type II hydrophobic destabilizing residues and not type I basic residues (Schmidt et al., 2009,

Dougan et al., 2010), suggesting the type I and type II branches of the n-end rule pathway might be phylogenetically separable (Mogk et al., 2007, Sriram et al., 2011). As a variation of the N-end rule pathway is present in bacteria, it suggests that it is an ancient pathway for regulating protein degradation and has been coopted to the UPS during evolution of Eukaryotes (Gibbs et al., 2014a). An equivalent of the N-end rule pathway has also been found in organelles of eukaryotic cells thought to derive from bacteria, in the chloroplasts of plant species and in yeast mitochondria (Lupas and Koretke, 2003, Vogtle et al., 2009).

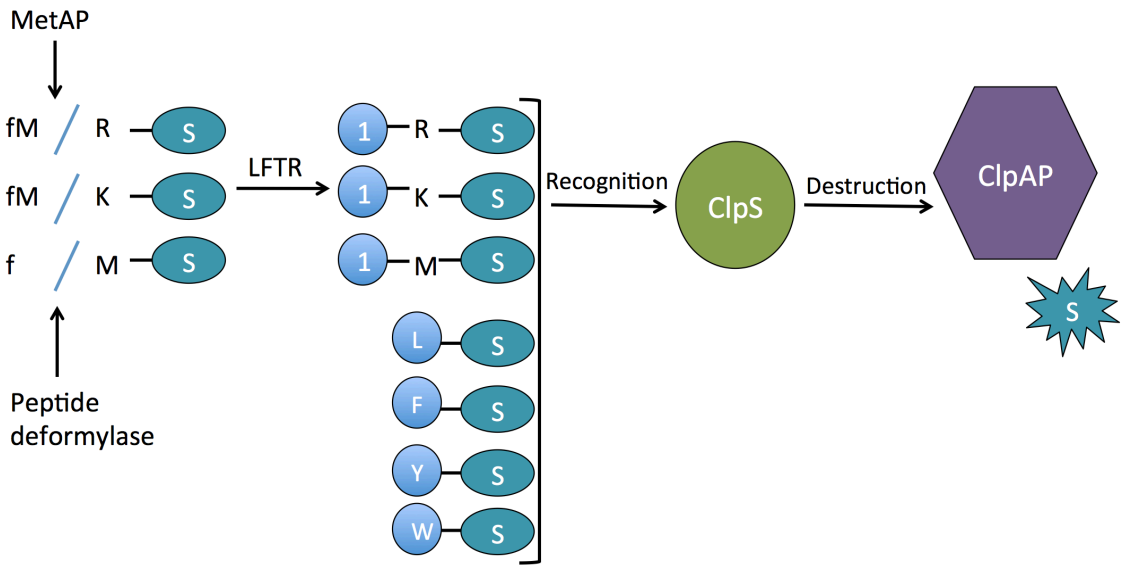

FIGURE 1.5 The N-end rule pathway in prokaryotes

Formylation occurs on formyl-methionine (fM). Peptide deformylase can remove this. Then methionine amino peptidase (MetAP) can remove the N-terminal methionine. Primary (leucine (L), phenylalanine (F), tyrosine (Y) and tryptophan (W)) and secondary (arginine (R), lysine (K) and methionine (M)) destabilizing amino acid residues are exposed by other amino peptidases. Primary destabilizing residues are added to the secondary destabilizing residues by L/F-tRNA-protein transferase (LFTR). When a primary destabilizing residue is at the N-terminus this is recognized by the caseinolytic protease (ClpS) and then the protein is targeted for destruction by the ClpAP protease complex.

1.3.5 Known substrates and the roles of the N-end rule pathway

A number of different substrates of the N-end rule pathway are known in different kingdoms. In Drosophila the N-end rule is known to have a role in the regulation of apoptosis (Piatkov et al., 2012a) as INHIBITOR OF APOPTOSIS 1 (IAP1) has been found to be a substrate (Ditzel et al., 2003, Tasaki and Kwon, 2007). The N-end rule pathway also has a role in apoptosis in bacteria through regulation of the substrate PUTRESCINE AMINOTRANSFERASE (PATase), which maintain homeostasis of the toxic chemical putrescine in bacterial cells, preventing apoptosis (Ninnis et al., 2009, Schmidt et al., 2009). In yeast, the N-end rule pathway has role in chromosome stability as endopeptidases were found to expose destabilizing residues in the substrate SISTER CHROMATID COHESION 1 (SCC1) (Rao et al., 2001). UBR1, the sole E3 ubiquitin ligase in yeast, recognizes the transcriptional repressor CUP9 by its internal degron (Turner and Varshavsky, 2000). The control of peptide movement is N-end regulated as CUP9 represses the peptide transporter PTR2 (Du et al., 2002). Mutations in E3 ligases could mean its substrates would become stable. Mutations in *UBR1* in humans have been shown to be the cause of Johanson-Blizzard syndrome (Zenker et al., 2005), meaning a functioning N-end rule is linked to the prevention of symptoms such as mental retardation, physical abnormalities and pancreatitis.

UBIQUITIN-SPECIFIC PROTEASE 1 (USP1) in mammals is a substrate of the N-end rule pathway and regulates genomic stability and DNA repair (Yan et al., 2006, Piatkov et al., 2012b). Also in mammals, the N-end rule has been

linked to neurodegenerative disorders (Brower et al., 2013). PINK1 is degraded by the N-end rule which is a protein associated with Parkinson's disease (Yamano and Youle, 2013). The N-end rule has functions in regulating autophagy (Kim et al., 2013), the sensing of heme (Hu et al., 2008), detecting misfolding of proteins (Eisele and Wolf, 2008, Heck et al., 2010, Sultana et al., 2012) and BRCA1 tumour suppressor protein is regulated by the N-end rule pathway (Xu et al., 2012).

The REGULATOR OF G PROTEIN SIGNALLING (RGS) is a known substrate of the Cys branch of the Arg/N-end rule pathway in mammals (Lee et al., 2005). Cell signalling by substrate G-protein regulators RSG4 , RGS5 and RGS16 links the Cys/Arg N-end rule to gas-sensing and cardiovascular development (Kwon et al., 2002). In plants the Arg/N-end rule pathway regulates seed germination (Holman et al., 2009), seedling establishment, shoot and leaf development (Graciet et al., 2009), leaf senescence (Yoshida et al., 2002) pathogen responses and response to abiotic stress (Sriram et al., 2011). The transcription factors, the group VII ethylene response factors (ERFVIIs) demonstrate that the N-end rule has a role in gaseous sensing in plants as they become stable in hypoxia and low nitric oxide (similar to the RGSs in mammals) and ERFVIIs are substrates of the Cys branch of the Arg/N-end rule pathway (Gibbs et al., 2011, Licausi et al., 2011, Gibbs et al., 2014a).

1.3.6 Oxygen and nitric oxide sensing via the N-end rule

Most eukaryotes rely on oxygen for growth and metabolic processes including

aerobic respiration and the production of energy in the form of ATP. If oxygen levels are depleted (hypoxia) then eukaryotic cells can respond by altering gene transcription levels in order to sustain ATP production anaerobically and to avoid any negative effects of low energy production (Gibbs et al., 2011, Licausi, 2011). Nitric oxide is an important signaling molecule in plants (Gibbs et al., 2014b). Plants rely on nitric oxide for is involvement in stress responses to pathogens and developmental processes such as seed germination/dormancy, stomatal closure, hypocotyl elongation and flowering (Mur et al., 2013). The N-end rule pathway has been shown to be the first oxygen and nitric oxide sensing mechanism discovered in plants, functioning by regulating key transcription factors in *Arabidopsis thaliana*. The Cysteine division of the Arg/N-end rule branch where the N-terminus begins with methionine and cysteine (MC) is present in plants and is a conserved method of gaseous signal transduction (Hu et al., 2005) (FIGURE 1.6). Cys is a primary destabilizing residue in eukaryotes other than yeast, with an in vitro half-life of approx. 1.2h (Gonda et al., 1989). The stability of substrates of the Cys-Arg/N-end rule pathway is related to oxygen and Nitric oxide (NO) availability. Exposure of Cys in an unacetylated protein in plants allows oxygen-dependent oxidation of Cys by PCOs. PCO1 and PCO2 are induced by hypoxia and are known to redundantly repress the anaerobic response and transcription mediated by the ERFVIIs (Weits et al., 2014). PCOs have specific affinity to N-terminal Cys and they catalyze the conversion of Cys to Cys-sulfinic or Cys-sulfonic acid by the incorporation of two oxygen to the thiol group of cysteine (Weits et al., 2014, White et al., 2017). Oxygenated Cys is then arginylated by the ATEs (Ikeuchi et al., 2015).

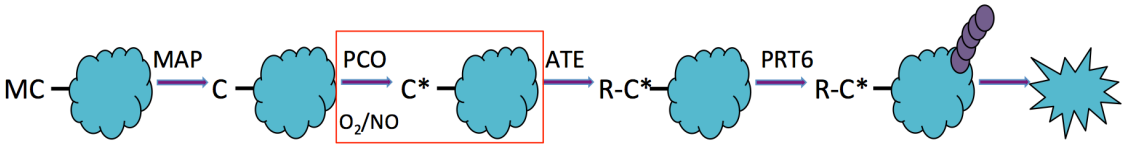

FIGURE 1.6 The Cys/Arg N-end rule pathway of proteolysis

A schematic representation of N-terminal processing events leading to degradation of Met-Cys- (MC)-proteins via the Arg(R)/N-end rule pathway: Single letter amino-acid codes are used. Methionine is cleaved by MAP methionine amino peptidase. Cysteine is oxidized by PCO plant cysteine oxidase. C* indicates oxidized Cys. An arginyl group (R) is added by the arginyl transferases. The E3-ligase PRT6 PROTEOLYSIS6 adds a polyubiquitin chain to the protein. The protein is then degraded by the 26S proteosome. Red box is the gas sensing step - as oxygen and nitric oxide (NO) are required for this stage to take place.

The nitric oxide and oxygen dependent step of the n-end rule pathway was first identified in mammals, where it was shown in conditions of hypoxia or lack of NO that the substrates RGS4, RGS5 and RGS16 levels increased (Hu et al., 2005). When oxygen was higher through vasodilation and nitric oxide levels were high through production by endothelial nitric oxide synthase, the RGS proteins were degraded. The conditional stability of RGS proteins regulate G protein signaling in the development of the cardiovascular system in mammals (Lee et al., 2012, Jaba et al., 2013). Hypoxia inducible factor 1alpha (HIF1α) is a subunit of hypoxia inducible factor 1 (HIF-1); a transcriptional regulator of cellular and developmental response to hypoxia, that has been shown in mammals to regulate transcription levels according to oxygen availability (Kaelin and Ratcliffe, 2008). Recently the N-end rule has been linked to oxygen and NO sensing in plants due to the discovery that the ERFVII transcription factors are substrates of the Cys-Arg/N-end rule pathway (Gibbs et al., 2011, Licausi et al., 2011). HIF1α is absent from plants and instead, the N-end rule controls the hypoxia response in plants via the ERFVII transcription factors. The ERFVIIs are constitutively degraded due to the Met-Cys (MC) initiating Nt.

Plants may experience hypoxic conditions during their normal development, especially in certain tissues such as the meristem (Considine et al., 2017). Oxygen enter plant tissues by simple diffusion, meaning the most internal areas may not get as much oxygen as surface tissues, meaning the meristems may naturally be hypoxic. Plants may also experience

waterlogging during flood in their natural environment, causing hypoxia in certain plant tissues. The plant senses the environment around it and responds to the hypoxic conditions via the N-end rule pathway because without the oxygen and nitric oxide step the ERFVIIs are stabilized. The ERFVIIs can then promote the expression of hypoxia response genes. The PCOs are only found in plants and are hypoxia response genes (i.e. they are up-regulated under hypoxic conditions), meaning ERFVIIs and other N-end rule substrates become stable. PCOs are required in this step because they oxidize the Cys residue using oxygen before the arginylation step of the pathway (Weits et al., 2014).

Nitric oxide (NO) is available in plants through nitrate reductase enzyme reactions (Gibbs et al., 2014b). Nitric oxide is also required in this gas-sensing step because it serves as a signaling molecule in plants (Mur et al., 2013), however whether it is directly involved in the oxidation of Cys or indirectly via other factors is currently unknown (Gibbs et al., 2018). By mutation of components of the Arg/N-end rule pathway, it has been found that Nitric oxide is involved in the regulation of development, breaking seed dormancy, elongation of the hypocotyl, in stomatal closure responses to the environment and in stress responses (Gibbs et al., 2014b). Nitric oxide promotes ERFVII degradation via the N-end rule pathway but whether NO affects Cys oxidation directly or acts indirectly is currently unknown.

As the mammalian RGSs and the plant ERFVIIs have been shown to be important regulatory substrates of the Arg/N-end rule, and they are both MC

initiating proteins it is interesting to speculate how many other MC initiating substrates there are that may also have important roles in gas sensing and in regulating proteins essential for plant development. The MC N-terminus of a protein is only one part of the N-degron, the lysine residue and tertiary structure exposing the N-terminus are also required. Nonetheless, one can hypothesize that other MC proteins across eukaryotes may be substrates of the Arg/N-end rule pathway (Gibbs et al., 2014a). One likely candidate investigated in this project is the MC initiating protein VERNALIZATION2 (VRN2), which has several known developmental functions, including seed development where it prevents cell differentiation (Roszak and Kohler, 2011, Ikeuchi et al., 2015), but it is best characterized as a positive regulator of flowering (Gendall et al., 2001). VRN2 is involved in vernalization; the process of flowering after experiencing prolonged cold conditions.

1.4 Vernalization

Vernalization is an adaptation of plants to delay flowering until a plant has overwintered. Plants can monitor the environment in which they grow to enable them to coordinate their growth and developmental changes so they coincide with seasonal cues (Song et al., 2012). The vernalization pathway and photoperiod pathway promote flowering in plants by integrating environmental cues to control when flowering occurs. The autonomous and gibberellin pathways also promote flowering but they act independently of photoperiod, temperature or other external signals (Gendall et al., 2001). A fifth pathway has also been identified related to flowering and that is the aging pathway (Srikanth and Schmid, 2011). The flowering time pathways control the expression of the floral pathway integrators *SUPPRESSOR OF OVEREXPRESSION OF CONSTANS 1* (*SOC1*), *FLOWERING LOCUS T* (*FT*) and LEAFY (*LFY*), and these genes then encode proteins that activate the floral meristem identity (Henderson and Dean, 2004).

A prolonged period of low temperatures is required for vernalization and this is normally experienced during winter but the process of vernalization is distinct from freezing tolerance and the acclimation response (Gendall et al., 2001). Only the shoot apical meristem needs to be exposed to low temperatures for all of the dividing cells in the whole plant to undergo vernalization and vernalization is mitotically stable, persisting throughout the plants development (Burn et al., 1993, Gendall et al., 2001, Song et al., 2012).

Vernalization occurs during mitosis but not meiosis so the epigenetic state is reset each generation and each generation requires vernalization (Sheldon et al., 2008, Choi et al., 2009, Crevillen et al., 2014). Vernalization is an epigenetic 'memory' where a plant 'remembers' it has experienced the cold and will then transition from a state of vegetative growth to a state of reproduction and floral promotion (Gendall et al., 2001), although there is a temporal separation between the environmental cue and the response. This adaptation allows a plant to be able to flower and produce seed in more favourable conditions generally experienced in spring (Song et al., 2012).

1.4.1 Vernalization Requirement in *Arabidopsis thaliana*

Many temperate plants require vernalization in order to delay flowering until they experience favourable growing conditions and this process has evolved independently between monocots and dicots (Michaels and Amasino, 1999). In this project we work with *Arabidopsis thaliana* (hereafter referred to as *Arabidopsis*). *Arabidopsis*, a member of the Brassicaceae family, is a small flowering plant that is widely used as a model organism in plant biology. Its whole genome has been sequenced and a collection of natural accessions, transgenics and mutant lines is available from the Arabidopsis Biological Resource Centre (ABRC) and the Nottingham Arabidopsis Stock Centre (NASC). *Arabidopsis* naturally grows around the world in variable climates and so native populations are exposed to different environmental conditions across the species' geographical range (Korves et al., 2007). This causes natural variation in *Arabidopsis* plants due to the differences in selection pressures. Some natural populations (ecotypes/accessions) have adaptations

to the particular climate they are from and this includes variation in alleles controlling the requirement for vernalization. Some commonly used ecotypes that are frequently used in research that provide different genetic backgrounds to work with are *Columbia* (Col), *Landsberg erecta* (Ler) and *Wassilewskija* (Ws).

In naturally occurring Arabidopsis accessions the *FRIGIDA* (*FRI*) and *FLOWERING LOCUS C* (*FLC*) genes determine flowering time variation and the requirement for vernalization (Gendall et al., 2001). The *FRI* gene encodes a protein that increases the mRNA level of *FLC*. *FLC* encodes a highly expressed MADS box transcriptional repressor protein, which negatively regulates genes that promote flowering, thus represses flowering (Gendall et al., 2001). During vernalization *FLC* is repressed and therefore flowering occurs (Michaels and Amasino, 1999, Sheldon et al., 1999). Some Arabidopsis accessions have evolved so they do not require vernalization. One of these is *Columbia-0* (Col-0) that evolved in warmer climates where the plant does not naturally experience cold. The cause of variation in vernalization requirement between Arabidopsis accessions is the allelic variation at *FRI* (Nappzinn, 1957). Col-0 has two, naturally occurring null deletion alleles of *FRI*, where the *FRI* gene has become non-functional. Non-functional *FRI* alleles will allow a plant to flower rapidly without the need for vernalization because *FLC* expression is low (Johanson et al., 2000). These plants are termed rapid-cycling or summer annual backgrounds, where the plants flower early and reproduce without the need for cold (Henderson and Dean, 2004). Ler is another ecotype that does not require vernalization.

However, *Stockholm* and *San Felieu2* (*Sf2*) ecotypes do respond to vernalization (Diallo et al., 2010) and these ecotypes have a dominant, functional *FRI* allele. A functional *FRI* allele will cause plants to delay flowering if they have not experienced vernalization (Nappzinn, 1957). These plants are late flowering, require vernalization and termed winter annual backgrounds (Henderson and Dean, 2004). Summer annuals will generally have fewer leaves when flowering and winter annuals will have many leaves if they have not experienced vernalization (FIGURE1.7). If winter annuals do experience vernalization the rosette leaf number will be similar to that of summer annuals at bolting.

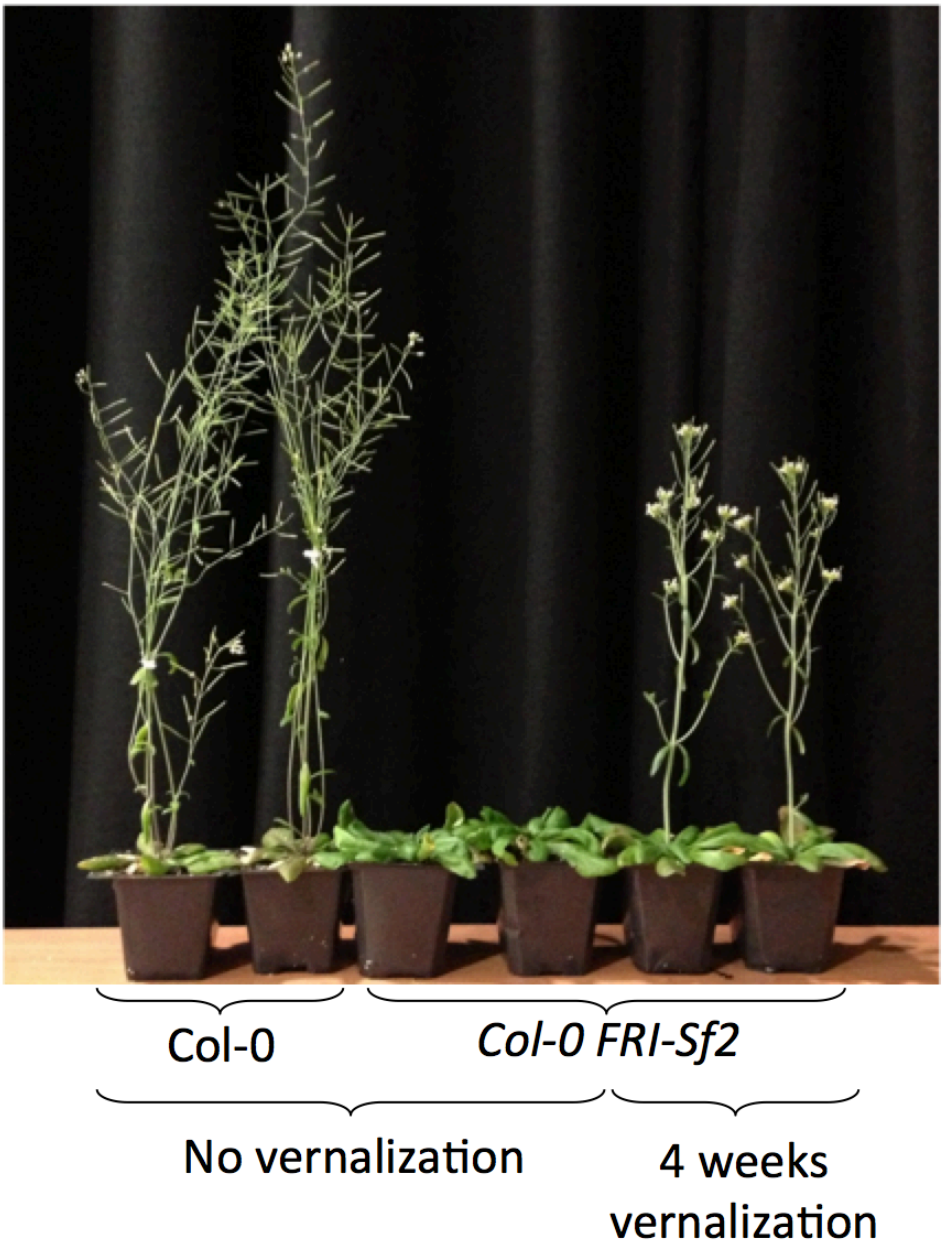

FIGURE 1.7 Flowering behaviour of summer and winter ecotypes of *Arabidopsis thaliana*

The summer ecotype Col-0 flowers rapidly without the need for vernalization due to a recessive FRIGIDA allele that has a 16 bp deletion. The winter ecotype Col-0 *FRI*-Sf2 flowers late with no vernalization but flowers rapidly if vernalized due to having an active, dominant *FRI* allele.

1.4.2 The Process of Vernalization in Arabidopsis

In Arabidopsis, vernalization causes epigenetic silencing of the key floral repressor gene *FLC* (Song et al., 2012) and this is partly controlled by the VERNALIZATION2 (VRN2) gene (accession no.AF284500). It is thought epigenetic repression is limited to *FLC* and this process is quantitative because flowering becomes progressively earlier when increasing the duration of the cold exposure (Sheldon et al., 1999, Sheldon et al., 2000, Gendall et al., 2001, Song et al., 2012). The reduction in *FLC* expression remains stable, as levels remain low after the cold exposure and when the plant is returned to optimal temperatures (Gendall et al., 2001). The *VRN2* gene encodes a zinc finger protein that is found in the nucleus (Gendall et al., 2001). *VRN2* is antagonistic to *FRI* because *VRN2* epigenetically maintains a decrease in *FLC* mRNA (via *FLC* histone methylation) and therefore promotes flowering, whereas *FRI* increases the mRNA level of *FLC*, delaying flowering. The longer the vernalization conditions, the less *FLC* is expressed and the faster the flowering time. In *vrn2* mutants the *FLC* mRNA will still decrease during cold treatment but when plants are returned to normal temperatures the *FLC* mRNA levels increase again. VRN2 is not the cause of the reduction in *FLC* mRNA but is responsible for its stable repression and cellular 'memory' of vernalization (Gendall et al., 2001). *VRN2* is constitutively expressed in the presence or absence of vernalization conditions but the VRN2 protein accumulates to high levels only during the cold (Wood et al., 2006). This suggests that *VRN2* is regulated post transcriptionally at the protein level and not at the gene expression level.

1.4.3 Polycomb Group Proteins and The Polycomb Repressive Complex2

Polycomb group (PcG) proteins are essential epigenetic regulators of gene expression, which function as multiprotein complexes to remodel chromatin and silence their target genes via histone methylation (Simon and Kingston, 2009, Schwartz and Pirrotta, 2013, Derkacheva and Hennig, 2014). PcG proteins were initially identified in *Drosophila*, however PcG proteins are part of a general regulatory mechanism in controlling gene expression of key developmental genes in all eukaryotes (Butenko and Ohad, 2011). The highly conserved PcG proteins were discovered in plants in 1997 (Hennig and Derkacheva, 2009). Gene expression controlling developmental pathways throughout the life cycle of an organism is controlled by PcG proteins due to their effect on transcription of their target genes. PcG proteins form large protein complexes that work in plants to maintain cell identity, fate and normal development. PcG proteins form multi-subunit complexes and examples of these include polycomb repressive complex 1 (PRC1), polycomb repressive complex 2 (PRC2) and polycomb-like PRC2 (pcl-PRC2).

In plants, PRC2 activity takes a role in numerous developmental processes such as the control of cell identity, flowering, seed development, shoot meristem development, root patterning and the establishment of environmental memory (Margueron and Reinberg, 2011, Butenko and Ohad, 2011, Mozgova et al., 2015). The PRC2 complex is highly conserved among plants and animals. The *Drosophila* PRC2 complex contains four subunits:

ENHANCER OF ZESTE (E(z)), EXTRA SEX COMB (ESC), SUPPRESSOR OF ZESTE (Su(z)12) and the p55 protein (Margueron and Reinberg, 2011, Schwartz and Pirrotta, 2013). Plants have one homologue of ESC and one homologue of p55 which are *FERTILIZATION INDEPENDENT ENDOSPERM* (FIE) and *MULTICOPY SUPPRESSOR OF IRA1* (MSI1) respectively. Plants encode multiple copies of the other PRC2 subunits allowing formation of functionally distinct complexes. The Arabidopsis genome encodes for three E(z) homologues: CURLY LEAF (CLF), SWINGER (SWN) and MEDEA (MEA) (Butenko and Ohad, 2011). *VRN2* is a homologue of (*SU(z)12*) (accession no. AF149047) (Birve et al., 2001, Song et al., 2012). Two other homologs of *SU[Z]12* in Arabidopsis are EMBRYONIC FLOWER2 (EMF2) (accession no. AB023044) (Yoshida et al., 2001) and FERTILIZATION INDEPENDENT SEED2 (FIS2) (accession no. AF096096) (Luo et al., 1999).

VRN2, EMF2 AND FIS2 (Su(z)12-like proteins) associate with the other core protein components to make different PRC2 complexes (FIGURE 1.8). FIS2-PRC2 inhibits seed development in the absence of fertilization (Yadegari et al., 2000). The EMF2-PRC2 complex suppresses flowering by repressing FLOWERING LOCUS T (FT) and AGAMOUS-LIKE 19 (AGL19) (Yoshida et al., 2001, Hennig and Derkacheva, 2009). The VRN2 protein is part of the VERNALIZATION (VRN) complex that is a PRC2-like complex controlling the pathway that allows flowering after vernalization by the silencing of *FLC* (Gendall et al., 2001, Hennig and Derkacheva, 2009). The EMF and VRN2 complexes both control flowering but the pathways they use are distinct (Jiang et al., 2008). As vernalization requires cells that are dividing by mitosis

(Wellensiek, 1962), this could be the mode of establishing stability of *FLC* repression during DNA replication because there is stability in the PcG epigenetic silencing of *FLC* (Hennig and Derkacheva, 2009). In the VRN2-PRC2 complex the VRN2 protein associates with CLF/SWN, FIE and MSI1 proteins (Wood et al., 2006, De Lucia et al., 2008). The complex functions by performing the methylation of lysine 27 of histone H3 (H3K27) on *FLC* chromatin (Margueron and Reinberg, 2011, Mozgova et al., 2015). This association of VRN2-PRC2 with the *FLC* locus is independent of exposure to cold, however during vernalization the amount of VRN2 that associates with *FLC* increases because VRN2 levels increases and the repressive H3K27me3 epigenetic mark spreads along the whole locus (Gendall et al., 2001, De Lucia et al., 2008, Hennig and Derkacheva, 2009). A plant homeodomain (PHD) protein *VERNALIZATION INSENSITIVE 3 (VIN3)* is known to associate with VRN2 as part of the PRC2 complex to form a PHD-PRC2 complex and VIN3 is required in the repression of *FLC* during vernalization (Sung and Amasino, 2004a).

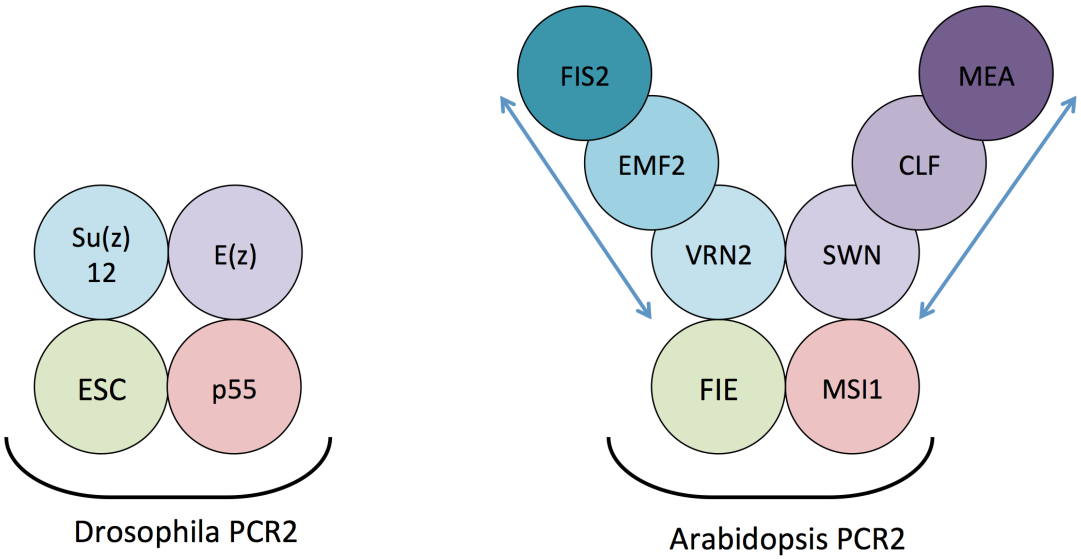

FIGURE 1.8 Polycomb Repressive Complex 2 (PRC2) variations

The *Drosophila* PRC2 complex contains four subunits: ENHANCER OF ZESTE (E(z)), EXTRA SEX COMB (ESC), SUPPRESSOR OF ZESTE (Su(z)12) and the p55 protein (Margueron and Reinberg, 2011, Schwartz and Pirrotta, 2013). In *Arabidopsis* VRN2, EMF2 AND FIS2 (Su(z)12-like proteins) associate with the other core protein components to make different PRC2 complexes. In the VRN2-PRC2 complex the VRN2 protein associates with SWINGER (SWN), FERTILIZATION INDEPENDENT ENDOSPERM (FIE) and MULTICOPY SUPPRESSOR OF IRA1 (MSI1) proteins (Wood et al., 2006, De Lucia et al., 2008). Blue double-ended arrows indicate either of the three proteins can be substituted into the complex (there are 4 proteins in the PRC2 complex in total).

1.4.4 The evolution of VRN2

Vernalization and flowering are characterized developmental pathways that may help characterize how genes and gene networks function throughout evolution to modern day plants. Su(z)12 in animals is typically only single copy but in plants there are three Su(z)12-like genes. VRN2 plays a major role in epigenetic regulation of gene expression along with its homologs EMF2 and FIS2 by silencing MADS-box genes. VRN2, EMF2 and FIS2 genes have co-evolved to be part of the PCG multi-protein complexes but they target different gene networks; vernalization-mediated flowering, vegetative development and seed development, respectively. All three of these genes share a VEF domain that is conserved in plants and animals (Chen et al., 2009). They also all share a C2H2 zinc finger domain. VRN2 is likely to have evolved from an EMF2-like ancestor and ancient land plant. When aligned, 45% of VRN2 and EMF2 amino acids are similar and the N-terminal domain sequence aligns, with the exception of the N-terminal cap (Chen et al., 2009) (FIGURE 1.9). The N-terminal cap of EMF2 is the sequence of amino acids from the first to the second Met (amino acid 21). It is possible that these genes have come about as a result of a historic gene duplication event and subsequent divergence has led to them becoming co-opted to different pathways and with different roles. Hypothetically, a gene duplication of an ancient EMF2-like protein led to the removal of the N-terminal cap, the removal of the E5-10 domain and the addition of the C-terminal repeat, resulting in VRN2.

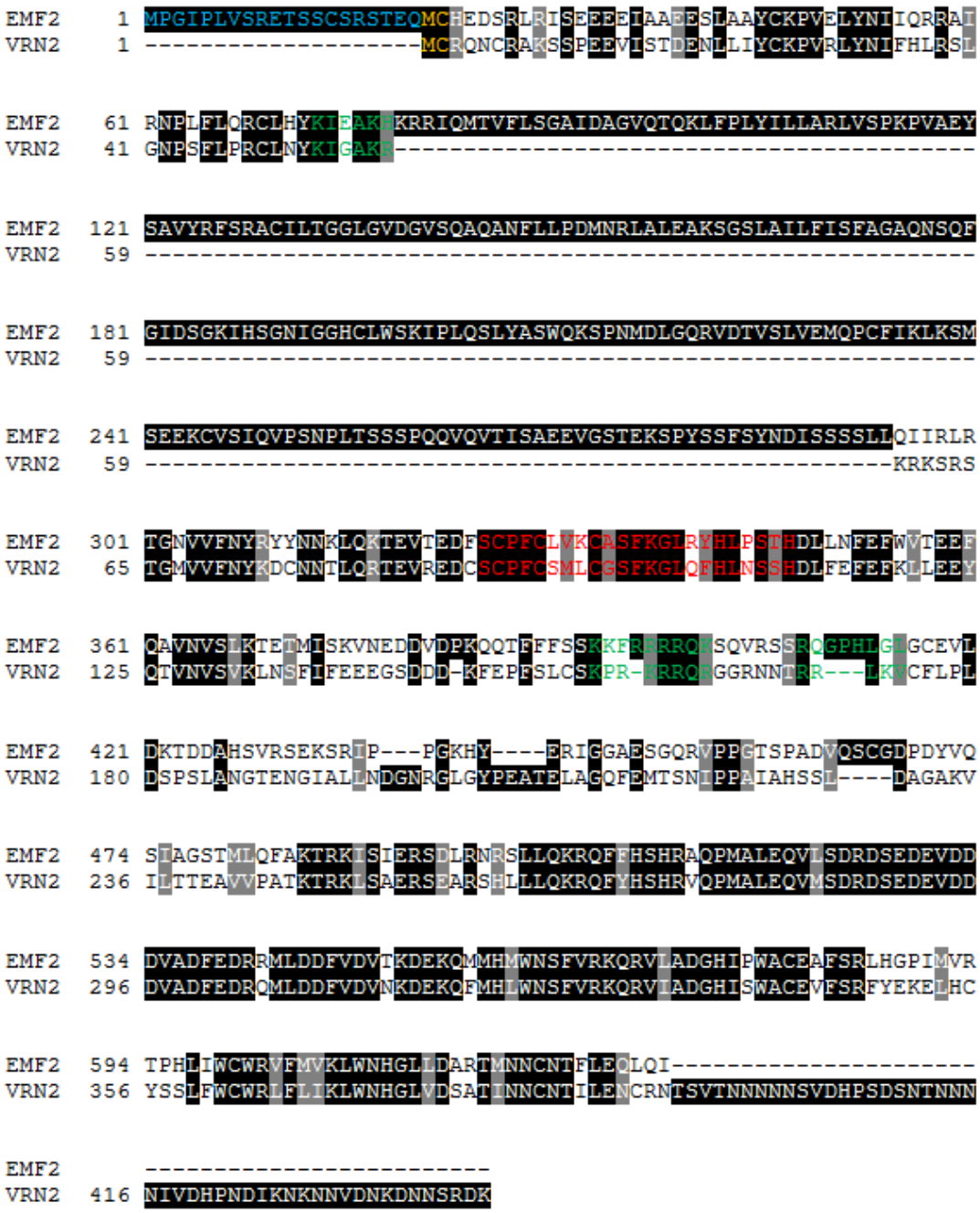

FIGURE 1.9 Alignment of Arabidopsis thaliana EMF2 and VRN2 protein sequences

Sequence alignment of EMF2 and VRN2 proteins from *A. thaliana*. Numbers refer to amino acid number. The VRN2 MC N-terminus aligns with an internal MC in the EMF2 proteins highlighted in yellow. Blue highlights N-terminal cap in EMF2 that is not present in VRN2. Green highlights a putative nuclear localization signal. Red highlights the zinc finger motif.
Black and grey shading denotes identical and similar amino acids respectively. Sequences were obtained from NCBI. Alignments were conducted at Clustal Omega using the default settings. https://www.ebi.ac.uk/Tools/msa/clustalo/
Alignments were then converted to this output using Boxshade 3.21, with fractional sequences that must agree for shading set at 1.

1.4.5 VRN2 in monocots and gymnosperms

Grasses developed 70 million years ago as part of the tropical forest understory but in modern times they have now diversified and adapted to cool climates (Kellogg, 2001) and cereals are now an economically important food crop (Woods et al., 2016). The *VRN2* gene in cereals is unrelated to the VRN2 gene in Arabidopsis but it has the same name as they are both involved in vernalization. Wheat *VRN2* is involved in vernalization requirement and Arabidopsis *VRN2* in the vernalization response. Homologs of Su(z)12 have however been identified in grasses including wheat (*Triticum eastivum*) and barley (*Hordeum vulgare*) (Chen et al., 2009). These core Pooideae have been characterized as vernalization responsive (Heide, 1994) and it is hypothesized that the vernalization response evolved when the grasses started to grow in more temperate climates (Fjellheim et al., 2014). VRN2 and EMF2 homologs have been observed in the ancient angiosperm -the poplar tree (*Populus trichocarpa*) but the most ancient homologs have been found in the gymnosperms spruce *Picea engelmannii* and pine *Pinus taeda*, the lycophyte spike moss *Selaginella moellendorffii* and the moss *Physcomitrella patens* (Chen et al., 2009).

1.5 AIMS

This study aims to provide information on how plants detect the environment in order to make developmental changes. Here, the molecular basis behind the increase in VRN2 during vernalization will be investigated. The hypothesis that VRN2 is a substrate of the N-end rule pathway will be tested and its stability will be monitored in various 'N-end' mutant backgrounds. VRN2 stability will also be monitored during vernalization treatments to test the hypothesis that VRN2 becomes stable in cold conditions. The localization of VRN2 will also be observed to confirm that VRN2 is found in the nucleus. Phenotypic analysis will be performed to see if VRN2 regulation of flowering can be linked to the N-end rule pathway and to determine if there is a possible link to stress response pathways. If VRN2 is found to be a substrate of the N-end rule, VRN2 stabilization will be investigated to implicate VIN3 association as a cause for VRN2 stability. Further, in this study I wanted to investigate the possible functional similarity of the monocot HvEMF2c and the dicot AtVRN2 to gain insight into the developmental evolution of VRN2 in flowering plants. Finally, I will investigate the hypothesis that VRN2 evolved from EMF2 via gene duplication and a truncation event that removed the N-terminal cap.

Chapter 2

Methods

2.1 Plant cultivation growth and harvesting

Recipes for normal and selective growth media are found in Appendix I.

2.1.1 Seed sterilization

Sterilization solution (10 %) was prepared using 45 ml Sterile distilled water (SDW) and 5 ml of Parazone™ bleach. The required amount of seeds were placed into a 1.5 ml Eppendorf. Seeds were imbibed in 500 µL of the bleach solution and left for 5 min on a tilting tray. The bleach solution was then removed and the seeds were washed twice with 1 ml SDW. The SDW was removed with 50 µL remaining to cover the seeds. Seeds were plated onto ½ Murashige and Skoog (MS) agar (Murashige and Skoog, 1962) using a 20 µL micropipette, inside a sterile laminar flow hood, pre-cleaned with 70 % ethanol. The ½ MS was supplemented with selective agents where required (Appendix I). Plates were sealed with Microporous tape.

2.1.2 Plant growth conditions

The sterile plates of *Arabidopsis thaliana* seeds were stratified at 5 °C for 2-3 days and then moved to the 22 °C Thermofrost Cryo constant temperature growth room 16h L: 8h D for 7 days. Square plates were stored vertically in the growth room, so the roots grew on the surface of the media whereas round plates were grown horizontally. 7-day old seedlings were transferred to soil (4:2:1 of Levington M3 compost: vermiculite: perlite) and grown in the glasshouse in a controlled environment of 20-22 °C, 16 h day length and with automatic watering each day. Plants were bagged with plant sleeves when they started to flower to prevent cross contamination.

2.1.3 Collecting seeds

Seeds were collected once siliques had turned brown. The stalk was cut at the base with scissors and the plant material stored in labelled glassine bags at room temperature (RT).

2.1.4 Crossing plants

Two plants were chosen and all but 3 stems were removed from one of the plants (acting as the female plant) with small scissors. Then all siliques and all open buds were removed. Next, closed buds were removed leaving only three closed buds at the end of the stem. The three buds from the end of the stem were dissected: The sepals, petals and stamens were removed so only the style was remaining. Using forceps, a flower was removed from the other plant (acting as the male) plant and the stamens rubbed onto the female plant so the pollen could be seen to stick to the stigma under a binocular microscope. The crosses were labelled with masking tape and left to grow until the seeds were ready to harvest. Seeds from crosses were collected using scissors into a 1.5 ml Eppendorf.

2.1.5 Plant lines used

Arabidopsis genetic resources were obtained from the National Arabidopsis Resource Centre.

Gene/mutant background	Gene acronym	gene ID	SALK/SAIL code	Source
VERNALIZATION 2	*vrn2-5*	AT4G16845.1	SALK_201153	(Gibbs et al., 2018)
PROTEOLYSIS 6	*prt6-1*	AT5G02310.1	SAIL_1278_H11	(Garzon et al., 2007)
FRIGIDA	*FRI*	AT4G00650	n/a (not mutant)	(Nappzinn, 1957)
Columbia 0 *FRIGIDA* San Felieu2	Col-0 *FRI*-Sf2	AT4G00650	n/a (not mutant)	(Johanson et al., 2000)
ARGINYLTRANSFERASE 1	*ate1*	AT5G05700.1	SALK_069686	(Holman et al., 2009)
ARGINYLTRANSFERASE 2	*ate2*	AT3G11240	SALK_040788	(Holman et al., 2009)

Table 1. Plant lines used to provide different mutant or allelic backgrounds for the study

2.2 Plant manipulations

2.2.1 Abscisic acid (ABA) treatment

The germination test was performed by sterilizing freshly harvested seeds and plating them onto agar plates supplemented with ABA. ABA was dissolved in methanol (MeOH) and then added to the ½ MS mixture to get concentrations of 0, 1, 2 and 5 μM ABA agar plates. Plated seeds were then stratified for 2 days and placed at 22 °C as described in section 2.1. Germination and establishment were scored after 6 days. Germination was scored as when the endosperm had ruptured, and the radicle had emerged. Establishment was scored as when the cotyledons had turned green.

2.2.2.1 Vernalization conditions

Seeds were sterilized, plated and grown on ½ MS plates for 7 days as described in section 2.1. For treatment under vernalization conditions seedlings were then transferred from the growth room to an incubator at 5 °C and 8h days for the desired number of weeks. They were then either transferred to soil in the glasshouse at 22 °C or seedling samples were frozen in liquid nitrogen and stored at -80 °C for RNA and protein extractions.

2.2.2.2 Flowering time assay

Seeds were sterilized and plated onto ½ MS plates. They were stratified at 5 C for 2 days and then grown at 22 C for 7 days. Seeds were then vernalized for 0, 1, 2, 3, 4 weeks at 5 °C and 8h days. After the required amount of vernalization plants were put onto soil in a staggered formation and placed at

22 C with 16 h days. The number of days to flowering was scored from the day of plating. In addition, the number of leaves at flowering was scored. Flowering was said to have occurred once the central bud was visible and the bolting shoot was 0.5 cm in length. For leaf counting, the first two leaves (the cotyledons) were removed and all leaves were counted thereafter. Leaves from the rosette were removed one by one with forceps and care was taken not to include leaves originating from the main central stem or leaves from lateral shoots.

2.2.3 Heat stress treatments

Four thermotolerance assays were performed as in the recent paper by Vicente et al. (2017). For the basal thermotolerance (BT) assay, 5-day-old seedlings were treated for 23 min and 26 min at 44 °C and then moved back to 22 °C for 13 d. For short-term acquired thermotolerance (SAT) assay, 5-day-old seedlings were acclimated for 1 h at 37 °C, recovered for 2 h at 22 °C, treated for 170 min at 44 °C and returned to 22 °C for 8 d. For the long-term acquired thermotolerance (LAT) assay, 5-day-old seedlings were placed at at 37 °C for 1 h, transferred to 22 °C for 2 d to recover. They were then treated for 60 min at 44 °C and then returned to 22 °C for 8 d. Seedling survival was scored after 8 days where the seedlings were established and green.

2.2.4 Salt stress treatment

Seeds were cleaned and plated on ½ MS, stratified and grown at 16 h light at 22 °C. 7-day old seedlings were transferred to soil and grown at under the

same conditions for another 10 days. 600 ml of 200 mM Sodium chloride solution was used to water the seedlings twice a week. Any excess water was tipped off after soaking for 30 min. Control plants were irrigated with tap water. Seedling senescence and survival was observed.

2.2.5 Plant transformation

Agrobacterium tumefaciens were transformed by electroporation with the desired constructs (see section 2.7.9.2 and 2.7.10.2). *A. tumefaciens* containing constructs to be transformed to plants was used to inoculate 200 ml LBB plus the appropriate selective agents and grown in a 1 litre conical flask with a foam bung and foil on the top. The ratio of bacteria to flask size was 1:5 to allow aeration of the culture. The flask was incubated at 28 °C and 200 rpm overnight. The bacteria were poured into 500 ml plastic bottles and centrifuged at 4500 rpm for 10 min. The supernatant was discarded. The bacterial pellet was then re-suspended in 400 ml of 5 % sucrose solution and poured into 500ml glass bottles for transport to the glasshouse.

Transgenic *Arabidopsis* seeds were sprinkled onto soil in 9 cm pots and grown at 22 °C in the glasshouse. Once established, plants were thinned out by removing them with forceps, until there were just four remaining in a pot. These plants were grown until they had flowers and then the stems were cut back to the base to promote more shoots. The plants were then allowed to grow until they had buds. Any flowers or open buds were removed the night before and the morning of dipping. Only closed buds were left. 80 µL of Siluett L77 (Wetting agent) was added to each re-suspension of the 400 ml of the

bacteria in sucrose (to 0.02 %). Plants were then dipped into the solution for 5-10 seconds, making sure all the inflorescences were coated. The plants in their pots were then sealed in an autoclave bag and left on their side in low light in the glasshouse for ~24 h. The next day the plants were taken out of the bags and grown in normal glasshouse conditions until seeds were ready for harvest. Seeds were collected once mature so the transgenic plants could be selected.

2.2.6 Plant selection

The plant transformation of the desired vector inserts a hygromycin phosphotransferase (HTP) gene into plants, allowing for selection. 0.7 % MS agar was supplemented with appropriate selective agent (20 mg/ml Hygromycin), autoclaved and left to set. The desired numbers of seeds from sample lines for selection were added to 15 ml Falcon tubes. Then 0.6 % agar was made and autoclaved. Before the agar was set it was poured into the tubes and mixed with the seeds by inversion. The mixture was poured on top of the agar plates in a flow hood and left to set. Plates were then stratified at 5 °C 3 days before placing in the 22 °C growth room. After 6 h at these conditions they were wrapped in a double layer of tin foil for 5 days to promote etiolation in order to differentiate transgenic seedlings more easily. The foil was removed and after a further 10 days the seedlings that had grown most were selected and planted into soil. Transgenic seedlings were green, healthy and etiolated. Seeds were collected from these and seedlings selected again on ½ MS supplemented with hygromycin. Lines showing 75 % seedling growth were grown on to the next generation. Of these, at least two

independent lines that had 100 % growth were homozygous and thus were used for further experiments.

2.2.7 Estradiol induction of transgenes

A solution of liquid MS was made, and this was autoclaved. 60 µL of a 10mM solution of β-estradiol was added to 100 ml ½ MS. 60 µL DMSO was added to another 100ml ½ MS as a control solution. 6 ml of the +/- estradiol solutions were added to wells of a 6 well plate. The seedlings were placed in the solutions and the plates were agitated gently on a rotary plate at RT. Seedling samples were taken and frozen after 24, 48 and 72 h of being soaked in the +/- estradiol solutions. These seedlings were then used for protein and RNA extractions.

2.3 Bacterial strains

Escherichia coli DH5α™ cells (Thermofisher Scientific)

F- φ80lacZΔM15 Δ(lacZYA-argF)U169 recA1 endA1 hsdR17(rk - , mk +) phoA supE44 thi-1 gyrA96 relA1 λ-

Escherichia coli ABLE® K cells (Agilent)

E. coli C lac (LacZω–) [Kan^r McrA– McrCB– McrF– Mrr– HsdR (r_K– m_K–)] [F´proAB lacI^{q}ZΔM15 Tn10 (Tet^r)].

Genes listed signify mutant alleles. Genes on the F´ episome, however, are wild-type. These are kanamycin and tetracycline resistant cells.

DB3.1 cells

gyrA462 endA1 Δ(sr1-recA) mcrB mrr hsdS20 glnV44 (=supE44) ara14 galK2 lacY1 proA2 rpsL20 xyl5 leuB6 mtl1

These are streptomycin resistant and ccdB resistant.

Agrobacterium tumefaciens GV3101 (GV3101pMP90)

C58 (RIF R) Ti pMP90 (pTiC58DT-DNA) (gentR/strepR) Nopaline

Disarmed *Agrobacterium tumefaciens* strain produced in a C58 background; it carries a rifampicin resistance gene on chromosome 1 and also harbours the disarmed pMP90 Ti virulence plasmid (pTiC5ΔT-DNA) that possesses the genes for T-DNA transfer but has no functional T-DNA region of its own. This Ti plasmid carries the gentamycin resistance genes (Koncz and Schell, 1986).

2.4 Bacterial growth conditions

Recipes for normal and selective growth media are found in Appendix I.

2.4.1 Glycerols of bacteria

A 60 v/v glycerol solution was made by adding 60 ml glycerol to 40 ml SDW before autoclaving.

300 µL glycerol solution and 900µL bacterial culture were added to a 1.5 ml Eppendorf to make the overall concentration of glycerol 15 %. The bacterial glycerol was then frozen immediately in liquid nitrogen and stored at -80 °C.

2.4.2 *E.coli*

One colony or sample from a bacteria glycerol stock (2.4.1) was streaked onto a plate or 100 ml of culture was spread onto a Lysogeny broth (LB) agar plate. Agar plates were inverted and left at 37 °C overnight for ~16 h. For liquid cultures, one colony or glycerol was picked using a cocktail stick and placed into 100ml LBB. *E.coli* liquid cultures were grown overnight for ~16 h at 37 °C on a rotary shaker at ~200 rpm. All inoculations were made under aseptic conditions by a Bunsen burner or in a laminar flow hood.

2.4.3 A. tumefaciens

Liquid cultures were grown for ~48 h at 28°C on a rotary shaker at ~200 rpm. 10ml of culture was grown in universal bottles and 100ml of culture was grown in sterile 1 litre conical flasks with a sponge bung wrapped in foil. Agar plates were inverted and left at 28°C for ~48 h. Inoculations of liquid culture and agar

plates were carried out under aseptic conditions. Liquid and ager media had rifampicin and gentamycin selection.

2.5 Cloning vectors

pDONR™221 (Invitrogen)

A Gateway® vector Including: Two recombination sites *att*P1 and *att*P2, for recombination cloning of the gene of interest from an *att*B PCR product. A kanamycin resistance marker for selection. M13 forward and reverse priming sites for sequencing of the insert. *ccd*B gene for negative selection. pUC origin for replication and maintenance of the plasmid in *E.coli*.

pDONR™zeo zeomycin M13 invitrogen

A Gateway® vector Including: Two recombination sites *att*P1 and *att*P2, for recombination cloning of the gene of interest from an *att*B PCR product. A zeomycin resistance marker for selection. M13 forward and reverse priming sites for sequencing of the insert. *ccd*B gene for negative selection. pUC origin for replication and maintenance of the plasmid in *E.coli*.

Per8GW /pB2GW7

Used for transformation of estradiol inducible genes into plants (Coego et al., 2014). A Gateway® compatible binary vector (Curtis and Grossniklaus, 2003). Contains *att*R1 and *att*R2 sites for recombination cloning and XVE estrogen receptor that mediates inducible gene expression (Zuo et al., 2000). Includes a hygromycin resistance marker. Contains the *ccd*B gene for negative selection. Has a *LexA* operator fused to a minimal promotor of Cauliflower Mosaic Virus 35S gene. Has the HTP gene, allowing for plant selection on hygromycin.

pTNT™ (Promega)

Used with the *in vitro* rabbit reticulocyte lysate expression system. Includes a kanamycin resistance marker. Contains the SP6 and T7 promotors adjacent to a multiple cloning site.

pE2c (Invitrogen)

A Gateway® compatible vector for C-terminal 3x HA tag fusion with the gene of interest. Contains *att*R1 and *att*R2 sites for recombination cloning and includes a kanamycin resistance marker.

2.6 Isolation of nucleic acids

Recipes for all solutions and buffers are in appendix II.

2.6.1 Preparation of plasmid DNA from bacteria

A QIAprep® Spin Miniprep Kit (Qiagen) was used to extract plasmid DNA from bacteria. The kits lyse the bacterial cells to extract the DNA plasmids. They then used a silica column to adsorb DNA in high salt conditions, the column is washed with ethanol and then the DNA is eluted with a base buffer. 2 ml of bacterial overnight culture was pelleted by centrifugation at 17900 x G for 3 min at room temperature (RT). Sometimes 10 ml of culture was used and centrifuged for 10 min if a high yield of plasmid was required. The pellet was resuspended in 250 µL buffer P1 (50 mM Tris-HCl pH 8.0,10 mM EDTA, 100 µg/ml RNaseA) and transferred to a 1.5 ml Eppendorf. 250 µL buffer P2 (1% sodium dodecyl sulfate (SDS)(w/v) and 200mM NaOH) was added and mixed by inversion. The 350 µL buffer N3 (Guanidinium hydrochloride 25-50%, Acetic acid 10-25%, pH 4.3) was added and mixed by inversion. The mix was centrifuged at 17900 x G for 10 min. 800 µL of the supernatant was applied to the QIAprep 2.0 spin column, centrifuged for 1 min at 17900 x G and the flow-through discarded. The column was washed with 750 µL buffer PE, centrifuged at 17900 x G for 1 min and the flow-through discarded. The column was centrifuged for a further minute to remove residual wash buffer. The column was placed into a clean 1.5 ml Eppendorf and the DNA was eluted in 50 µL of Buffer EB (10 mM Tris-Cl, pH 8.5). DNA was stored at -20 °C.

2.6.2 Preparation of genomic DNA from plants

A leaf samples from each plant was collected with forceps and placed into a 1.5 ml Eppendorf. These could be frozen and the DNA extracted at a later date or used fresh. A GenElute™ Plant Genomic DNA miniprep kit (Sigma) was used to extract the DNA. 350 µL of lysis solution part A was added to the sample and the sample was ground using a sterile mini-pestle. 50 µL was added and the sample was vortexed. Samples were then incubated at 65 °C in a heat block for 10 min, inverting occasionally. 130 µL of precipitation solution was added, inverted and placed on ice for 5 min. Samples were centrifuged at 16000 x G for 5 min to pellet the cellular debris. The supernatant (approx. 530µL) was pipetted onto a GenElute™ filtration column at centrifuged at max speed for 1 min. The filtration column was discarded and 700 µL binding solution added to the flow through liquid and mixed by inversion. GenElute™ Miniprep Binding Columns were prepared by washing with 500 µL of column preparation solution and centrifuged at 12000 x G for 1 min. 700 µL of the sample was added to the binding column and centrifuged at max speed for 1 min. The flow-through was discarded and the rest of the sample added to the binding column, centrifuged at max speed for 1 min and the flow-through discarded. The column was put into a fresh 2 ml collection tube and washed twice with 500 µL wash solution (containing ethanol). It was centrifuged first for 1 min at max speed and then 3 minutes to dry the column. The binding column was then placed into another fresh 2 ml collection tube. 100 µL of pre-warmed (65 °C) elution solution (Tris) was placed on the column, left to stand for 1 min and centrifuged at max speed for 1 min to elute the DNA. Eluate was stored at -20 °C.

2.6.3 Preparation of total RNA from plants

RNA was extracted from material that had been frozen in liquid nitrogen and stored at -80 °C. The RNA was extracted using the RNeasy® plant mini kit (Qiagen). For each sample, 4.5 µL β-Mercaptoethanol was added to 450 µL of RLT buffer (containing a high concentration of guanidine isothiocycanate, which supports the binding of RNA to the silica membrane). The sample was ground in the buffer mix using a micro-pestle, vortexed and kept on ice. The sample was placed on a lilac QIAshredder™ spin column and centrifuged at 17900 x G for 2 min. The supernatant was transferred to a clean tube, 0.5 volume of ethanol was added and mixed by pipetting. The sample was transferred to a pink column, centrifuged at 10 000 rpm for 15 s and the flow through discarded. The column was washed with 700 µL RW1 buffer by centrifuging 10 000 rpm for 30 s. RW1 contains guanidine salt and ethanol and helps remove large molecules such as protein, carbohydrate and lipid from the membrane during the wash. The column was placed into a fresh 2ml tube. 500 µL RPE buffer was added, centrifuged as before and the flow through discarded. 500 µL RPE buffer was added again but this time centrifuged at 10 000 for 2 min and the flow through discarded. RPE removes salts from earlier washes in the protocol. The column was spun for a further minute to remove residual ethanol from the membrane. The column was placed into a clean 1.5ml Eppendorf and the RNA was eluted in 30 µL RNase-free water. This was centrifuged for 1 min at 10 000 rpm, transferred to a microcentrifuge tube and frozen at -20 °C.

2.7 Nucleic acid manipulations

2.7.1 Estimation of nucleic acid concentration

DNA and RNA concentrations were determined using a nanodrop spectrophotometer (ND-1000; Labtech International). It measures absorbance rations at different wavelengths (260/280) and converts this into a nucleic acid concentration.

2.7.2 Digestion of DNA with restriction enzymes

Typically, a 20 µL reaction was used for each sample when checking the correct DNA had been inserted into a vector. In each reaction there was 10 µL plasmid DNA, 2 µL NE buffer 2.1, 2µL Bovine serum albumin (BSA), 0.5 µL BsrGI enzyme and 5.5 µL SDW. Reactions were incubated at 37 °C for 1.5 h. Plasmid DNA was incubated for a further 1 h after the addition of 1 µL calf intestinal phosphatase to dephosphorylate the vector in order to prevent self-ligation. 2 µL of DNA loading buffer was added to the samples and then they were run on a 1 % gel by electrophoresis. MluI enzyme was used instead of BsrGI to digest pDONR.

When digesting DNA fragments and vectors before ligation a 100 µL reaction was used. 40 µL of PCR product/vector were mixed with 10 µL buffer, 45 µL SDW and 2.5 µL of enzyme 1 and 2.5 µL enzyme 2. Enzymes 1 and 2 were either MluI and XbaI or EcoRI and KpnI. Different enzymes were used for each end of the DNA to prevent fragments inserting in an incorrect orientation. Restriction enzymes and the appropriate buffers were obtained from New

England Biolabs. Expected fragment lengths were found using Serial Cloner software.

2.7.3 Agarose gel electrophoresis of DNA and RNA

For RNA and DNA, 1 % (w/v) agarose gels were prepared in 1 X Tris-borate/EDTA (TBE) buffer. For *FRIGIDA* (*FRI*) genotyping a 3 % gel was used so the small difference in size of fragments could be seen. 1 µl ethidium bromide (1.5 µm/ml) was added per 50 ml of the molten gel shortly before pouring in order to visualise the nucleotides. 5 µl of 1kb plus DNA ladder (Invitrogen) (20 µL Ladder, 20 µL of 1 X DNA loading buffer, 160 µL SDW) was used to estimate the DNA/RNA size and concentration. 10-15 µl each sample was loaded onto the gel in each well. Samples containing Red *Taq* were suitable to load directly but other samples needed 1 X DNA loading buffer. All gels were compared to a SDW control PCR reaction with no DNA template. A Bio-Rad gel electrophoresis tank and Bio-Rad Power/pac 300 were used and gels were run at constant voltage of 100 V for 1 hour. For *FRI* genotyping, gels were run at 80 V for 3 h. DNA was visualised on a ChemiDoc™ MP Imaging System (Bio-RAD) at 700 nm and images were taken using ImageLab software.

2.7.4 cDNA synthesis

First strand cDNA synthesis was performed using Superscript II Reverse Transcriptase (RT) (Invitrogen). A 20 µL reaction volume was used. 2000 ng of RNA was added to 1 µL of Oligo DT primers, 1µL dNTPs, and made up to 12 µL volume with SDW. This was placed in a heat block at 65 °C for 5 min

then put onto ice. Then 4 µL 5 x first strand buffer, 2 µL 0.1M DTT and 1 µL RNase OUT were added and mixed by pipetting. This was placed at 42 °C for 2 min. 1 µL Superscript II RT enzyme was added and the mixture returned to 42 °C for 50 min. The mixture was finally placed at 70 °C for 15 min. The cDNA was amplified using PCR with gene specific primers and checked by gel electrophoresis.

2.7.5 PCR product purification -PEG

The attB sequences were incorporated onto genes to be cloned using primers. PCR products were purified to remove primer dimers and products < 300 base pairs (bp). First, the PCR reaction was diluted 4-fold with TE (10 mM Tris-HCl (pH 7.5-8), 1 mM EDTA). Then half volume of 30% PEG 8000/30mM $MgCl_2$ was added and the mixture vortexed. The mixture was centrifuged at 17 900 x G for 15 min and the supernatant removed. The pellet was then resuspended in 15 µL of TE.

2.7.6 Gene cloning

2.7.6.1 Extraction of digested DNA from agarose gels

A 1 % gel was made with double wells to load samples into. Sample plasmid and insert DNA were pre-digested and the amount loaded was approximately 500 µL. The gel was run at 100 V for 1 hour as in section 2.7.3. Bands were viewed using a UV light box and cut out using a scalpel. The DNA gel samples were weighed in 1.5ml Eppendorfs. The DNA was purified by adsorption to a silica column using a Qiagen gel extraction kit according to manufacturer's instructions and eluted in 30 µL Elution Buffer. 3 µL of the

sample was run on another gel by electrophoresis to check the extraction was successful prior to being used in ligation reactions.

2.7.6.2 Ligation into vector DNA

This method was used to clone genes into the pTNT vector. Ligation reactions were carried out using T4 DNA-Ligase (New England Biolabs). 300ng of gene insert were mixed with 100ng of vector (a 1:3 ratio). (If this ratio was unsuccessful other ratios were used.) 2 µL T4 DNA ligase buffer, 1 µL T4 DNA ligase and 5 µL SDW were then added to make the reaction volume 20 µL. The reactions were kept at 16 °C overnight for ~16h and then this was used for transformation of chemically competent *E.coli*.

2.7.6.3 Gateway recombination cloning

2.7.6.3.1 BP reaction

This method was used to clone genes into the pDONR vector. Cloning of the gene of interest into its vector was done using Gateway® BP Clonase™ II enzyme mix kit (Invitrogen). A 150 ng concentration of the attB-PCR product was added to 150 ng of the donor vector (pDONR221/pDONRzeo) and made up to 8 µL with TE buffer (pH8). 2 µL of the BP Clonase™ II enzyme mix was added to each sample. The mixture was vortexed and incubated at RT for 1 h. To terminate the reaction 1 µL Proteinase K was added and samples were placed at 37 °C for 10 min. The samples were stored at -20 °C until needed.

2.7.6.3.2 LR reaction

Thermofisher Scientific Gateway® LR Clonase® II enzyme mix was used to transfer the gene from the entry vector to the destination vector. Typically, 150 ng of all vectors (destination vector per8GW and the pDONR221/zeo entry vector) was used. This was made up to 8 µL volume with TE buffer pH8. 2 µL LR Clonase™ II enzyme was added to each reaction and the mix was incubated at RT for 1 h. 1 µL Proteinase K was added to each sample and incubated at 37 °C for 10 min to terminate the reaction. Samples were stored at -20°C until required for transformation into *E.coli* by heat shock.

2.7.7 DNA sequencing

Sequencing of DNA was carried out by the Functional Genomics Laboratory at the University of Birmingham. They use the dideoxy chain termination method of sequencing. 300ng of plasmid/PCR product was used for each sample as well as 1µL of 3.2 pmol of sequencing primer (see Appendix III for primers used). This was then made up to 10 µL with SDW and taken to the sequencing laboratory. Sequencing reagents were added to the samples by Roboseq 4204s and then placed in the Primus HT 96-well plate thermocycler (MWG Biotech) according to manufacturer's instructions. Reactions were then purified, eluted in diformamide and sequenced in the ABI3700 sequencer (Applied Biosystems).

2.7.8 Polymerase chain reaction (PCR)

2.7.8.1 Oligonucleotides

The *vrn2-5* and *prt6-1* mutants were produced by the SALK institute using transfer DNA insertion mutagenesis (Baulcombe et al., 1986). Primers were designed for genotyping these mutants to the left and right border of the inserts and gene specific primers. Gene and plasmid sequences were used for cloning and sequencing. The Arabidopsis Information Resource (TAIR) was used to find coding DNA sequences for *VRN2, PRT6, VIN3, FRI* and *EMF2*. Primers were designed for genotyping, cloning and for sequencing using these sequences on the National Centre for Biotechnology Information (NCBI) website, reverse compliment website, OligoPerfect™ designer on the Thermofisher Scientific website, the Invitrogen perfect primer design tool online and using the Microsoft Word application. Eurofins supplied all primers. All primers and their uses can be found in Appendix III.

2.7.8.2 PCR techniques

PCR was used for amplifying gDNA when genotyping transgenic plants, amplifying plasmid DNA in cloning, adding restriction sites and recombination sites in cloning and in amplifying cDNA. The enzymes used were either Phusion® polymerase (New England Biolabs) or red *Taq*® PCR Ready Mix™ (Sigma-Aldrich), used according to manufacturers' instructions. Reactions were set up according to manufacturer's guidlelines using recommended buffers and volumes of reagents. PCR amplification was carried out in 0.2ml thermotubes. Primers were made up in SDW at an initial concentration of 100μM and then diluted further, to 10 μM in a 100 μL volume.

A typical **PCR mix** for a reaction volume of 20μL would be:

10 μL red *Taq* Ready Mix,

0.5 μL Forward primer,

0.5 μL Reverse primer,

1μL DNA template,

8μL SDW.

A typical **PCR mix** for a reaction volume of 50μL would be:

0.25 μL Phusion polymerase (NEB),

1 μL Forward primer,

1 μL Reverse primer,

1 μL 10mM dNTPs (Invitrogen),

10 HF Buffer (NEB),

1 μL DNA,

35.75 μL SDW.

PCR cycling conditions

If using Phusion® polymerase 98 °C is needed for denaturation, whereas with red *Taq*® PCR Ready Mix™ 95 °C is needed. Between 25-35 cycles were used.

Typical **PCR cycles** using Phusion® would be as follows:

gene	*VRN2*		*PRT6*		*FRI*	
	temperature	time	temperature	time	temperature	time
initial denaturation	98	5min	98	30s	98	2min
denaturation	98	30s	98	20s	98	30s
annealing	60	30s	60	30s	60	30s
extension	72	1min	72	2min	72	20s
final extension	72	7min	72	5min	72	1min
hold	10	Hold	10	Hold	10	Hold

gene	*HvEMF2c*		*VIN3*		*ACTIN2*	
	temperature	time	temperature	time	temperature	time
initial denaturation	98	30s	98	5min	98	5min
denaturation	98	30s	98	30s	98	30s
annealing	64	30s	60	30s	60	30s
extension	72	40s	72	1min15s	72	40s
final extension	72	7min	72	7min	72	7min
hold	10	Hold	10	Hold	10	Hold

Table 2. Typical PCR conditions used for amplifying genes of interest

2.7.8.3 Single colony PCR

A colony was suspended in 20 µL SDW using an inoculation loop. PCR was done with conditions described in 2.7.8.2. The PCR product was run on a 1 % gel by electrophoresis. The remainder of the re-suspended colony was used to inoculate an overnight culture and grown with appropriate antibiotics at 28 °C 200 rpm.

2.7.9 Preparation of competent cells

2.7.9.1 Preparation of chemically competent *E.coli* DH5α cells

From the *E.coli* DH5α glycerol, bacteria were streaked onto an LB agar plate and grown at 37 °C for ~16 h. Then 10 ml of LB broth was inoculated with a single colony and grown at 37 °C for ~16 h at 200 rpm. 2 ml of this culture was added to 200 ml of fresh LB broth in a 2 L flask and grown 2-3 h at 37 °C and 200 rpm until the optical density (OD_{600}) was 0.5-0.6. At this point the cells were chilled on ice for 15 min in order for them to stop growing. The cells were then spun at 5000 X G at 4 °C for 10 min. The supernatant was discarded, the pellet was re-suspended in 80 ml of Tfb1 buffer and the cells kept on ice for 5 min. Cells were spun again at 5000 X G for 5 min at 4 °C, re-suspended in 8ml of Tfb2 buffer and kept on ice for 15 min. 560 µL DMSO was added drop wise to the cells and mixed gently. The competent cells were moved to the 4 °C constant temperature room where the cells were snap frozen in 50 µL aliquots into pre-chilled Eppendorf tubes into liquid nitrogen. Cells were stored at -80 °C until needed.

2.7.9.2 Preparation electrocompetent *A. tumefaciens* GV3101 cells

From the glycerol stock, a 10 ml starter culture of *A. tumefaciens* was grown for ~48 h at 28 °C in LB broth with rifampicin and gentamycin selection. 5 ml of this culture was used to inoculate 200 ml of LB-rifampicin and gentamycin broth and grown at 28 °C, 200 rpm for 4-6 h until the OD_{600} reaches 0.5-0.8. celled were chilled on ice for 5 min. Then the cells were spun at 5000 X G for 5 min at 4 °C and re-suspended in 10 % glycerol. The competent cells were

snap frozen in 100 µL aliquots in liquid nitrogen and stored at -80 °C until needed.

2.7.10 Transformation of bacterial cells

2.7.10.1 Transformation of *E.coli* by heat shock

DH5α cells were thawed on ice for 10 min. (DB3.1 cells were used for transformation of empty vectors.) 5 µL of the vector (~100 ng) was added to the 50 µL aliquot of bacterial cells and this was left on ice for 30 min. The cells were shocked at 42 °C for 30 s then placed back onto ice for 2 min. 950 µL of LBB was added and the cells placed at 37 °C on a shaker ~200 rpm for 1 h. 100 µL of the culture was plated on LBA with appropriate antibiotic selection. The remaining 900 µL was centrifuged at 17 900 x G for 2 minutes, the supernatant tipped off and the cells re-diluted with 100 µL LBB. The concentrated culture was also plated onto LBA using a sterile plastic spreader in a flow hood. Colonies that grew were selected and grown in LBB, with appropriate antibiotics overnight at 37 °C and 200 rpm. Plasmid DNA was then extracted from the overnight cultures.

2.7.10.2 Transformation of *A.tumefaciens* by electroporation

Aliquots (~100 µL) of *Agrobacterium* GV3101pMP90 competent cells were thawed on ice for 10 min. 1 µL of vector was added to one aliquot of cells and returned to ice. The mixture was transferred to a 0.2 cm electroporation cuvette and left on ice for 20 min. In the 5 °C constant temperature room the electroporator (BioRad Micropulser) settings were set for Agrobacteria to EC2 (2.5 kV and 5-6 ms). The cuvette was tapped on the bench top to ensure cells

settle at the bottom and placed in the cradle of the electroporator. The pulse button was pressed for 1 s so electricity was passed through the sample. Following electroporation, 1 ml LBB was added to the cuvette and mixed by pipetting. The cells were then transferred to a clean 1.5 ml Eppendorf and recovered for 3-4 h at 28 °C 200 rpm. 100 µL of bacteria were then added to LBA plates using a sterile plastic spreader inside a flow hood. 300 µL Gentamycin, 1200 µL Rifampicin and 300 µL of antibiotics specific to the vector used were added to every 300 ml of LBA. Plates were inverted and left at 28 °C for 3 days. The same selection was used for overnights of these cultures.

2.8 Protein manipulations

Recipes for solutions and buffers are found in appendix II.

2.8.1 Protein extractions from plants

150µL of protein extraction buffer was added to each sample in a 1.5ml Eppendorf. The sample was ground with a micropestle and kept on ice. It was centrifuged at 13200 rpm for 30 min at 4 °C. 80µL of the supernatant was mixed with 20µL protein loading dye and this was placed in a heat block at 95°C for 15 min. These samples could then be stored at -20°C for use in western blots. In addition, 4 µL of supernatant was added to 16 µL SDW and these samples were used to measure protein concentration.

2.8.2 Estimating protein concentration

Proteins were quantified using a Bradford Protein Assay. Known concentrations (0, 1.25, 2.5, 5, 10 ng/µL) of Bovine serum albumin were diluted in the same way as the proteins (by adding 4µL to 16µL of SDW), as a control. 3 x 4µL of the diluted controls/samples were pipetted into a 96 well plate. A spectrostar nanostar spectrophotometer was used to quantify the protein at 595nm optical density. Microsoft Excel was then used to get an average reading for each sample and comparing to the BSA control standard curve. Using this we could calculate how much protein sample to load in the Western Blot.

2.8.3 Sodium dodecyl sulphate - Polyacrylamide gel electrophoresis (SDS-PAGE)

Proteins were analysed by SDS-PAGE using BioRad self-assembly kits. Gels were made according to the table in appendix IV. Most of the time a 10 % gel was chosen. The gel was held between two pieced of glass and was 1mm thick. A 10 or 15 well comb was used. The running gel was pipetted between the glass, levelled with saturated butanol and allowed to set. Then the stacking gel was pipetted on top, the comb inserted and allowed to set. If the gel was not used immediately it was stored at 5 °C in damp tissue and wrapped in cling film. Proteins to be loaded were mixed with 5 x protein loading buffer with β-mercaptoethanol and heated to 95 °C for 5 min prior to loading. 5 µL of protein ladder and the calculated amount of sample were loaded into the gel. Gels were run in Tris-glycine SDS (TGS) buffer (100 ml of 10 x TGS, 900 ml SDW) at 120 V for 2 h.

2.8.4 Western Blotting

2.8.4.1 Protein transfer

The gel was removed from the glass and the stacking gel was cut off the top. The gel was then placed onto Whatman™ blotting paper that had been soaked in Tris-glycine (TG) transfer buffer. Polyvinylidene difluoride (PVDF) transfer membrane (Hybond-P, Sigma-Aldrich) was dipped into methanol then SDW and placed on top of the gel, making sure the gel was covered. The gel and membrane were then covered with another piece of soaked blotting paper, sandwiched between two electroblotting pads (BioRad) and held in a plastic case. This was put in an electroblotting tank (BioRad) with a block of

ice. The tank was filled with TG buffer (200 ml of 10 x TG, 400 ml methanol, 1400 ml SDW) and the gel was transferred to the membrane at 80 V for 2 h using BioRad powerpacks. The membrane was then removed and washed with milk wash solution (25 g Marvel milk powder, 500 ml Phosphate buffered saline (PBS), 500 µL Tween) for 1-2 h at 4 °C to block the membrane.

2.8.4.2 Antibody probing

The solution was removed, and 10 ml milk wash solution added to the membrane with the appropriate amount of primary antibody and rocked overnight at 4 °C. The antibodies and amounts used are shown below.

αHA mouse (Sigma)	1:10000
αFLAG mouse	1:1000
αGFP rabbit	1:2000

The primary antibody mix was removed, and the membrane was washed three times with milk wash solution for 10 min. 10ml milk wash solution was added to the membrane along with 1 µL of the secondary antibody (HRPα Mouse/Rabbit at a 1:10000 dilution) and rocked for 1 h at RT. The membrane was washed three times with a mix of 500ml 10% PBS and 500µL 1% Tween for 5 min.

2.8.4.3 Enhanced chemiluminescence (ECL) detection

A 50/50 mix of western blot substrate (Thermofisher) was made and 2ml added to cover each membrane to detect the secondary antibody. The membrane was placed face down on flat acetate with no creases or air

bubbles. This was taped into place in a cassette and developed in the dark room onto photographic film (Hyperfilm-ECL, Sigma-Aldrich). Developing times varied according to the strength/quantity of protein and ranged from 5s to 20min. Images were then scanned and analysed using Quantity One software (BioRad). Wherever comparisons of protein levels were determined, blots were exposed for the same length of time.

2.8.4.4 Coomassie blue staining

In a plastic dish Coommasie blue was poured to cover the membrane and washed for 20 min. This was tipped off and a destain added to cover the membrane and washed for 10 min on a tilting machine. The membrane was then left to air dry. The membranes were scanned and analysed using Quanity One software (BioRad).

2.8.5 *in vitro* protein degradation assay

The Rabbit Reticulocyte Lysate System (Promega L4960 and L4151) was used for the expression of the cloned gene of interest *in vitro*. For one reaction a mix of 12.5 µL Rabbit reticulocyte, 1 µL buffer, 0.5 µL T7 polymerase, 0.25 µL leucine AA, 0.25 µL methionine and 0.5 µL RNase OUT were used. 15 µL of this mix was added to 10 µL of the DNA sample (the pTNT™ containing the gene of interest fused to HA). Reactions were incubated at 30 °C for 30 min. To stop the reaction 1 µL cyclohexamide (CHX) 2.7 nM was added. 1 µL bortezomib was added (at the same time as CHX) as a control to inhibit the 26S proteasome, otherwise 1 µL SDW was added. Samples were kept at 30 °C and 6 µL was taken every 30 min (or every hour)

and added to protein loading buffer containing β-mercaptoethanol, mixed gently and kept on ice. 10 µL of these samples would then be loaded onto the SDS-PAGE gel and analysed using western blotting.

2.9 Microscopy

2.9.1 GUS staining

2.9.1.1 Staining

12ml of GUS stain solution was made. To this 12 µL (1/100) of 100 mM potassium ferricyanide and 12 µL (1/100) of 100 mM Potassium ferrocyanide was added fresh. 1 ml of the GUS staining mixture was added to each well of a 12 well plate. 3 seedlings were placed in each well and then left to stain in the dark at 37 °C for 4 h and 24 h.

2.9.1.2 Clearing and fixing

The GUS staining mixture was removed from the seedlings by pipette and 1 ml of fixative was added. The seedlings were left overnight on a rotary tilter at RT in natural light conditions. This process was repeated for 3-5 days until it was considered to be an appropriately cleared. The fixative was removed by pipette and 1 ml 50 % glycerol was added to cover the seedlings. The seedlings were then put on a glass slide in glycerol with a large cover slip. The seedlings were imaged using LAS EZ software.

2.9.2 Imaging YFP lines by confocal microscopy

Seedlings were grown on ½ MS for 3-5 days and placed on a slide with a coverslip in water. Immersion oil was put onto the slide. Seedlings were then viewed under the confocal microscope (Dig Sci DLight 2000 and Olympus BxUCB) to visualise the expression of *VRN2-YFP* in Col-0 and *prt6-1* backgrounds under the YFP excitation wavelength of ~514nm. Propidium

iodide was used to stain the cell walls. Smart capture software was used to take stacks of the seedlings and to edit the images.

2.10 Appendix I - growth media

Bacterial growth media

LB broth

10 g/l tryptone

5 g/l yeast extract

10 g/l NaCl

LB agar

LB broth plus 15 g/l agar

Bacteria and Plasmid Selection

50 µL/ml Kanomycin was used with pDONR221 and pDEX.

50 µL/ml Zeomycin was used with pDONRzeo (which was needed for entry into pDEX to avoid entry and destination vector having the same selection).

50 µL/ml Spectinomycin was used with Ω35s, per8GW and PUBC.

For *A. tumefaciens* 300 µL Gentamycin, 1200 µL Rifampicin and 300 µL of antibiotics specific to the vector used were added to every 300 ml of LBA.

50 µg/ml rifampicin for *A. tumefaciens*

50 µg/ml gentamycin for *A. tumefaciens*

50 µg/ml Streptomycin for DB3.1 cells

50 µg/ml Tetracyclin for ABLE® K cells

50 µg/ml for pTNT vector

Plant medium

½ Murashige and skoog (MS) agar

To make 1% plates:

1 litre of Sterile distilled water (SDW)

2.2 g Murashige & Skoog (MS) powder.

pH 5.7 with either 0.5 M HCL or 0.5 M KOH

10 g of agar

The mixture was then autoclaved and, once cool, it was poured into square Petri dishes to approximately 7.5 mm depth, inside a fume hood.

Plant Selection

0.7 % plates of Hygromycin ½ MS:

600 ml SDW,

1.32 g MS powder

4.2 g agar

600 µL Hygromycin to cooled media.

2.11 Appendix II - general solutions

Nucleic acid gel electrophoresis solutions

DNA loading buffer

40 % (v/v) glycerol

0.25 % bromophenol blue

5 x TBE buffer

0.45 M Tris

0.45 M Orthoboric acid

12.5 mM EDTA

Competent *E.coli* cell solutions

Tfb1

30 mM potassium acetate
10 mM rubidium chloride
10 mM Calcium chloride
50 mM Manganese chloride
15 % (v/v) glycerol
pH 5.8

Tfb2

10 mM MOPS
75 mM Calcium chloride
10 mM Rubidium chloride
15 % glycerol
pH 6.5

Protein electrophoresis and Western blotting solutions

5 x SDS loading dye

67.5 % (v/v) Tris-HCl (2M, pH 6.8)

10 % (w/v) SDS

50 % (w/v) glycerol

5 % β-mercaptoethanol

0.005 % (w/v) bromophenol blue

Protein transfer buffer

25 mM Tris

190 mM glycine

20 % methanol

pH8

Milk wash solution

500 ml SDW

5 x PBS tablets

25 g Marvel milk powder

500 µL Tween

Coomassie stain

0.1 % coomassie blue R-250

45 % (v/v) SDW

45 % (v/v) methanol

10 % glacial acetic acid

Coomassie destain

30 % (v/v) methanol

10 % (v/v) glacial acetic acid

Biochemistry solutions

Protein inhibitor cocktail (PIC)

1 x PIC tablet (Roche)

1.5 ml SDW.

Protein extraction buffer

150 µL PIC

100 µL 10% SDS

50 µL Tris-HCl pH7.5

700 µL SDW

GUS Staining solutions

GUS stain solution

Mix 3.9 ml of 1 M Monosodium phosphate (A) and 6.1 ml of M Disodium phosphate (B) at a ratio of 39:61 (A: B). Add 90 ml of SDW to get 100mM of buffer pH7. Add 0.104 g of X-Gluc (5-bromo-4-chloro-3-indoyl-beta-D-glucuronic acid) substrate and vortex until completely dissolved. Add 0.1 % (v/v) Triton X-100 by pipette and invert until completely mixed.

Fixing solution

37.5 ml 100 % ethanol

12.5 ml 100% glacial acetic acid

500 µL Tween

2.12 Appendix III - PCR primers

GENOTYPING

vrn2 F	GTTTGTTCATCATGACACCCC
vrn2 R1	TTTGAGTCACTGGGATGATCC
vrn2 SALK LBb1.3	ATTTTGCCGATTTCGGAAC
prt6 F	GGAGTTTTCTATGTCCAGTGAGAGTTT
prt6 R	GTCTCCAATGACACGTTCACTTGTCT
prt6 BP	GCCTTTTCAGAAATGGATAAATAGCCTTGCTTCC
prt6 F2	AGTGGTTGAAATGCTTCTGGA
prt6 R2	AACTCCCGGTGTTCATGTGT
FRI_SF2_F	AGATTTGCTGGATTTGATAAGG
FRI_SF2_R	ATATTTGATGTGCTCTCC
vin3 F	ATGCAAGCTGCTTCGCTCTC
vin3 R	ATGCCAAAGCTTGAGGCAG

CDNA ANALYSIS

vrn2 start	ATGTGTAGGCAGAATTGTCGCGCG
vrn2 stop	TTACTTGTCTCTGCTGTTATTGTCC
prt6 start	ATGGAGACCAACTCTTCTCTTTTT
prt6 stop	TTAATGTAAGACGGCTCCAATTGTG
VIN3START	ATGAAGCTGCTTCGCTCTC
VIN3STOP	ATGCCAAAGCTTGAGGCAG

actin2F	ATGGCTGAGGCTGATGATATTC
actin2R	AGAAACATTTTCTGTGAACGATTC
ACTIN7_F	CTGGAATGGTGAAGGCTGGT
ACTIN7_R	GTGCCTAGGACGACCAACAA

VRN2_YFP_F	AGTCGATGACGATGTTGCAG
VRN2_YFP_R	TGGTGCAGATGAACTTCAGG
YFP_F	CCTGAAGTTCATCTGCACCA
YFP_R	GTTCACCTTGATGCCGTTCT
VRN2_GUS_R	TCATTGTTTGCCTCCCTGCT
GUS_R	TGCCCAACCTTTCGGTATAA
VRN2_HA_R	ATAGGATCCTGCATAGTCCG

CLONING

vin3attb1	GGGGACAAGTTTGTACAAAAAAGCAGGCTGGATGCAAGCTGCTTC
vin3attb2	GGGGACCACTTTGTACAAGAAAGCTGGGTCATGCCAAAGCTTGAG
vin3HAattb2	GGGGACCACTTTGTACAAGAAAGCTGGGTCGGCGTAGTCGGGCAC
vin3R1HA	GGCGTAGTCGGGCACGTCGTAGGGGTAATGCCAAAGCTTGAGGCA
HVEMF2C_MCF	AAAAGAATTCATGTGCCGTCAACCGTCCACGCC
HVEMF2C_MAF	AAAAGAATTCATGGCCCGTCAACCGTCCACGCC
HVEMF2C_R	AAAAGGTACCGTACTGTCGGCGGTGTAAGATTGC

EMF2_MP_F	AAAATGCCAGGCATTCCTCTTGTTAGTCGTG
EMF2_MC_F	AAAATGTGCGGCATTCCTCTTGTTAGTCGTG
EMF2_TRUNCMC_F	AAAAGAATTCATGTGCCATGAAGACTCCCGTC
EMF2_TRUNCMA_F	AAAAGAATTCATGGCCCATGAAGACTCCCGTC
EMF2_R	AAAAGGTACCAATTTGGAGCTGTTCGAGAAAGG

SEQUENCING

vin3 seqR1	AAGCATCACAAGTAAGCCATAAACT
vin3 seqF1	GCTTGTAGAGCTGCGCTTG
vin3 seqF2	CCGTGAGAGTAGAAGAGATTCAAG
vin3 seqF3	AAAGCAAGGAGGGAATAAAAGATT
attb seq F	AAGTTTGTACAAAAAAGCAGGC
attb seq R	ACTTTGTACAAGAAAGCTGGG
M13 F	GTAAAACGACGGCCAG
M13 R	CAGGAAACAGCTATGAC
pTNTF	TAAGGCTAGAGTACTTAATAC
pTNTR	CCCCAAGGGGTTATGCTA

RESTRICTION
ENZYME SITES

MluI	ACGCGT
XbaI	TCTAGA
EcoRI	GAATTC
KpnI	GATATC
BsrGI	TGTACA

2.13 Appendix IV - preparation of SDS-PAGE gels

	Running gel			Stacking gel	
	10%	12%	15%		
SDW	4ml	3.3ml	2.3ml		3.4ml
Acryl/Bisacryl	3.3ml	4ml	5ml		0.83ml
Tris pH8.8	2.5ml	2.5ml	2.5ml	Tris pH6.8	0.63ml
SDS (10%)	0.1ml	0.1ml	0.1ml		0.05ml
APS (10%)	0.1ml	0.1ml	0.1ml		0.05ml
Temed	4uL	4uL	4uL		5uL

Chapter 3

Investigating the relationship between the N-end Rule Pathway and VRN2 Function

3 Investigating the relationship between the N-end Rule Pathway and VRN2 Function

3.1 Introduction

This project focuses on the post-translational modifications of proteins that control protein stability or degradation. As discussed earlier, the N-end rule pathway of targeted proteolysis is a specific branch of the ubiquitin proteasome system that targets proteins for destruction based on the nature of their N-terminus (the N-degron) (Bachmair et al., 1986). The N-terminus (Nt) can contain stabilizing or N-degron destabilizing amino acid residues (Varshavsky, 2005). The project focuses on cysteine as a destabilizing residue in proteins that begin with MC, that are the basis of the MC/Arg N-end rule pathway (FIGURE 1.6).

It has previously been shown in animals and plants that the “Cys-Arg/” branch of the N-end rule pathway plays a key role in oxygen and nitric oxide (NO) sensing, through controlling the stability of proteins that initiate with the residues ‘Met-Cys’ (MC) (Kwon et al., 2002, Hu et al., 2005, Gibbs et al., 2011, Licausi et al., 2011, Gibbs et al., 2014). In plants, the only confirmed substrates of this pathway are the ERFVII transcription factors, which regulate the homeostatic transcriptional response to oxygen and NO availability (Gibbs et al., 2011, Licausi et al., 2011, Gibbs et al., 2014a). Under hypoxic or reduced NO conditions, Cys oxidation does not occur and thus ERFVIIs accumulate to initiate the low-oxygen transcriptional response. In this study it was hypothesized that there may be other MC-initiating proteins in plants that

are regulated by the Cys/Arg N-end rule pathway that may also act as oxygen and NO sensors.

Su(z)12 is a PRC2 protein, identified in *Drosophila*, that epigenetically regulates gene expression (Birve et al., 2001). Arabidopsis VRN2 is a homologue of Su(z)12, containing the zinc finger domain for epigenetic gene suppression (Gendall et al., 2001). MC-initiating Su(z)12 homologues (i.e. VRN2-like proteins) throughout the flowering plant lineage were identified by comparing all proteins that begin with MC. These VRN2 orthologous sequences were aligned using Clustal Omega (FIGURE 3.1) and this was used to form a probability plot (FIGURE 3.2). From the alignments and probability plot it was observed that the MC N-terminus was highly conserved. More than 200 proteins have been found in *Arabidopsis* that have MC at the N-terminus (Gibbs et al., 2011) and of these, VRN2 was identified as an interesting potential candidate to be a substrate of the Cys/Arg N-end rule pathway as it has a role in vernalization and the control of flowering. This is because the MC N-terminus is evolutionally conserved and therefore of biological significance. There is also a highly conserved lysine at amino acid 26 that could be a further indication that VRN2 may be a substrate of the N-end rule because this could be ubiquilylated by the E3 ligase PRT6. The MC terminus would also have to be accessible by the N-recognin for VRN2 to be a substrate. VRN2 has previously shown to be degraded in an N-end rule system *in vitro* (Gibbs et al., 2011). The main purpose of this project was to test whether VRN2, and its homologues in plants, are *in vivo* gas sensors

regulated by the Cys/Arg N-end rule, linking stress perception to flowering and developmental control.

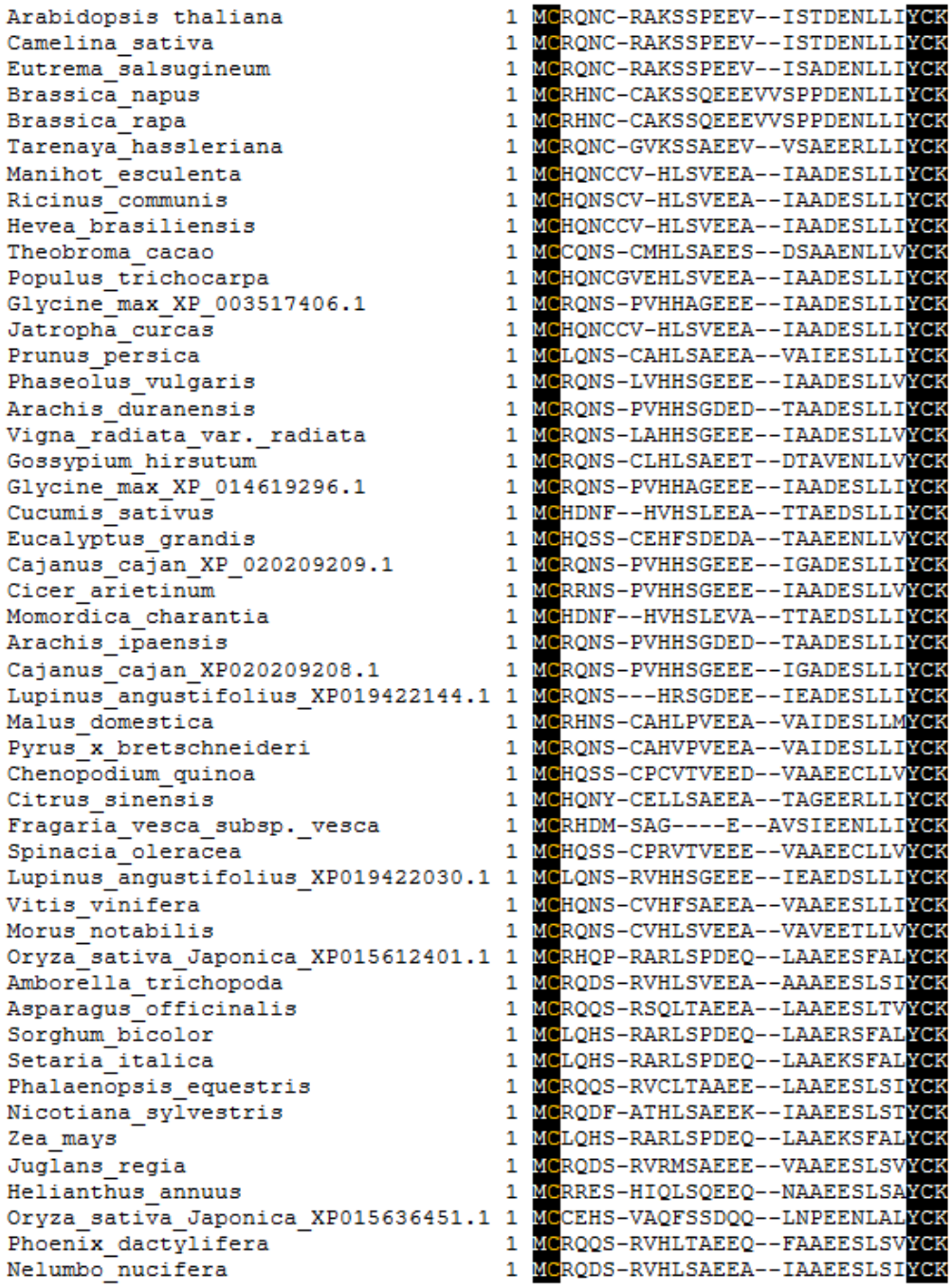

FIGURE 3.1 Alignment of VRN2 orthologous sequences representing diverse clades of flowering plants.

Alignment of 49 VRN2-like proteins highlights the conserved MC N-terminus (Nt) (cysteine shown in yellow) and also a conserved lysine residue a short distance from the N-terminus where proteins could potentially be ubiquitylated. (Sequences obtained from the 1KP initiative. Alignments made with Clustal Omega.)

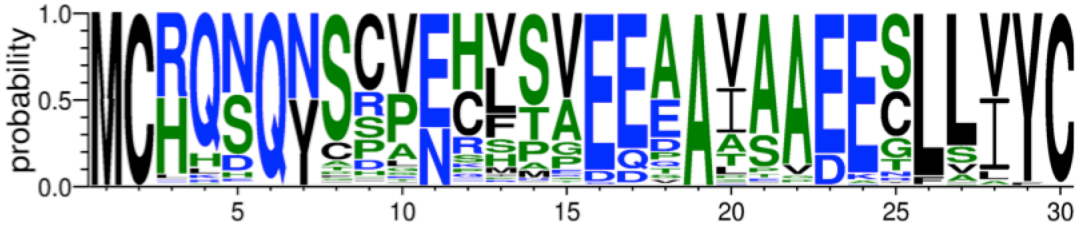

FIGURE 3.2 MC is conserved across angiosperms in VRN2-like proteins

Sequence logo of the N-terminal region of VRN2-like proteins from all sequenced flowering plants shows 100% conservation of the N-terminal MC dipeptide. (Sequences obtained from the 1KP initiative.) There is also a conserved Lysine residue at amino acid position 26 where the proteins could potentially be ubiquitylated. Image generated using Weblogo.

3.2 Confirmation of VRN2 as an N-end rule substrate *in vitro*

To confirm the hypothesis that VRN2 is regulated by the N-end rule pathway as observed in Gibbs et al., (2011), a rabbit reticulocyte lysate system was used (Lee et al., 2005) that contains all the components needed for transcription and translation of the *VRN2* gene (tRNA, ribosomes, amino acids, initiation, elongation and termination factors). Components of the N-end rule such as ATE, MAP and E3 ubiquitin ligases are conserved in eukaryotes (Graciet et al., 2010) and so they are present in the system. Rabbit lysate was chosen as wheat germ lysate has been shown to not contain an active proteosomal system (Takahashi et al., 2009). *VRN2* was cloned by ligation into the pTNT vector with a haemagglutinin (HA) tag at the C-terminus. The pTNT vector was chosen as it is designed for highly efficient synthesis of RNA using *in vitro* expression systems and it has a T7 polymerase promotor adjacent to the multiple cloning site. *E.coli* DH5α that had the vector containing the gene were selected for with Ampicillin. The plasmids were then used in an *in vitro* protein degradation assay (FIGURE 3.3). The reactants were incubated for 30 min and then cyclohexamide was added to all samples to block further translation of the gene. VRN2 stability was then measured by taking samples over a time course (0, 30 and 90 min). From an anti-HA western blot of the *in vitro* samples it was observed that WT MC-VRN2-HA levels decrease over time following CHX treatment, whereas if bortezomib was added, which inhibits the 26S proteosome, it was observed that MC-VRN2-HA is stabilized. Lee et al. (2005) used a C2A point mutation in mammalian RGS proteins; the N-degron is removed and so the substrate of

the N-end rule pathway is stabilized. It is confirmed in this study that the instability of VRN2 is related to its N-terminus because a C2A point-mutation (i.e. MA-VRN2-HA) led to constitutive stabilization of VRN2 to similar levels as were observed for the bortezomib treatment. The Coomassie stain of the membrane shows that there was even loading, therefore the difference in protein level is due to degradation of protein and not how much protein was loaded onto the blot. This supports our hypothesis that VRN2 is a substrate of the N-end rule pathway and that it is regulated in the same way as the ERFVII transcription factors. The next step was to confirm further that it is a substrate by observing VRN2 stability *in vivo* and looking at VRN2 stability in different mutant backgrounds (*prt6* and *ate1ate2*) that are components of the Cys/Arg N-end rule pathway.

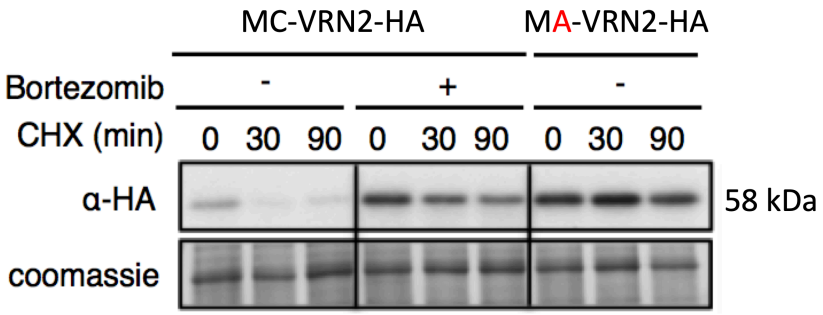

FIGURE 3.3 VRN2 is a substrate of the Cys/Arg N-end rule pathway *in vitro*

Western blot showing an *in vitro* cyclohexamide (CHX) chase of WT MC-VRN2-HA and mutant (Ala2) MA-VRN2-HA (+/- bortezomib; BZ). MC-VRN2-HA is degraded over time whereas MA-VRN2-HA is stable. Bortezomib causes MC-VRN2 HA to become stable. Coomassie blue staining was used as a loading control.

3.3 Confirmation of VRN2 as an N-end rule substrate *in vivo*

WT MC-VRN2-HA was degraded *in vitro* over a 90 min time course, whereas MA-VRN2-HA was stable, but was this the case in vivo? It had previously been shown that VRN2-FLAG was unstable following CHX treatment in transgenic Arabidopsis seedlings but was stable following treatment by bortezomib (Gibbs et al., 2018). This indicated that *in vivo*, VRN2 protein degradation was regulated by the 26S proteasome. To confirm whether the protein stability was linked to the N-end rule pathway, *Arabidopsis* lines that have *VRN2* fused to β-glucuronidase (GUS) at the C-terminus driven by approximately 2 kb of its native promotor were generated. Two independent plant lines were generated in the *prt6-1* E3 ligase mutant and the *ate1ate2* mutant by crossing the *VRN2-GUS* transgene into the mutants. (Two independent lines would provide more conclusive evidence than a single line.) In addition, MC-VRN2 and MA-VRN2 stability was studied by creating transgenic plants in the Col-0 background of VRN2 fused to GUS with either the MC or MA N-terminus. Plants were grown for 7 days and protein extracts were prepared. From performing an anti-GUS western blot, it was observed that steady state levels of MA-VRN2-GUS were higher than MC-VRN2-GUS in Col-0 (FIGURE 3.4). This is in agreement to the *in vitro* results, which indicates the importance of the Cysteine as a tertiary destabilizing residue at the N-terminus and the presence of cysteine as a requirement of Cys/Arg N-end rule substrates. In *ate1ate2* mutants VRN2-GUS was more stable than MC-VRN2-GUS in Col-0. This is what is expected if VRN2 were a substrate of the N-end rule, as the *ate1ate2* mutants lack the ability to arginylate the N-

terminal oxidized Cys. VRN2 would therefore not be recognized by the N-recognin and would not be able to be ubiquitylated and targeted for degradation. In the *prt6-1* E3 ligase (N-recognin) mutant, WT VRN2-GUS was also significantly more stable than WT. This links the degradation of VRN2 directly to PRT6, as expected for a target of the Cys/Arg N-end rule. Coomassie staining showed equal protein loading and there were no significant differences in mRNA levels between WT and the other backgrounds. Taken together, these results support the hypothesis that VRN2 is regulated *in vivo* by the Cys/Arg N-end rule pathway.

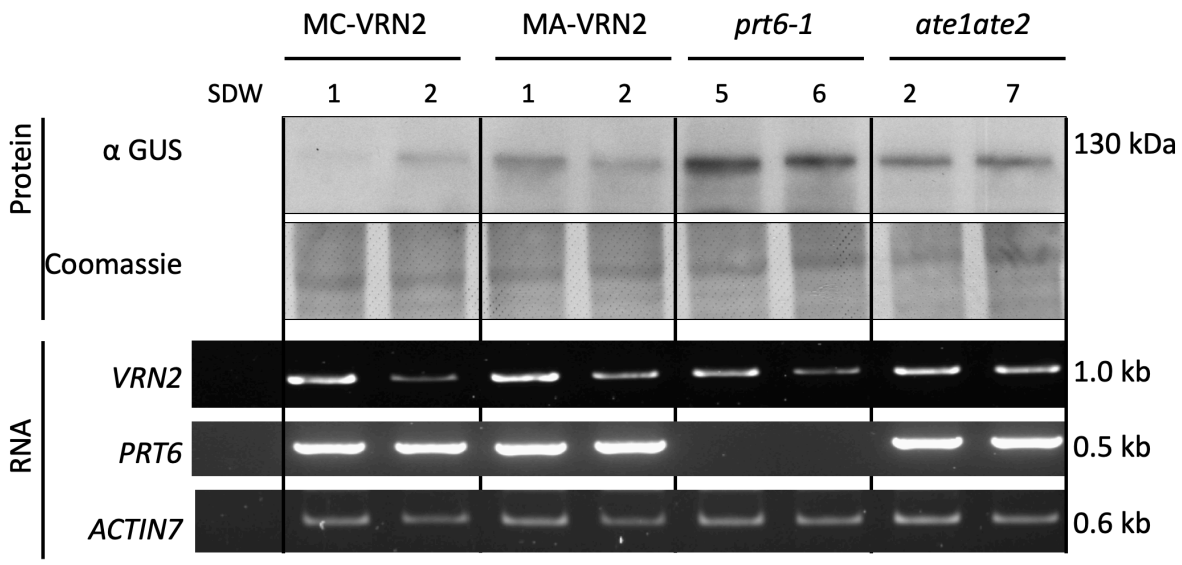

FIGURE 3.4 MC-VRN2-GUS stabilization *in vivo*

Western blot showing that MC-VRN2-GUS is unstable, whereas MA-VRN2-GUS is more stable. MC-VRN2-GUS is stable in *prt6-1* and *ate1ate2*, Coomassie staining shows equal loading. Numbers (1+2, 1+2, 5+6, 2+7) denote names of two independent lines of each genotype tested.

PCR of cDNA synthesized from total RNA extractions shows transcription of *VRN2* is similar between lines (although this is semi-quantitative as it is not qPCR). There is no *PRT6* transcript in the *prt6-1* mutant and *ACTIN7* is used as a control.

To provide further evidence linking VRN2 stability to the N-end rule, histochemical staining of VRN2-GUS was performed, in order to visualize the spatial distribution of VRN2 stability in the different N-end rule mutant backgrounds. Seedlings were grown for 7 days and histochemically stained for GUS activity for 4 h and 24 h before fixing onto glass slides (FIGURE 3.5). In MC-VRN2-GUS Col-0 seedlings there was a lot less staining overall compared to the other lines and WT VRN2-GUS protein in Col-0 was restricted to the meristem and vasculature. This indicates that VRN2 is present at low levels in the seedlings except for the shoot meristem and the root tip. The meristems are thought to be areas of the plants that have low levels of oxygen (hypoxic) (Considine et al., 2017). If VRN2 is regulated by the N-end rule pathway, the gas-sensing step of the pathway would not be able to occur in these tissues and so VRN2 would be stable, which agrees with the results. In the MA-VRN2-GUS plants the staining is darker than in MC-VRN2-GUS and in the *ate1ate2* and *prt6-1* backgrounds staining is darker than the other lines, showing strong stabilization and accumulation of VRN2-GUS present in all tissues throughout the seedling. These results confirm the observations made by western blotting, supporting the hypothesis that VRN2 is regulated *in vivo* by the Cys/Arg N-end rule pathway. Furthermore, the distribution of the staining suggests that the N-end rule pathway restricts VRN2 to meristematic regions under normal growth conditions.

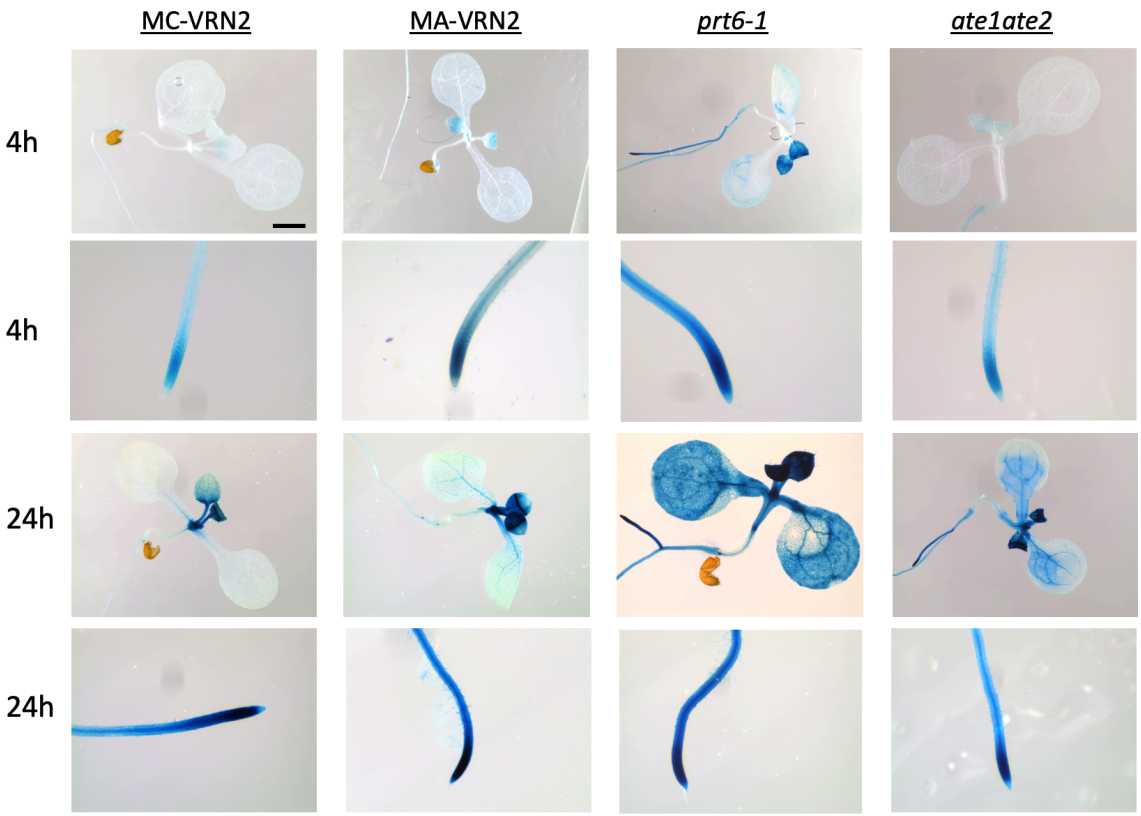

FIGURE 3.5 VRN2 is unstable in MC-VRN2-GUS except in the vasculature and meristem

Histochemical staining of 7-day-old seedlings expressing MC-VRN2-GUS in Col-0, mutant (Ala2) VRN2-GUS in Col-0 and MC-VRN2-GUS in *prt6-1* and *ate1ate2*. Stained for 4h and 24h. Images are representative of three repeat experiments. Scale bar 500μm.

3.4 VRN2 subcellular localization

Results so far indicate that VRN2 is a substrate of the N-end rule pathway when using C-terminal HA and GUS tags attached. To provide further evidence, yellow fluorescent protein (YFP) fusions were used to confirm VRN2 as a substrate of the N-end rule pathway and to visualize the localization of VRN2 in the cell. PcG proteins share a conserved region in the N-terminus that contains a putative nuclear localization signal (NLS) and VRN2 has been found to be distributed unevenly in the nucleus but not throughout the nucleus (Gendall et al., 2001). Therefore, more work needs to confirm if it is only nuclear localized and whether the NLSs are functional. Gendall et al. (2001) used an Nt GFP::VRN2 fusion (instead of GFP fused to the C-terminus) so it is not known if this is actually true localization because the N-terminus has been altered, Further, the N-terminal residue of the protein would not have N-end rule regulation unless the GFP was cleaved. ERFVIIs are known to move between the cytosol and the nucleus (Licausi, 2011, Kosmacz et al., 2015), providing additional justification to study subcellular localization of VRN2. VRN2 has also been found to interact with LIKE HETEROCHROMATIN PROTEIN 1 (LHP1) in the nucleoplasm *in vivo* (Hecker et al., 2015). However, not a lot is known about the subcellular localization of VRN2 during its entire presence from translation to degradation. The work of Sung and Amasino (2004a) shows that VRN2 represses transcription of *FLC* by chromatin modification, which is also consistent with VRN2 nuclear localization.

To conduct the VRN2 localization experiment Col-0 and *prt6-1* lines were transformed with the MC-VRN2 fused to yellow fluorescent protein (YFP), driven by VRN2's native promotor. Homozygous transformed lines were identified by selection with hygromycin. Seeds from the T3 lines with 100% germination were used in this experiment.

Western blotting (FIGURE 3.6 A) confirms expression of the VRN2-YFP fusion protein and again indicates that there are higher levels of MC-VRN2-YFP protein in the *prt6-1* mutant than in Col-0. Ponceau staining of the membrane shows there was equal loading of the proteins. This is consistent with the earlier western blot results of VRN2-GUS (FIGURE 3.4) and also with the hypothesis that VRN2 is a substrate of the N-end rule because the *prt6-1* mutant lacks the E3 ligase cannot ubiquitylate VRN2 and so it is not labelled for destruction by the 26S proteasome.

Confocal microscopy was used to visualize the localization of VRN2 in the roots of the MC-VRN2-YFP WT and *prt6-1* lines. VRN2 was found to be localized in the nucleus of all root tips (FIGURE 3.6 B). VRN2 is known to put the H3K27me3 epigenetic mark onto chromatin (De Lucia et al., 2008) so it was expected that VRN2 would be a nuclear protein. VRN2 was also found in some nuclei further up the root (in the region of maturation) and on some images, it was observed that VRN2 was also cytosolic (FIGURE 3.6 B). The PCOs and the proteasomes are also found in the cytosol as well as the nucleus (Weits et al., 2014) and so it follows that VRN2 could be present in both also. However, this result was not conclusive, and one reason could be

because the Propidium iodide (PI) that was used to stain the cell walls emits light at ~625nm a similar wavelength to YFP at ~525nm and there could be some overlap of their emission wavelengths. It is therefore difficult to distinguish whether the emission is due to VRN2 being present in the cell wall, in the cytosol or whether it is actually due to the PI. This will need to be repeated by looking at seedlings with no PI staining and perhaps seedlings that have had their cells plasmolyzed so the cytosol would not be against the cell wall, or another option would be to separate protein from nuclear and cytosolic fractions and perform a western blot in order to detect VRN2-YFP (Kim and Michaels, 2006). If VRN2 present in the nucleus and cytoplasm it could mean that at different stages of development VRN2 may be in the PRC2 complex in the nucleus and at other times VRN2 may be free to move through the cell. VRN2 may therefore have other functions outside of the PRC2 complex that have not yet been discovered.

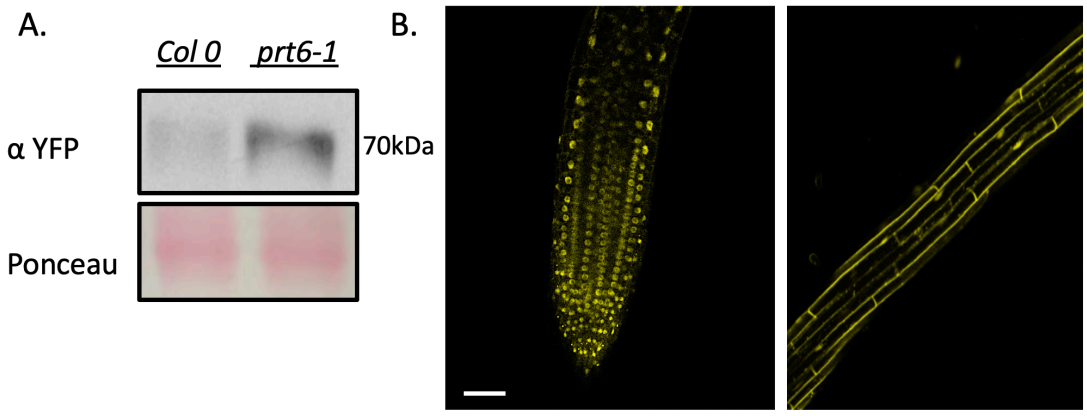

FIGURE 3.6 VRN2 is found in the nucleus

(A) Western blot showing steady state MC-VRN2-YFP protein levels in Col-0 and *prt6-1*. MC-VRN2-YFP is unstable in Col-0 whereas it is stabilized in the *prt6-1* mutant. Ponceau staining of the membrane shows equal sample loading.
(B) Confocal image showing MC-VRN2-YFP is localized to the nucleus in root tips of Col-0 and *prt6-1* plants. Further up the root, in the region of maturation, VRN2 appears to be cytosolic as well as in the nucleus. Scale bar 50μm.

3.5 When is VRN2 stable?

This study has shown that VRN2 is a substrate of the N-end rule pathway *in vivo* and that it can be found in the meristem and vasculature of seedlings and in the nucleus at the root tip under normal growth conditions (22 °C 16 h L: 8 h D). The next step was to find out when VRN2 is expressed and when VRN2 would be degraded or stabilized throughout the development of the plant. It is known that VRN2 becomes stabilized in the cold during vernalization (Wood et al., 2006). It was hypothesized that this cold-induced stabilization was related to the N-end rule. To test this hypothesis, the MC-VRN2-YFP transgenic WT and *prt6-1* lines were used. Seeds were cleaned, plated and stratified for 2 days at 5 °C. Seedlings were then grown for 10 days at 22 °C 16 h light (L), 8 h dark (D). Seedlings were then placed in vernalization conditions (5 °C, 8 h L: 16 h D) and seedlings were sampled over a time course of 0, 2, 4 weeks vernalization and also 4 weeks vernalization followed by 1 week back at 22 °C. Total protein was extracted from the samples and quantified using a Bradford assay. Western blotting showed VRN2 protein levels became more abundant with increased vernalization time in WT plants (FIGURE 3.7). MC-VRN2-YFP levels appeared low at 0 weeks, as there was a very faint band present. At 4 weeks, protein levels had increased, and a strong band could be observed. When plants were returned to 22 °C VRN2 levels were depleted. VRN2 levels in the *prt6-1* seedlings were higher than in WT at 0 weeks showing a similar level to 4 weeks in WT seedlings. There is a slight increase in VRN2 levels at 2 and 4 weeks and then at 4 + 1 weeks VRN2 levels deplete in a similar way to WT. This could mean that there is an

E3 ligase (other than PRT6) yet to be found that is able to ubiquitylate VRN2, leading to its degradation. The Coomassie stain of the membrane shows equal loading on the blot. The RT-PCR indicates the *prt6-1* mutant is not expressing *PRT6* and the *ACTIN2* control shows that cDNA levels are consistent between lines. Gendall et al. (2001) found *VRN2* gene expression is not altered by vernalization but it might be a low abundance transcript or expressed in a small subset of cells. The RNA analysis in this experiment also shows that VRN2 protein accumulates during vernalization in the absence of changes in mRNA levels, therefore transcription remains fairly constant throughout and it is the protein levels that are changing. This is consistent with the hypothesis that VRN2 protein is stabilized post-translationally in an N-end rule dependent manner during vernalization.

These data using MC-VRN2-GUS and MC-VRN2-YFP confirm similar results obtained using MC-VRN2-GUS, (data not shown); that VRN2 in *prt6-1* is constitutively stable and does not change in response to cold treatments, suggesting that the N-end rule acts to restrict VRN2 protein localization to the meristem and vasculature under non-vernalized (warm) conditions. The spatial stabilisation of VRN2 protein during cold is opposite to that that seen for *FLC* promoter activity (Kim and Michaels, 2006), which correlates with its known function in the maintenance of reduced *FLC* expression. As it has now been shown that VRN2 is stabilized in an N-end rule dependent manner and that VRN2 levels increase in the cold, it was decided to investigate further, the functional relevance of this regulation in relation to flowering and stress responses.

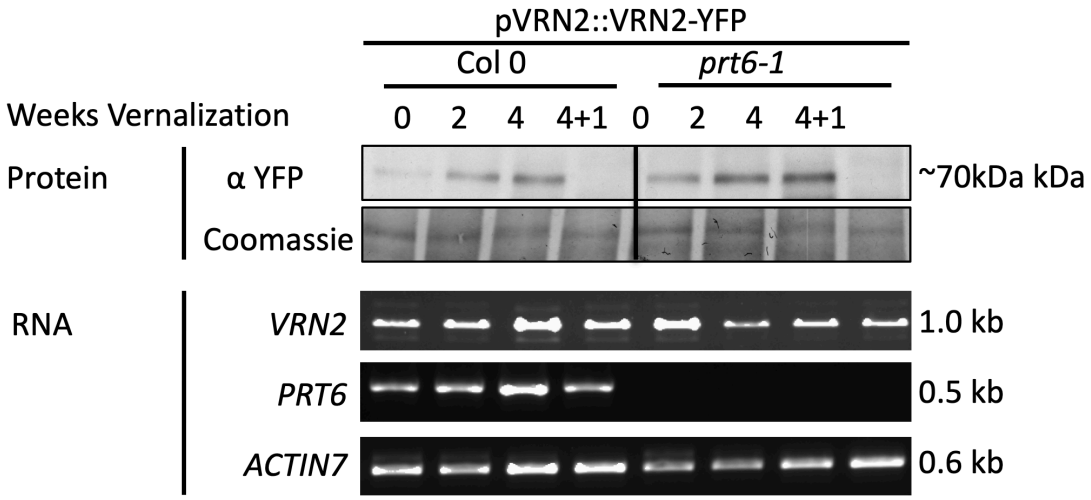

FIGURE 3.7 VRN2 becomes stable with increased vernalization but is degraded when returned to optimal growing conditions

Western blot showing VRN2-YFP stabilization and mRNA levels of WT VRN2-YFP in vernalized Col-0 and *prt6-1* seedlings. MC-VRN2-YFP transgenic WT and *prt6-1* lines were used. Seeds were cleaned, plated and stratified for 2 days at 5 °C. Seedlings were then grown for 10 days at 22 °C 16 h light (L), 8 h dark (D). Seedlings were then placed in vernalization conditions (5 °C, 8 h L: 16 h D) and seedlings were sampled over a time course of 0, 2, 4 weeks vernalization and also 4 weeks vernalization followed by 1 week back at 22 °C. 4+1 refers to 1 week 'recovery' at 22°C following vernalization. VRN2 becomes stable with increased vernalization at 5 °C 8 h light: 16 h dark but is depleted on return to 22 °C 16 h light: 8 h dark. PCR of cDNA synthesized from total RNA extractions shows transcription of *VRN2* is similar between lines.

3.6 Functional relevance of VRN2 regulation by the N-end rule pathway

The next aim of the project was to explore how regulation of VRN2 by the N-end rule pathway contributes to the known function of VRN2 in coordinating cold-responsive flowering (vernalization). VRN2 and FLC play a key role in the vernalization response. FLC acts in the leaves and meristem by repressing genes such as *FT* and delaying flowering (Alexandre and Hennig, 2008). As VRN2 is a substrate in the N-end rule pathway, it is ubiquitylated by the E3 ligase PRT6 and targeted for degradation by the 26S proteasome. However, when the plant experiences cold during vernalization, the VRN2 protein accumulates. The VRN2 protein facilitates H3K27me3 of *FLC*, repressing *FLC* and therefore allowing the plant to flower (Gendall et al., 2001). To investigate the functional relevance of VRN2 regulation by the N-end rule pathway it was decided to generate mutant lines of *vrn2*, *prt6-1* and the *vrn2 prt6-1* double mutants in order to then perform flowering time assays.

The first step to create the transgenic plants needed was to obtain homozygous *vrn2* and *prt6-1* single and double mutants in a Col-0 background, (early flowering and not requiring vernalization). This is because the available T-DNA knockouts are only available in Col-0 accessions and because Col-0 is fast growing and can be easily checked for a mutation that produces complete gene knockouts. The T-DNA insert for *prt6-1* allele is SAIL _1278_H11. The T-DNA insert for the *vrn2* mutant is SALK_201153. The *vrn2* mutant is a new allele obtained from the SALK collection at the *Arabidopsis* stock centre that has been called *vrn2-5* in this study and it has not been

published previously. FIGURE 3.8 (A) shows the gene map of the *vrn2-5* mutant. The SALK_201153 tDNA insertion site is at bp 993 in the CDS, corresponding to just after arginine (R) 331 in the protein. This disrupts the VEFS-box domain (aa 250-387), a conserved domain at the C-terminus, characterized by an acidic cluster and tryptophan/methionine rich sequence.

Plants that were homozygous for *vrn2* were crossed with homozygous *prt6-1* plants. The F1 seeds from the cross were collected, grown and genotyped for both T-DNA inserts by performing DNA extraction and PCR. The F1 generation was found to be heterozygous for both genes. Heterozygous plants for *prt6-1* and *vrn2* were grown on to the next generation to also find a *vrn2 prt6-1* homozygous double mutant. Plants were again genotyped using PCR on genomic DNA with primers designed either side of the T-DNA insert for each gene. The *vrn2* homozygous mutant and the *vrn2 prt6-1* homozygous double mutant were identified by PCR analysis of genomic DNA (FIGURE 3.8 B). Total RNA was also extracted from the seedlings and cDNA generated using reverse transcriptase and Oligo dT primers. PCR was performed on the cDNA using primers specific for the *VRN2* and *PRT6* start and stop codons of the coding sequence. A longer extension time was used to enable amplification of the whole *PRT6* gene (approximately 6000bp long). The cDNA analysis confirmed that the T-DNA insertion in the mutants produced a complete knockout of the genes (FIGURE 3.9 C). Once the lines had been generated, they could be used for phenotypic analysis to provide an insight into the functional relevance of VRN2 and its regulation by the N-end rule pathway.

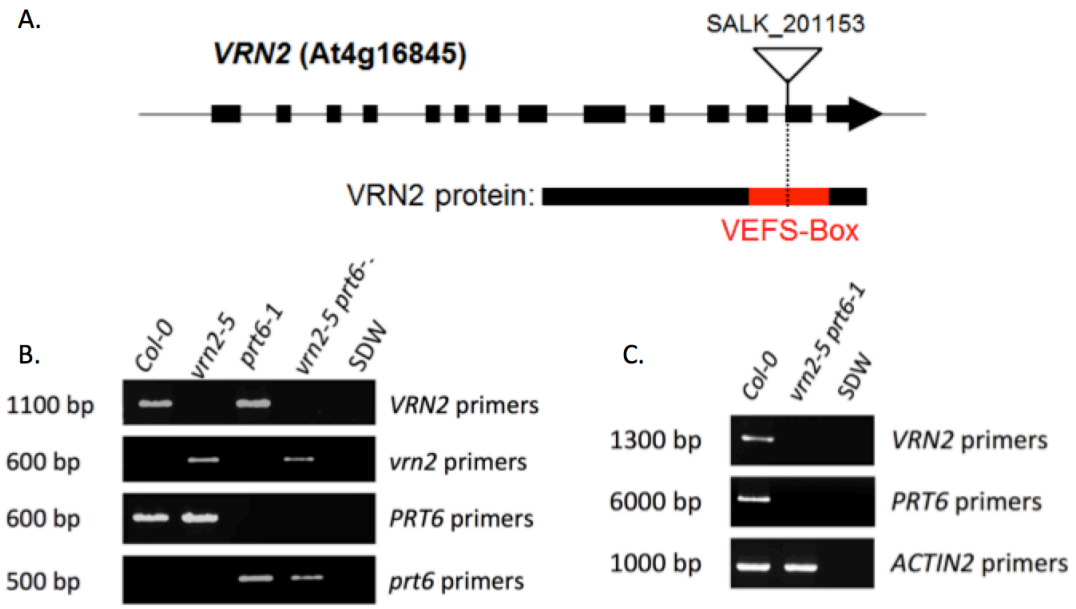

FIGURE 3.8 Genotyping confirms *vrn2-5* and *prt6-1* single and double mutants in Col-0 plants

(A) Schematic diagram of the *VRN2* gene structure and SALK_201153 tDNA insertion site at bp 993 in the CDS, corresponding to just after arginine (R) 331 in the protein. This disrupts the predicted VEFS-box domain (aa 250-387), a conserved domain at the C-terminus characterized by an acidic cluster and tryptophan/methionine rich sequence. Black boxes denote exons.
(B) PCR from genomic DNA confirming mutant lines for the *vrn2-5* and *prt6-1* single and double mutants in the Col-0 background.
(C) Full length RT-PCR from cDNA to confirm complete gene knockout.

3.6.1 Phenotypic analysis – ABA germination assay

It has been shown previously that the N-end rule pathway has a function in seed after ripening, breaking dormancy, seedling establishment and abscisic acid (ABA) signalling through PRT6 and ATE1/2 (Holman et al., 2009, Gibbs et al., 2014b). ABA is known to repress germination and promote seed dormancy. PRT6 was shown to be implicated in the regulation of seed sensitivity to ABA and in seedling establishment from seed to seedling, indicating a role of the N-end rule pathway in germination (Holman et al., 2009), where *prt6*-1 and *prt6-4* mutants showed extreme hypersensitivity to ABA treatment, halting testa rupture and endosperm rupture. Gibbs et al. (2014b) showed *prt6-1* hypersensitivity to ABA but remarkably, they found that the *prt6-1rap2.1rap2.2rap2.3* (*prt6-1, ERFVII*) quadruple mutant showed reduced sensitivity to ABA, demonstrating that the ERFVIIs N-end rule substrates participate in the regulation of germination. As VRN2 has also been found to be an N-end rule substrate, it was hypothesized that VRN2 might also contribute to the germination phenotype of *prt6-1*. Creating a *vrn2 prt6-1* double mutant should remove the hypersensitivity of *prt6-1* if the hypothesis was correct. To test this hypothesis a germination assay was performed on 3 x 40 seeds of WT Col-0*, vrn2, prt6-1* and *vrn2prt6-1* lines on ½ MS containing ABA hormone at concentrations of 0, 1, 2 and 5 μM. All seeds used were harvested from plants and grown at the same time so as to minimise differences in after ripening and dry storage time of seeds. All seeds were stratified at 5 °C for 2 days and then placed at 22 °C. Germination was

scored after 6 days, observing endosperm rupture, radicle emergence and how many seedlings established (i.e. cotyledons had turned green).

The *vrn2-5 prt6-1* and *prt6-1* show significant sensitivity to 2 μM ABA for germination, whereas the WT and *vrn2-1* have significantly higher germination. This suggests VRN2 is not involved in the ABA response during germination. Results do however show that in fact the single *vrn2-5* mutant had a significant delay in establishment relative to WT with 1 μM ABA treatment (FIGURE 3.9). *vrn2-5 prt6-1* shows hypersensitivity to ABA, similar to *prt6-1*, in relation to establishment. This suggests that VRN2 and the N-end rule pathway do contribute to the regulation of establishment due to the *prt6-1* phenotype but VRN2 may not be the substrate involved. The double mutants behave similarly to the single *prt6-1* mutant for germination and so the reason for the sensitivity cannot be due to VRN2 stabilization because there is no VRN2 present in the double mutant.

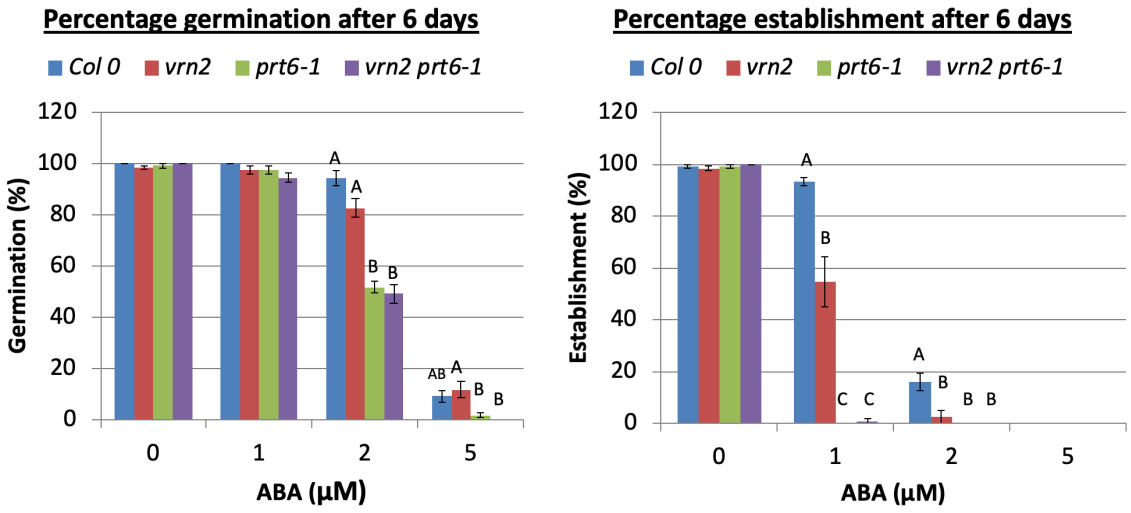

FIGURE 3.9 VRN2 is not involved in the ABA response during germination but may be involved in establishment

Germination and establishment under abscisic acid (ABA) treatment. Seeds used were all the same age and were all stratified at 5 °C for 2 days. The *vrn2-5 prt6-1* mutant shows a similar sensitivity to ABA as the *prt6-1* single mutant suggesting that VRN2 is not involved in the ABA response during germination. *vrn2-5* shows a significant decrease in establishment compared to WT at 1µM ABA, suggesting VRN2 may be involved in the ABA response during establishment. Germination was scored as radicle emergence through the endosperm. Establishment was recorded when cotyledons were fully expanded and green. Error bars indicate SEM and letters represent ANOVA (Tukey's test).

3.6.2 Phenotypic analysis – Flowering time in Col-0

Although the Col-0 ecotype does not require cold exposure in order to flower, developmental flowering time can still be monitored in Col-0 to see if there is an observable difference in flowering time between these available T-DNA mutant lines. Although the cold is not required for the plants to flower, there may still be an effect of VRN2 protein levels on flowering time. Seeds were sterilized and plated onto ½ MS and stratified at 4 °C, then seedlings were placed into soil. Flowering time was determined by counting the total leaf number in the rosette and also by counting the number of days until bolting.

After examining the flowering phenotypes of the mutant lines in the Col-0 background the general trend showed that without vernalization the *vrn2-5* mutant and double *vrn2-5 prt6-1* mutant flowered later than the WT and later than *prt6-1* when scoring days to flowering (temporal flowering time), although there was no statistically significant difference here (FIGURE 3.10). When measuring numbers of leaves (developmental flowering time) *vrn2-5* had significantly fewer leaves than *vrn2-5 prt6-1* at flowering, indicating the double mutant flowered significantly later than the single *vrn2-5* mutant. The overall trend suggests that *vrn2-5 prt6-1* flowers later than all other lines from the leaf number and days to flowering scores but more replication would be required to add confidence to this observation. These results highlight that the presence of VRN2 could be important for flowering time regulation but to test the true role of VRN2 it was decided to look at flowering in plants with a vernalization requiring background.

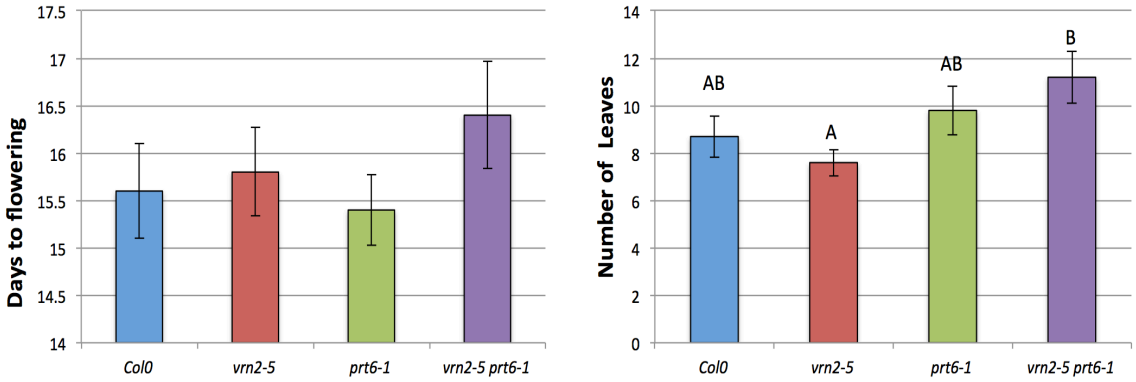

FIGURE 3.10 Flowering time of *vrn2-5*, *prt6-1* and *vrn2-5 prt6-1* mutants in the Col-0 ecotype

Days to flowering and rosette leaf number at flowering of Col-0 Arabidopsis plants under long days 16 h Light: 8 h Dark conditions. The *vrn2-5 prt6-1* double mutant flowers later than the other lines when measuring flowering time (days) and significantly later when measuring rosette leaf number. Error bars indicate SEM and letters represent ANOVA (Tukey's test).

3.6.2.1 Generation and confirmation of *vrn2-5* and *prt6-1* mutants in Col-0 *FRI*-Sf2 background

To perform true vernalization experiments and observe the role of the N-end rule pathway and VRN2 in flowering, the flowering time assays needed to be done in an ecotype that requires vernalization. In vernalization requiring plants *FLC* is activated by *FRIGIDA (FRI)* (Nappzinn, 1957). A dominant allele of *FRI* will transcriptionally activate *FLC* and so inhibit flowering (Michaels and Amasino, 1999, Sheldon et al., 1999). When the plant experiences cold during vernalization, VRN2 levels will increase and will overcome the effect of *FRI* by repressing *FLC* and allow flowering (Sung and Amasino, 2004a). Backgrounds such as *fca-1* or *fve-1* mutants are vernalization responsive genotypes (Gendall et al., 2001) but for this study it was decided to use a Col-0 *FRI*-Sf2 background (Johanson et al., 2000); a Col-0 ecotype that has a dominant *FRI* allele from the naturally occurring Sf2 ecotype introgressed into it. It was used because this allowed us to utilize the mutants already isolated in the Col-0 background. Col-0 has the recessive allele of *FRI* and this recessive allele has a 16bp deletion, meaning the plants do not require vernalization to flower because this allele is inactive. The 16 bp difference was used to distinguish the Col-0 and Sf2 alleles of *FRI* using gel electrophoresis.

Both *vrn2-5* and *prt6-1* were crossed into the Arabidopsis Col-0 *FRI*-Sf2 ecotype. PCR was performed to genotype the F1 plants, amplifying the *FRI* alleles. Since there is only a 16bp difference between the dominant and

recessive *FRI* allele and the PCR product is small (Johanson et al., 2000), a 3% gel was used and electrophoresis was performed at a low voltage to ensure distinction between plants with the dominant Sf2 *FRI* allele (larger band) or the recessive Col-0 *FRI* allele (Col-0). Single *vrn2-5* or *prt6-1* mutants were identified. Individuals that were homozygous for *FRI*-Sf2, homozygous for one mutant gene and heterozygous for the other gene were taken forward and grown. From these F2 plants the *vrn2 prt6-1* in the Col-0 *FRI*-Sf2 background was identified and eventually all required homozygous mutants that necessitate vernalization were produced (FIGURE 3.11). cDNA analysis was not done here as it had already been shown that *vrn2-5* and *prt6-1* were full length gene knock outs.

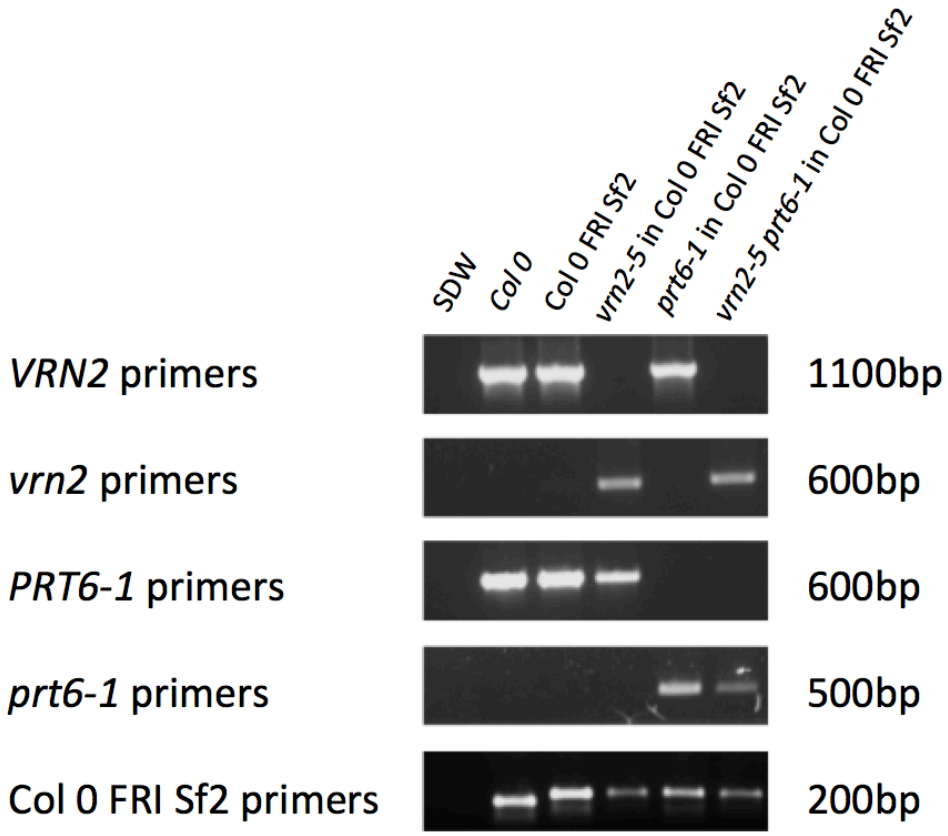

FIGURE 3.11 Genotyping confirms *vrn2-5* and *prt6-1* single and double mutants in Col-0 *FRI*-Sf2 plants

Ethidium bromide stained agarose gels of PCR products from genomic DNA confirming mutant lines for the *vrn2-5* and *prt6-1* single and double mutants in the Col-0 *FRI*-Sf2 background. The Col-0 *FRI*- amplicon is smaller than the Col-0 *FRI*-Sf2 allele due to a 16 bp deletion.

3.6.2.2 Phenotypic analysis – Flowering time in Col-0 *FRI*-Sf2

Using the *prt6-1* and *vrn2-5* mutants generated in the vernalization-requiring Col-0 *FRI*-Sf2 background the flowering time assay was repeated. It was predicted that Col-0 *FRI*-Sf2 WT plants would flower late with no vernalization but flower earlier with increased vernalization as VRN2 becomes stable and accumulates, in accordance with previous studies in this line (Gendall et al., 2001). *vrn2-5* was predicted to flower later, even with vernalization due to the lack of the VRN2 protein. *prt6-1* was predicted to flower earlier than WT because it lacks the E3-ligase to ubiquitylate VRN2 and target it for degradation, and so VRN2 levels would be high. For the *vrn2-5 prt6-1* mutant the prediction was that it would most likely act as the *vrn2-5* single mutant and flower later temporally (number of days) and developmentally (number of leaves) as there would be low VRN2 levels. It was also predicted that late flowering plants would have more leaves as it is well established that late-flowering plants form more leaves at flowering time (Koornneef et al., 1991). The different vernalization lengths could be then used with the flowering responses over time in the four lines to provide a definitive link between the N-end rule, VRN2 and flowering.

Seeds were cleaned and plated onto ½ MS and stratified at 5 °C. then seedlings were placed into soil. There were 6 plants of each genotype in each tray and 5 trays in total. Each tray of seedlings was grown under a different vernalization treatment, either 0, 1, 2, 3 or 4 weeks vernalization at 5 °C before moving to 22 °C with long days. Flowering time was estimated by

calculating the average total leaf number in the rosette and also by calculating the average number of days until bolting.

Here, the increasing the length of vernalization treatments reduced the length of time plants took to flower in all four lines (FIGURE 3.12 A and B), however this response was slower in the *vrn2-5* and *vrn2-5 prt6-1* lines when compared to WT. The *vrn2-5 prt6-1* plants showed a significant delay in flowering at 0 weeks vernalization when scoring days to flowering (FIGURE 3.12 A). With 0 weeks vernalization *prt6-1* showed a similar delay in days to flowering but as vernalization increased to 2 and 3 weeks the *prt6-1* single mutant shows a significant decrease in flowering time to *vrn2-5* with the *vrn2-5 prt6-1* double being somewhere in-between. The general trend observed is that *vrn2-5* and *vrn2-5 prt6-1* mutants flower later than *prt6-1* and Col-0 *FRI*-Sf2. The *vrn2-5 prt6-1* mutants flowers at a significantly higher number of leaves than the other lines under non-vernalized long day conditions (FIGURE 3.12 B). This result is similar to the *vrn2-5 prt6-1* in Col-0 but in Col-0 *FRI*-Sf2 the affect is more pronounced.

Overall, the trend appears to be as predicted; that *vrn2* and *prt6-1 vrn2-5* mutants flower later than Col-0 *FRI*-Sf2 and *prt6-1* lines, although there is not a statistically significant difference between flowering with all treatments, possibly due to the number of plants used. A previous study showed that *vrn2-1* in Col-0 *FRI*-Sf2 did not respond to vernalization treatments (Gendall et al., 2001) but in this experiment these plants still respond to vernalization, taking less time to flower with increased length of vernalization. The previous

study was on the mutant allele *vrn2-1* but in this study we have identified the new mutant allele *vrn2-5* which is in a similar location on the gene. As the plants in this experiment do respond to vernalization, this suggests that *vrn2-5* is not a complete functional knockout and there may still be some functional VRN2 (i.e. truncated) produced in these plant lines.

A.

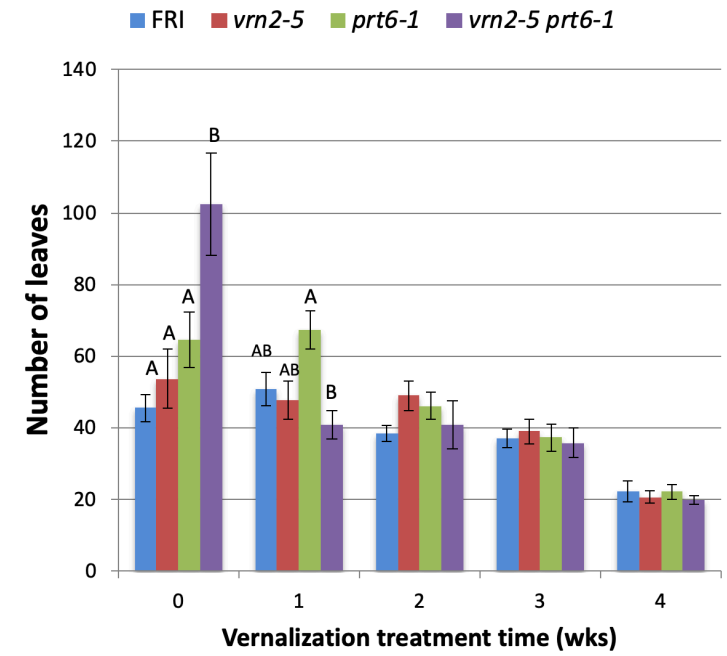

B.

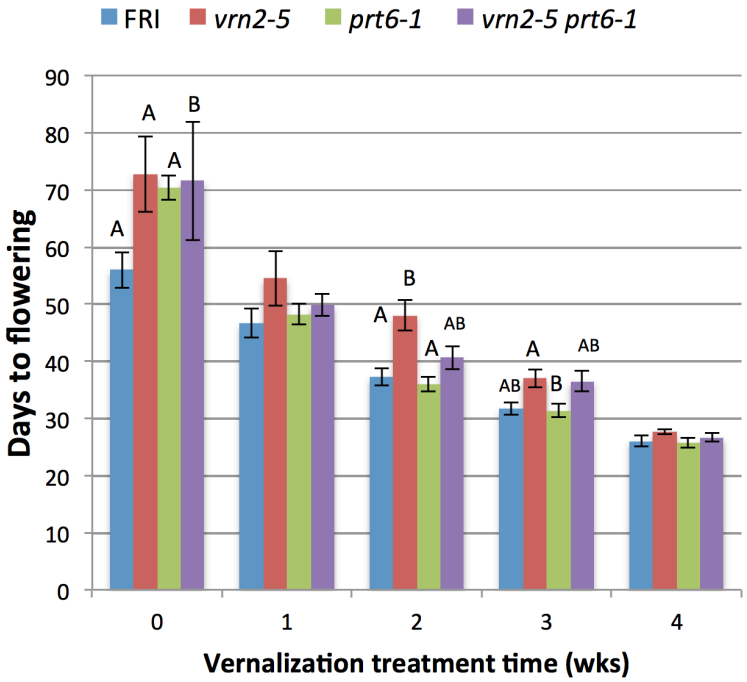

FIGURE 3.12 Flowering time of *vrn2-5*, *prt6-1* and *vrn2-5 prt6-1* plants in Col-0 *FRI*-Sf2

Flowering time as measure by average number of days to flowering and average rosette leave number at flowering. Error bars indicate SEM and letters represent ANOVA (Tukey's test).
(A) Differences in rosette leaf number are more pronounced at 0 weeks where the *vrn2-5 prt6-1* double mutant flowers significantly later than the other lines.
(B) Flowering time is decreased with increased vernalization when scoring days to flowering. *vrn2-5* and *vrn2-5 prt6-1* plants flower significantly later than Col-0 and *prt6-1* with 2 weeks vernalization.

3.6.3 Is VRN2 involved in abiotic stress responses?

Plants are sessile organisms and are subject to fluctuations in their environment. Some environmental changes can be extreme or sudden and a plant has to sense and respond to these changes in order to survive. Abiotic stresses such as flooding, salt and heat can have a negative effect on the growth and development of plants, can cause premature flowering and can have a negative impact on the quality and yield of crops. Recent work has shown that the Cys/Arg N-end rule pathway is a general sensor of abiotic stress via its capacity to sense oxygen and NO (Vicente et al., 2017). It was shown that N-end rule regulation of the stabilization of ERFVII transcription factor substrates can regulate the stress response by interaction with chromatin remodelling proteins. As VRN2 is a sensor of oxygen and nitric oxide and is also regulated by the N-end rule pathway it was hypothesized that VRN2 might have a role in abiotic stress response and enhanced plant survival, similar to the ERFVIIs.

3.6.3.1 Heat stress

One stress a plant may experience is heat. A large number of genes that are induced or repressed by heat have been identified but uncovering heat stress response phenotypes has proved difficult (Yeh et al., 2012). The function of some heat stress response genes might be obscured due to gene redundancy problems, which prevents the identification of stress sensors (Zhu, 2016). Vicente et al. (2017) showed that increased thermotolerance caused by *prt6* was diminished by the removal of ERFVII (N-end rule substrate) function, demonstrating that ERFVIIs are required for the enhanced thermotolerance

shown in *prt6*. A potential role for the Cys/Arg N-end rule substrate VRN2 in abiotic stress tolerance was thus explored, initially testing heat stress tolerance. Plants have diverse mechanisms to respond to temperature changes in the environment and have a complex regulatory network of proteins in response to heat stress (Zhu, 2016). There is post-translational regulation of certain proteins, causing histone modifications and chromatin remodelling that enable plants to acquire thermotolerance and epigenetic heat stress 'memory' (Ohama et al., 2017). Four distinct types of plant thermotolerance have been identified which are Basal thermotolerance (BT), Short term acquired thermotolerance (SAT), Long-term acquired thermotolerance (LAT) and thermotolerance to moderately high temperatures (TMHT), suggesting diverse mechanisms are present in plants to respond to temperature changes (Yeh et al., 2012). Further motivation to investigate a potential role for VRN2 in heat responses, in addition to ERFVIIs, came from an accidental observation that *vrn2-5* and *vrn2-5 prt6-1* mutants had increased survival relative to *prt6-1* when the growth chamber malfunctioned and overheated (to temperatures ~35 °C although the exact temperature was unknown) (FIGURE 3.13). It was therefore decided to investigate heat stress with the *vrn2-5* and *prt6-1* lines we had generated.

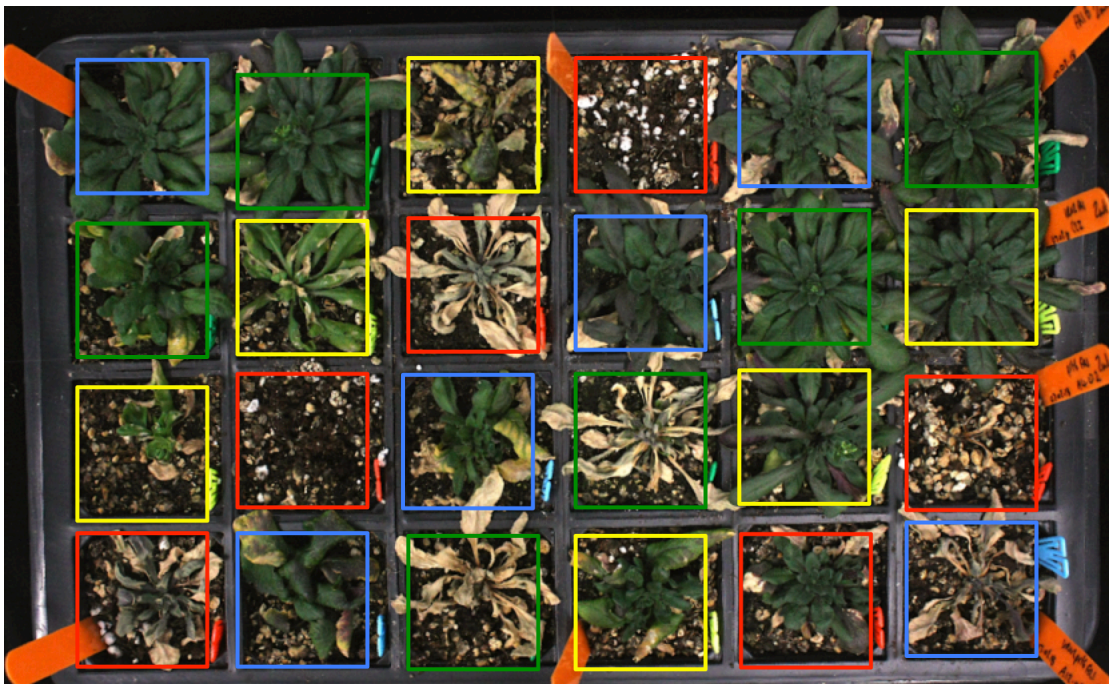

FIGURE 3.13 *vrn2-5* and *vrn2-5 prt6-1* mutants are more heat tolerant than *prt6-1*

Image of heat-stressed mature plants when the incubator reached temperatures over 35°C for 3 days. Colored squares surround each plant line. Green – Col-0, yellow – *vrn2-5*, red – *prt6-1*, blue – *vrn2-5 prt6-1*.
vrn2-5 and *vrn2-5 prt6-1* plants are larger with green leaves whereas *prt6-1* plants are dry, brown and shriveled.

It was decided to first test Basal thermotolerance (BT) (the ability to withstand a non-lethal heat stress) in the four lines in the Col-0 *FRI*-Sf2 background. Seeds were surface sterilized and plated on ½ MS in round Petri dishes. Seedlings grown at 22 °C Long days for five days and then subject to 44 °C in an incubator for 26 min and then returned to the 22 °C growth chamber. Plants were scored after a further 13 days and were assessed to be alive if they were green and dead if they were bleached (FIGURE 3.14 B shows an example of green and bleached seedlings but there was high variability between plates). Although there was no significant difference between lines, the *prt6-1* (where VRN2 protein levels would be high) appeared to show some indication of a tolerance to BT heat stress compared to *vrn2-5* and *vrn2-5 prt6-1* (where there would be low VRN2 protein levels) (FIGURE 3.14 A). The results here show that the *vrn2-5* and the *vrn2-5 prt6-1* mutants had a lower BT and were sensitive to BT heat stress. This is a similar result to Vicente et al. (2017) where at 44 °C for 23 min and 26 min the *prt6-1* and *prt6-5* showed a very high BT. This result supports the hypothesis that stabilized N-end rule substrates such as VRN2 may have a role in heat stress tolerance because without the E3 ligase, high VRN2 levels could increase the BT in these plants. Although PRT6 does have the ERFVIIs and other unknown substrates, the trend in the data suggests a possible link between the N-end rule substrate VRN2 and abiotic stress tolerance.

Although the BT test did not show statistically significant differences between genotypes, average survival still suggested some promise, so it was decided to continue further experiments to test the acquired thermotolerance. Due to time constraints only the SAT (the plant's capacity to acquire thermotolerance

to a normally lethal heat stress by preconditioning with a milder heat stress) was tested with four repeats. Lines with the Col-0 background and lines with the Col-0 *FRI*-Sf2 background were tested. Seeds were cleaned and plated onto ½ MS round Petri dishes and grown under long days at 22 °C. They were then moved to 37 °C for 1 h, returned to 22 °C for 2 h to recover, placed at 44 °C for 170 min and then returned to 22 °C. The results were scored after a further 13 days. Plants were assessed to be dead if they were bleached. Remaining plants that were alive were divided into normal larger, green healthier plants and delayed plants that were green but smaller. A previous study by Vicente et al. (2017) showed that *prt6-1* had a high SAT compared to a mutant lacking the ERFVII N-end rule substrates. In contrast, the results of this study showed that plants in the Col-0 *FRI*-Sf2 background lacking PRT6 or VRN2 did not differ in SAT between lines (FIGURE 3.15 B). However, the trend for plants in the Col-0 background was that *prt6-1* had a lower SAT compared to other lines and the N-end rule substrate *vrn2-5* single and *vrn2-5 prt6-1* mutants had higher SAT, similar to WT (FIGURE 3.15 A). This would suggest that VRN2 has a negative effect on heat stress response for SAT because the plants not expressing VRN2 have higher survival percentages. This is in contrast to VRN2 having a possible positive role with BT but is possible, as the stress response in plants is so complex. These are however only preliminary results and further repeats need to be done with these experiments and also to investigate LAT and TMHT responses in these lines.

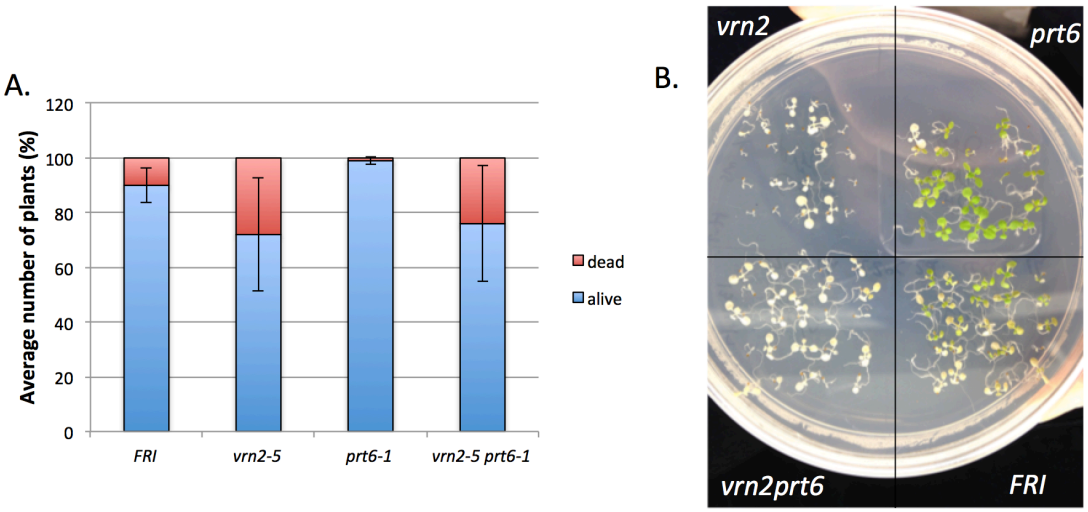

FIGURE 3.14 Basal thermotolerance response of Arabidopsis seedlings to heat stress treatment:

BT, basal thermotolerance 44 °C for 26 min.
(A) A graph showing *prt6-1* plants have higher BT than the *FRI*-Sf2 WT, *vrn2-5* or *vrn2-5 prt6-1* mutant plants.
(B) Image showing 7-week-old seedlings put under heat stress of 44 °C for 26 min. Green plants were scored alive and white plants were scored dead. In this example plate *prt6-1* has more plants that survived the BT test.
Error bars indicate SEM.

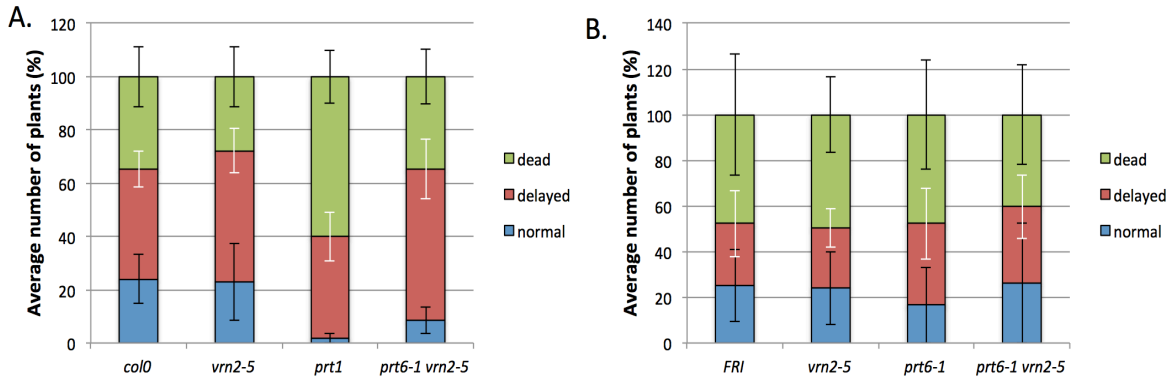

FIGURE 3.15 Short term acquired thermotolerance of Arabidopsis seedlings to heat stress treatments:

(A) SAT (short-term acquired thermotolerance) in Col-0 background. *prt6-1* is sensitive to the 44 °C heat stress whereas *vrn2-5* and *vrn2-5 prt6-1* mutants have on average a higher percentage of normal and delayed plants and therefore a higher SAT.
(B) SAT in Col-0 *FRI*-Sf2 background. Plant lines show no statistical difference in SAT, as averages numbers of plants alive, delayed or dead are similar.
Error bars indicate SEM.

3.6.3.2 Salt stress

The salinity of the soil plants grow in has a great effect on their development (Ma et al., 2015). In many plant species flowering is delayed when the plant experiences salt stress (Van Zandt and Mopper, 2002) and it is known that high salt levels delay the onset of flowering in *A. thaliana* (Achard et al., 2006), although the molecular mechanisms behind this remain largely unknown. The N-end rule has previously been linked to salt stress response via the ERFVIIs (Vicente et al., 2017) so here it was decided to see if VRN2 was also involved. Salt stress was applied to WT, *vrn2-5*, *prt6-1* and *vrn2-5 prt6-1* lines in Col-0 background to ascertain if there is a link between the N-end rule regulation of VRN2 in tolerance to salinity stress.

Seeds were sterilized, placed onto soil and grown under optimal conditions (22 °C, long days) for 12 days. For the initial experiment 6 plants were grown from each line and staggered across the tray so lines were spread evenly. One tray was then watered twice a week with 600 ml 200mM NaCl solution, whilst the other tray was watered as usual with water. Plants watered with water were all healthy, green and had started to flower. From the images taken of plants watered with salt water (FIGURE 3.16) it appeared that the *vrn2-5 prt6-1* double mutants (highlighted in yellow) were more salt tolerant, as the general trend is that these plants are larger and greener. The *vrn2-1* single mutant plants (highlighted in blue) were larger but do show browning and drying of the leaves. *erfvii* were not salt tolerant, similar to (Vicente et al., 2017). However, single *prt6-1* mutants showed little to no tolerance to salt stress, in contrast to the results in Vicente et al. (2017) where they observed a

significant increase in *prt6-1* seedling survival in the NaCl treated plants. It is unclear whether the salt tolerance in *vrn2-5 prt6-1* is caused by VRN2, PRT6, or both, as there was no observable difference in tolerance between the single mutants. Further study needs to be done to see if this result can be repeated and to see if VRN2 does or does not have a role in the salt stress response. It is also difficult to see the differences between the WT and *ERFVII* lines by images alone, so further work is needed to produce quantifiable results perhaps by scoring conductivity (electrolyte leakage) of the leaves of these plants so they can be compared by statistical analysis.

FIGURE 3.16 *vrn2-5 prt6-1* double mutants are more tolerant to salt stress

An image of 4-week-old seedlings. Seedlings were watered twice a week with 600 ml 200 mM NaCl. Orange tags – Col-0, Blue tags – vrn2, Green tags – prt6, Yellow tags – vrn2-5 prt6-1, Pink tags – ERFVII (*rap2.12 rap2.2 rap2.3 hre1 hre2*) mutants. Green and large plants were considered tolerant, whereas brown withered seedlings were intolerant to salt.

3.7 Discussion

Western blotting confirmed that VRN2 is stabilized in the presence of bortezomib *in vitro*, supporting the hypothesis that VRN2 is targeted by the 26S proteasome. VRN2 was stabilized when the cysteine of the Nt MC is mutated to an alanine, highlighting the importance of cysteine as a destabilizing amino acid residue at the N-terminus in the Cys/arg N-end rule pathway. Stabilization of VRN2 in *prt6-1* and *ate1ate2* mutants *in planta* also supports the hypothesis that VRN2 is regulated by the N-end rule pathway.

Histochemical staining of 7-day old seedlings demonstrated that VRN2-GUS is present at high levels in the vasculature and meristems of WT plants but is present throughout MA-VRN2-GUS, *prt6-1* and *ate1ate2* seedlings. Furthermore, VRN2-YFP confocal images show that VRN2 is located in the nucleus of roots tips in both the Col-0 and *prt6-1* plants, which agrees with previous reports that VRN2 modifies chromatin by placing the H3K27me3 mark on *FLC* and other targets. However, further work with VRN2-YFP lines needs to be carried out to confirm VRN2 localization in other plant tissues, as some images suggest that VRN2 may be cytosolic further from the root tip, but the results were not conclusive. There was also no clear difference between Col-0 and *prt6-1* in the confocal images despite the differences being observed by western blot so future work could include quantification measure of YFP intensity.

VRN2 stability increases with increased length of vernalization treatment, but it was unstable when the plants were returned to optimal conditions. A new T-DNA insertion mutant allele of VRN2 was isolated (*vrn2-5*) and this was used to generate *vrn2-5*, *prt6-1* and *vrn2-5 prt6-1* lines in a vernalization requiring background Col-0 *FRI*-Sf2 to examine the functional relevance of VRN2 regulation by the N-end rule. Flowering time assays showed that in general the *vrn2-5* and *vrn2-5 prt6-1* lines flowered later than *prt6-1* and WT plants in the Col-0 background. In addition, *vrn2-5* and *vrn2-5 prt6-1* plants also flowered later in the vernalization-requiring Col-0 *FRI*-Sf2 background. These results support the prediction that plants with low VRN2 levels would flower later and plants with high VRN2 levels would flower earlier than WT. All lines responded to vernalization although the general trend for but *vrn2-5* and *vrn2-5 prt6-1* mutants was that they responded slower than Col-0 *FRI*-Sf2 or *prt6-1* plants. The fact that *vrn2-5* mutants still respond to vernalization was not as predicted. This may mean that there is still functional VRN2 protein (perhaps truncated) present in the newly identified *vrn2-5* mutant. More repeats need to be done on the flowering time experiment to see if this may be the case. More PCR and cDNA analysis in the Col-0 *FRI*-Sf2 plants can confirm if the gene is a complete knockout or if there are any truncated PCR products and therefore truncated protein fragments present with possible functionality. Although there were 6-10 plants per line in this experiment, more repeats need to be done to improve the statistical analysis. The initial results here support the hypothesis that VRN2 regulation by the N-end rule pathway is linked to its accumulation during vernalization and most likely its effect on flowering time, however the experiments should be repeated to confirm this.

Phenotypic analysis revealed that VRN2 was not involved in the ABA response during germination could be involved in establishment. Recent results comparing ERFVII N-end rule substrates and *prt6-1* and *prt6-5* mutants by Vicente et al. (2017) showed a role of ERVII in heat stress tolerance (BT, SAT, LAT and TMHT). Conversely, we found the preliminary heat stress experiments showed almost opposite results in SAT heat stress experiments but similar results with BT suggesting VRN2 may have a role in heat stress tolerance, but further research needs to be undertaken to include more replicates and optimize the heat stress conditions. The preliminary salt stress experiment revealed that *vrn2-5 prt6-1* mutants appeared more salt stress tolerant, but more repeats and quantitative experiments should be performed to confirm the link with N-end rule regulation of VRN2 and abiotic stress tolerance.

Results in this chapter have confirmed VRN2 is a substrate of the N-end rule pathway and established that VRN2 is stabilized under cold vernalization conditions. The next aim of the project was to identify a potential mechanism causing VRN2 stabilization in the cold. VRN2 is expressed and degraded in normal conditions via the N-end rule pathway but in the cold it becomes stable. One mechanism could be a cold-specific shielding of the N-terminus that prevents post-translational modifications by components of the Cys/Arg N-end rule pathway that lead to its degradation. This mechanism and approaches use to test this hypothesis are discussed in the next chapter.

Chapter 4

Investigating a mechanism for VRN2 stabilization

4.1 Introduction

In the previous chapter it was determined that VRN2 is stabilized in cold conditions. However, the mechanism behind the switch from VRN2 being degraded, to VRN2 becoming stable during temperature decreases is unknown. An aim of this project was to see if a mechanism for VRN2 stabilization could be found. Data in chapter 3 show VRN2 is a substrate of the N-end rule pathway but substrates of the N-end rule are often only targeted conditionally. Some proteins have been shown to be substrates usually but then become stable once associated with other proteins in a multisubunit protein complex. One such example is the component of oligomeric complex 1 (COG1) which is a subunit of the Golgi complex (Shemorry et al., 2013). Once in complex with other proteins, the N-terminus of COG1 is shielded and the protein is unable to be targeted by the N-end rule. When the protein dissociated the N-degron was exposed and so it was recognized by its N-recognin and it was degraded. In the case of VRN2, one hypothesis could be that another protein interacts with VRN2 and shields its N-terminus, stabilizing it during the cold.

It is known that VRN2 suppresses and epigenetically maintains *FLC* repression (Gendall et al., 2001). Work by Sung and Amasino (2004b) identified seedlings from mutant screens that could not suppress and maintain *FLC* repression and has highlighted proteins other than VRN2 that are involved in vernalization. One of these proteins is VERNALIZATION 1 (VRN1) (Levy et al., 2002), a protein only found in plants that possesses DNA binding domains. Another protein known to be required in the repression of *FLC*

during vernalization is a plant homeodomain (PHD) finger protein, *VERNALIZATION INSENSITIVE 3* (*VIN3*) (Sung and Amasino, 2004b). *VIN3* contains one PHD that is that is usually found in proteins that are involved in chromatin remodelling complexes structure (Aasland et al., 1995, Fair et al., 2001). It has also shown previously that VIN3 interacts with VRN2 in the PRC2 complex and that the response to vernalization is blocked in *vin3* mutants, similar to *vrn2-5* mutants (Wood et al., 2006). VIN3 also has a fibronectin type III domain and these are known to often be involved in protein-protein interactions (Main et al., 1992). It is possible therefore, that VIN3 shields the N-terminus of VRN2 through interaction during *FLC* suppression.

Transcription of *VIN3* is only induced during cold exposure but mRNA is not detectable when returned to warm temperatures (Sung and Amasino, 2004b, Alexandre and Hennig, 2008). This is similar to the pattern observed for VRN2 protein stabilization (FIGURE 4.1). VIN3 first appears after 2 weeks of cold exposure and reaches a maximum level after 4 weeks of vernalization but is not detected in non-vernalized plants (Shindo et al., 2006). VIN3 is known to initiate the modification of chromatin structure in *FLC* and in *vin3* knockouts *FLC* is not repressed during vernalization (plants will be late flowering) (Wood et al., 2006). However, the constitutive expression of *VIN3* does not affect the flowering vernalization response phenotype without the cold, therefore other proteins must be involved. Epigenetic silencing of *FLC* requires VIN3, VRN1 and VRN2 (Wood et al., 2006). It is proposed that VIN3 is responsible for the initial *FLC* suppression and the process to distinguish the length of exposure

to cold temperatures and works upstream from VRN1 and VRN2 (Sung and Amasino, 2004b). As *VIN3* is expressed early in the vernalization response before VRN2 becomes stable, it follows that VIN3 could be the factor facilitating VRN2 stabilization.

The induction of *VIN3* occurs in the shoot and root apical meristems (Wellensiek, 1962, Michaels and Amasino, 2000). This correlates with the tissues in which VRN2 was found to be most stable (see Chapter 3 FIGURE 3.6) and is also where *FLC* suppression occurs during vernalization (although FLC can be found in all tissues and then silenced throughout (Sung and Amasino, 2004b, Kim and Michaels, 2006, Mylne et al., 2006, Crevillen et al., 2014)). The meristem was the location where vernalization was first recognised as an epigenetic memory (Lang and Melchers, 1947). Like VRN2, VIN3 also has a putative nuclear localization signal as part of its structure (Sung and Amasino, 2004a) so it is likely to be found in the nucleus at the same time as VRN2. Therefore, the cold-induced expression and the localization of VIN3 is consistent with the hypothesis that VIN3 has a role in VRN2 stabilization. Other findings have revealed that VIN3 interacts with the VRN2-PRC2 complex and that this complex is responsible for histone deacetylation by VIN3 of *FLC* (Sheldon et al., 2002, Sung and Amasino, 2004a) and methylation at *FLC* by VRN2 (Wood et al., 2006). This is further evidence that supports the hypothesis that VIN3 could facilitate VRN2 stabilisation. For these reasons VIN3 was chosen as a candidate gene to research in this study and it was hypothesised that VIN3 may act by shielding the N-terminus of VRN2 (FIGURE 4.2), preventing post-translational

modifications and thus preventing its degradation by the N-end rule pathway. The rest of this chapter will discuss the possibility of VIN3 being the cause of VRN2 stabilization.

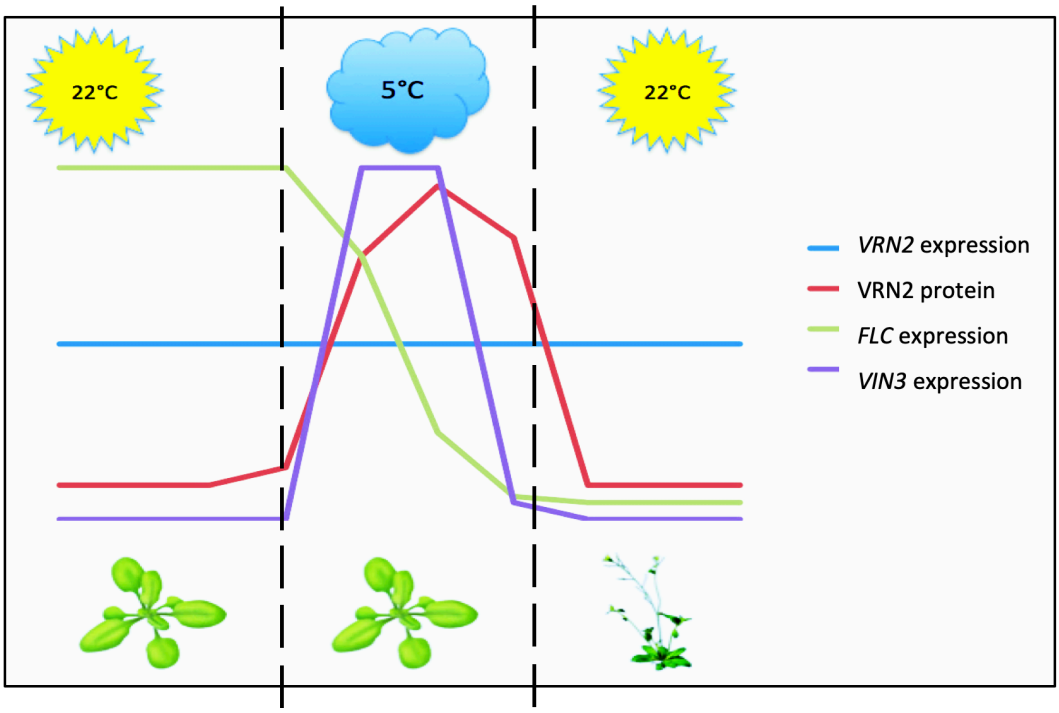

FIGURE 4.1 VRN2 protein becomes stable in the cold at the same time *VIN3* expression is increased

During varying environmental conditions *VRN2* expression remains constant and VRN2 protein is degraded via the N-end rule. During vernalization VRN2 protein levels increase as it becomes more stable. Once returned to warm conditions the amount of VRN2 protein becomes unstable and returns to low levels. As VRN2 levels increase *FLC* expression decreases and is epigenetically supressed (Song et al., 2012). *VIN3* expression increases during vernalization at the same time VRN2 becomes stable and it also decreases on return to warm conditions (Sung and Amasino, 2004b, Wood et al., 2006).

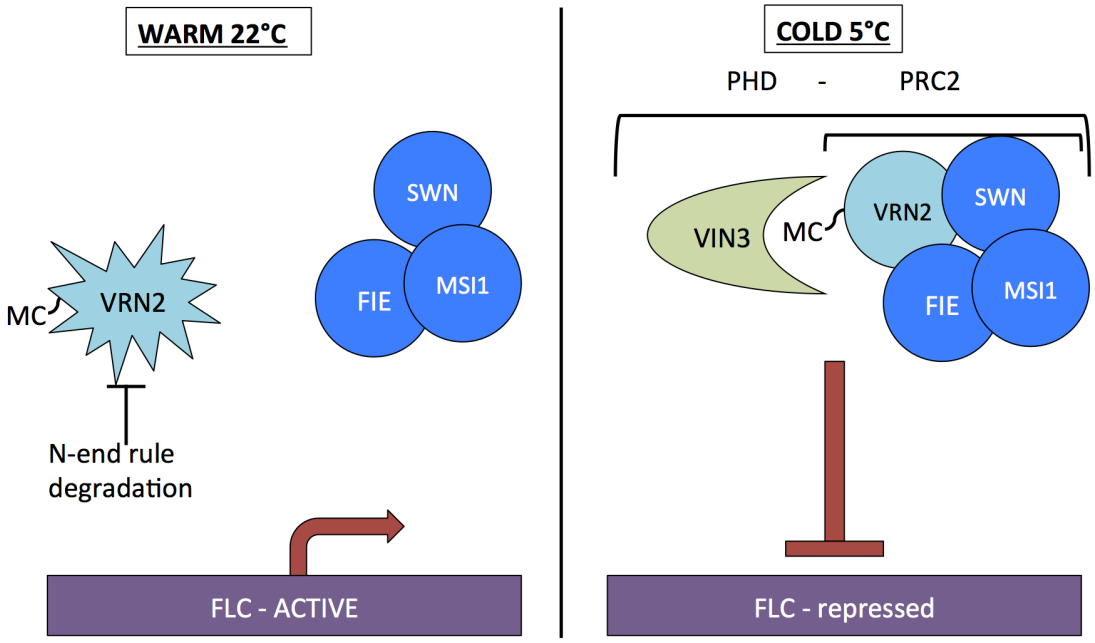

FIGURE 4.2 VIN3 interacts with the PRC2 complex in the cold

In warm conditions VRN2 protein is degraded by the Cys/Arg N-end rule pathway, *VIN3* is not expressed and *FLC* is active. In cold conditions VRN2 forms part of a PRC2-like complex that also includes FERTILIZATION INDEPENDENT ENDOSPERM (FIE), CURLY LEAF (CLF) and SWINGER (SWN). This complex is thought to associate with VIN3 and is involved in H3K27me3 epigenetic silencing of the *FLC* locus (Wood et al., 2006). The hypothesis in this study is that when VIN3 interacts with the PRC2 it may shield the N-terminus of VRN2, causing VRN2 to become stable.

4.2 The effect of VIN3 on VRN2 stabilization *in vitro*

To be a substrate of the Cys/Arg N-end rule pathway a protein must have MC amino acids at the N-terminus, a downstream lysine for ubiquitylation and the N-terminus needs to be easily accessible on the outside of the protein. I hypothesized that VIN3 might shield the N-terminus of VRN2, causing its stabilization. To test the effect of VIN3 on VRN2 stability, full length VIN3 cDNA was cloned in order to co-express VIN3 and VRN2 together in the *in vitro* protein degradation assay.

RNA was extracted from 2 wk vernalized seedlings as VIN3 is not expressed normally and cDNA was synthesized from this. Restriction cloning with MluI and XbaI was used to ligate VIN3 into pTNT for the *in vitro* protein degradation assay. Following digestion, bands of the correct size were observed by gel electrophoresis and sequencing confirmed full length VIN3 had been cloned.

VIN3-pTNT was co-expressed *in vitro* with the existing VRN2-pTNT construct in a protein degradation assay (Chapter 3, section 3.2) to test whether the presence of VIN3 would stabilize VRN2. 500ng each of VIN3 and VRN2 constructs were mixed *in vitro*, expressed and translated into protein by incubating for 30min. VIN3 + empty pTNT and VRN2 + empty pTNT were also mixed and incubated as controls. Cyclohexamide (CHX) was then added (to inhibit any more protein synthesis) and samples were taken after 0, 60 and 120 min. Western blotting with HA anitbody showed that when expressed

individually, VIN3-HA was stable over the time course whilst VRN2-HA was degraded over time, (confirming previous findings for VRN2 in chapter 3, FIGURE 3.4). When VIN3-HA and VRN2-HA were co-expressed then VRN2-HA was again degraded over time (FIGURE 4.3). This suggests VIN3 is not the cause for VRN2 stability *in vitro*, as VRN2 is still unstable if VIN3 is present. However, it was difficult to make comparisons between the single and co-expression experiments. Bands were fainter after 120 min for VRN2 but the extent of its degradation was not clear over that time period. To address this, the degradation assay was repeated over a longer time course in order to see more clearly if VRN2 degradation was affected by VIN3. VRN2 with bortezomib (bort) was also included as a control to show that proteasome inhibition stabilizes VRN2. Samples were taken 0, 1, 2, 3 and 4h.

The results (FIGURE 4.4) again showed that expressed alone, VRN2 degrades over the time course, present at a high amount at 0 h and decreasing over the 4 hours. Once again, expressed alone, VIN3 levels remain constant over the time course. When VRN2 was co-expressed with VIN3, VRN2 levels still decreased over time, showing a faint band at 4 h compared to 0 h, whilst VIN3 levels remained constant. When bortezomib was added, VRN2 protein levels remained high in all experiments, confirming that the VRN2 depletion was due to proteasomal activity. These results suggest that although VIN3 interacts with VRN2 in the PRC2 complex, it does not cause VRN2 stability *in vitro*. The results do not support the hypothesis that VIN3 shield the MC terminus of VRN2, preventing ubiquitylation and degradation. However, the interaction between VRN2 and VIN3 may require

the presence of other proteins that are not present in this lysate system or may require specific environmental conditions to take place.

As VIN3 and VRN2 co-expression did not produce conclusive results, another method was used for detecting a stabilizing effect of VIN3 on VRN2 *in vitro*. Firstly, *VIN3* was expressed *in vitro* for 1 h in order to produce high levels of VIN3 protein present. The products of this reaction were then added to the VRN2pTNT reactants at the beginning of VRN2 incubation. This would ensure that VIN3 would be present right from the beginning of VRN2 synthesis to see if VIN3 has any effect post-translationally and would mimic natural VIN3 expression upstream from VRN2 (Sung and Amasino, 2004b). The rabbit reticulocyte reaction containing VIN3-HApTNT or empty pTNT vector control reaction was incubated for 1h. Another reaction was then set up using VRN2pTNT and mixed with the pre-synthesized VIN3pTNT/empty PTNT reaction. This reaction was incubated for 30min before the addition of CHX and samples were taken at 0, 2 and 4h. Western blotting with HA antibodies showed that even though there were strong bands indicating high levels of VIN3, VRN2 levels still decreased over time, with decreasing abundance of protein present over the 4 h time course (FIGURE 4.5). In the control where pTNT only was added to VRN2, there was less VRN2 present to begin with but the results showed a similar pattern of VRN2 degradation over time. The Coomassie stain shows that the results are due to VRN2 depletion and not loading errors. These results do not support the hypothesis that VIN3 causes VRN2 stabilization *in vitro*.

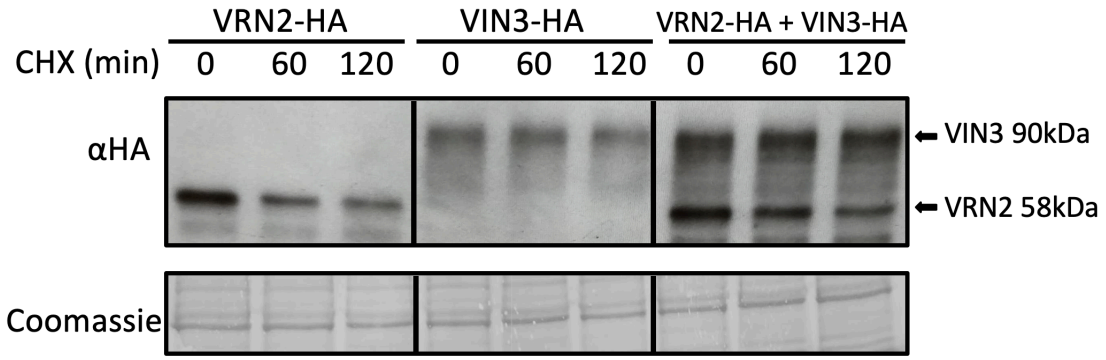

FIGURE 4.3 VRN2 levels decrease irrespective of VIN3 co-expression *in vitro*

Western blot with HA antibody showing an *in vitro* cyclohexamide (CHX) chase in a rabbit reticulocyte lysate system. VIN3-HA levels are consistent over the time course whereas VRN2-HA is degraded over time. When VIN3 and VRN2 are in the same reaction VRN2 is still degraded, meaning it is unlikely VIN3 is the cause of VRN2 stability during vernalization. Coomassie shows equal protein loading.

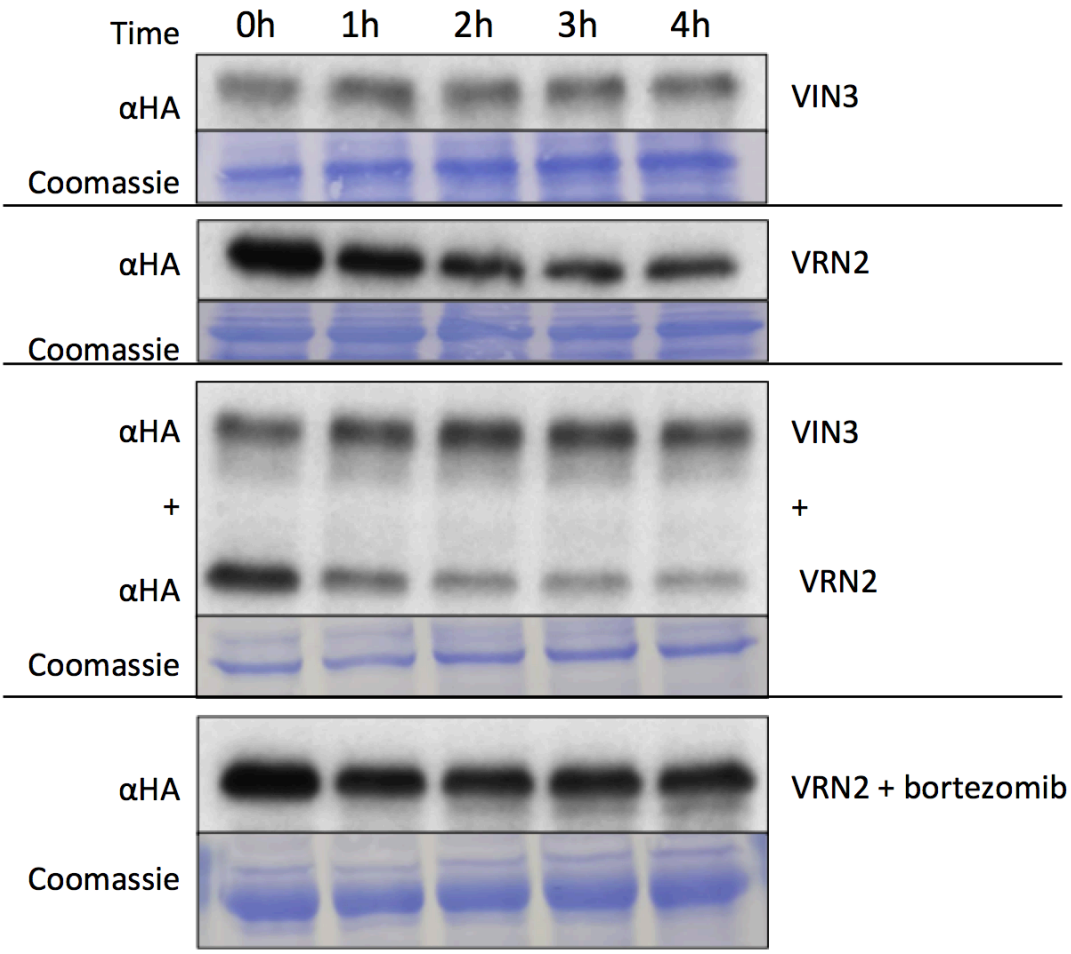

FIGURE 4.4 VRN2 is degraded over a 4 hour period in the presence of VIN3 *in vitro*

Western blot showing an *in vitro* cyclohexamide (CHX) chase. VIN3-HA levels are consistent over the time course whereas VRN2-HA is degraded over time. In the presence of bortezomib VRN2-HA becomes stable. When VIN3 and VRN2 are in the same reaction VRN2 is still degraded over the time course to low levels, indicating VIN3 does not affect VRN2 stability. Coomassie shows equal protein loading. VIN3-HA is 90kDa. VRN2-HA is 58kDa.

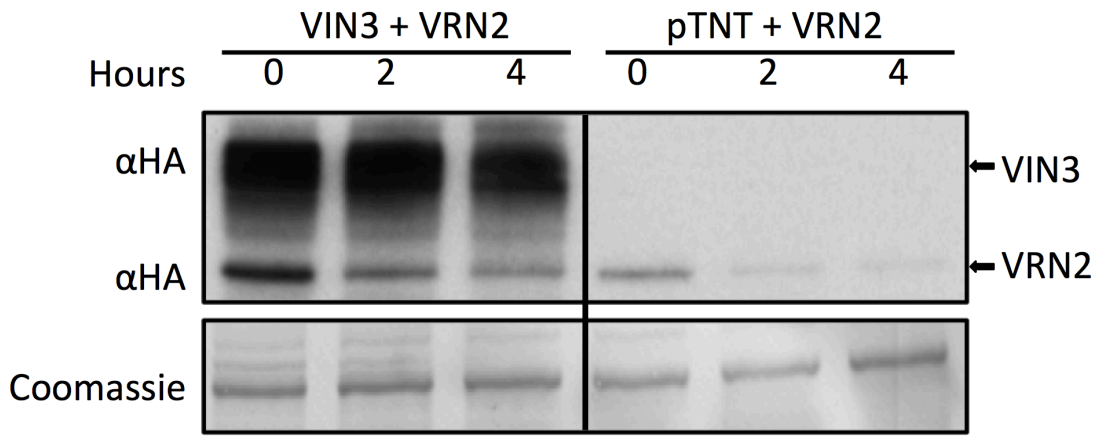

FIGURE 4.5 VRN2 is degraded over a 4 hour time course *in vitro* in the presence of high levels of pre-synthesized VIN3

Western blot showing an *in vitro* cyclohexamide (CHX) chase. Pre-synthesised VIN3 was added to the reaction from the beginning and empty pTNT vector was used in the control reaction. VIN3-HA levels are consistent over the time course whereas VRN2-HA is degraded over time. When VIN3 and VRN2 are in the same reaction VRN2 is still degraded over the time course to low levels, indicating VIN3 does not affect VRN2 stability. Coomassie shows equal protein loading. VIN3-HA is 90kDa VRN2-HA is 58kDa.

4.3 The effect of VIN3 on VRN2 stabilization *in vivo*

Although VIN3 was not seen to stabilize VRN2 *in vitro*, it might not be the case *in vivo*. This could be due to limitations of the rabbit reticulocyte lysate system. The rabbit system enzymes are not identical to plant enzymes, thus plant PRT6 may be more sensitive to Nt-shielding, or VIN3 and VRN2 may require other protein modifications not present in this system for the interaction. The HA tags at the C-terminus of the proteins could block VIN3 shielding of the VRN2 N-terminus and other PCR2 complex proteins may be required for VIN3 to shield the Nt-MC of VRN2. Therefore, the effect of VIN3 on VRN2 stabilization was investigated *in vivo*. To do this an estradiol inducible VIN3 construct was produced. This enabled comparison of uninduced and induced plants to test the effect of conditional *VIN3* expression on VRN2 stability *in vivo*.

In order to clone *VIN3*, seedlings were exposed to 2 weeks of vernalization, since *VIN3* is only induced in the cold, and the plant T-RNA was extracted for cDNA synthesis. PCR was used to add the *att*B sequence to the VIN3 coding sequence so it could be used in Gateway cloning (the addition of the HA tag by PCR was unsuccessful). The successful PCR amplicon was purified using PEG and the BP Gateway reaction was performed in order to insert *VIN3* into the pDONR221 vector. The correct insert was confirmed by restriction digest with BsrGI restriction enzyme and also confirmed by sequencing using M13 F, M13 R primers. *VIN3* was mobilized from pDONR221 into per8GW (Coego et al., 2014) by the LR reaction and correct constructs were confirmed with

restriction digest. The per8GW vector allows manipulation of *VIN3* expression as it allows *VIN3* expression to be induced by estradiol. The estradiol is a way of inducing *VIN3* without needing cold treatment as the vector contains the XVE estrogen receptor that mediates inducible gene expression (Zuo et al., 2000).

The per8GW-VIN3 construct was transformed into *Agrobacterium tumefaciens* (strain GV3101pMP90) and then dipped into *A. thaliana*. Transgenic MC-VRN2-FLAG lines in a Ler *vrn2-1 fca-1* background were used, as these contain FLAG-tagged VRN2 and would allow detection of VRN2 levels following VIN3 induction. The MC-VRN2-FLAG lines were selected until plants were homozygous for the *VIN3* insert (see methods section 2.2.6). At least one individual from three different independent lines (1A, 2E, 5 B/C/E) showed 100 % hygromycin resistance. Seedlings of these lines along with VRN2-FLAG control were grown for 6 days and then treated with either DMSO control or with DMSO + estradiol in liquid MS for 24 h and then frozen in liquid nitrogen prior to protein extractions. Western blotting (FIGURE 4.6) showed that there was a possible stabilization of VRN2 in estradiol-treated plants in all lines, with 2E and 5E showing the most promising results. However, it was not conclusive as there was only slight variation in the intensity of the protein band for 1A, 5B and 5C for this preliminary blot, cDNA analysis was not done as this experiment was repeated for lines 1A, 2E and 5E with the inclusion of material collected for cDNA analysis to confirm VIN3 expression.

The estradiol treatment was repeated with lines 1A, 2E and 5E, collecting samples at 24, 48 and 72 h to see the effect of length of *VIN3* induction on VRN2 stability. The samples were put on a moving plate to ensure even distribution of estradiol to all seedlings. Once again, seedlings were frozen in liquid nitrogen, this time samples were split into two, for protein and RNA extractions. There was no tag for the VIN3 so expression could only be detected by reverse transcription (RT)-PCR. cDNA was synthesized from RNA and PCR was performed using *VIN3* specific primers to confirm *VIN3* induction by estradiol treatments.

For 24 h estradiol treated seedlings the RNA analysis showed *VIN3* expression was not detected in untransformed VRN2-FLAG plants (FIGURE 4.7). The VRN2-FLAG plants do not have *VIN3* as they haven't experienced cold. *VIN3* transcript levels were similar in all estradiol-induced plants, although estradiol treatment did induce more *VIN3* expression in lines 1A and 2E compared to plants not treated. The transgenic plants containing the *VIN3* construct show *VIN3* expression with or without estradiol treatment, indicating there is some 'leaky' expression of *VIN3* at low levels all the time so it is difficult to assess if this is having an effect on VRN2. *ACTIN2* and *VRN2* were included as controls and bands shows consistency across treatments, so any effect on protein stability would be post-translational (i.e. not transcriptional). *ACTIN2* expression appeared to be slightly varied but this could have been due to variations in cDNA production and the amount of template present. The western blot showed no difference in VRN2-FLAG stability between estradiol treated or non-treated seedlings, i.e. with or without *VIN3* induction. In line 2E

there appeared to have some increased stability of VRN2 with estradiol. However, in the absence of the VIN3 construct VRN2 also appeared to increase with estradiol treatment (FIGURE 4.7), although the coomassie did show slightly more loading here. The results do not support the hypothesis that VIN3 is the cause of VRN2 stability.

Finally, a cyclohexamide chase was conducted on the estradiol inducible VRN2 line 2E with VRN2-FLAG (with no inducible VIN3) as a control with 24 h +/-estradiol treatment. Cyclohexamide was added and samples were then taken 0, 2, 4 and 8 h. cDNA analysis shows that *VIN3* is not expressed in the VRN2-FLAG line and *VIN3* is expressed in 2E only with the addition of estradiol (FIGURE 4.8). Western blotting showed that VRN2 levels remain fairly constant through the time course in all treatments. Estradiol treatment does not cause higher VRN2 levels in line 2E but does in the control, which is not as expected. Estradiol should not have an effect on VRN2 levels in the control. The presence of VIN3 in estradiol treated plants (2E) does not cause an increase in VRN2 stabilization over time. Overall the results do not support the hypothesis that VIN3 causes VRN2 stability by shielding the N-terminus *in vivo*, which confirms observations from the *in vitro* assay.

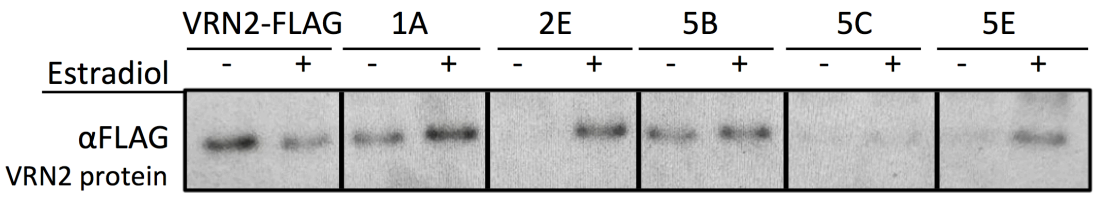

FIGURE 4.6 VRN2 protein stability in estradiol inducible VIN3 lines

Estradiol inducible *VIN3* lines were treated with estradiol in ½ MS solution for 24 h. Results show that VRN2 was present at higher levels in line 2E and 5E. In 1A, 5B and 5C the VRN2 levels appeared to be similar +/- estradiol. VRN2 was more stable in the control without estradiol. VRN2-FLAG is 70kDa.

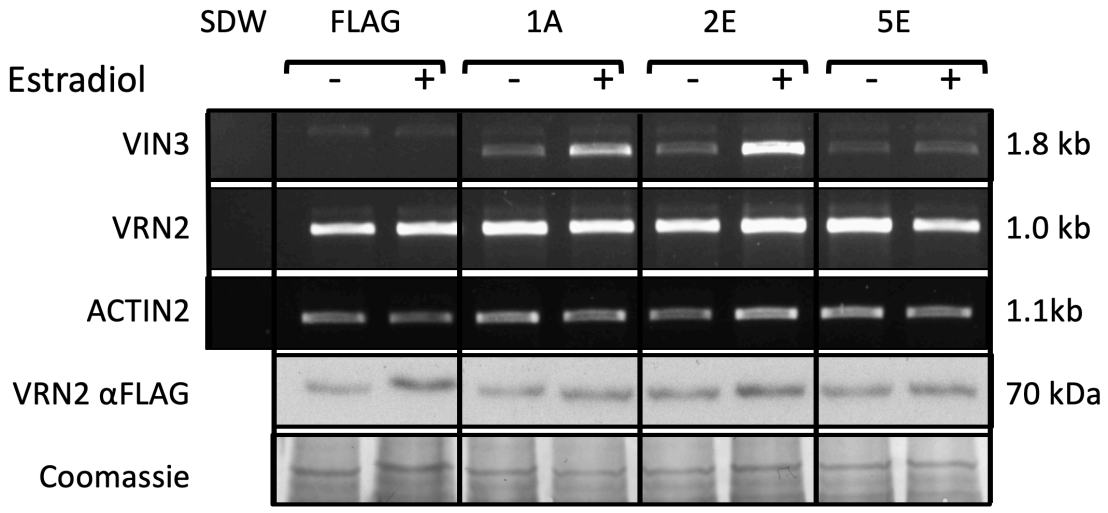

FIGURE 4.7 VRN2 is not more stable in the presence of VIN3 *in vivo*

Western blot of VRN2-FLAG in seedlings expressing VIN3 driven from an estradiol inducible promoter, +/- estradiol showed that VRN2 levels did not increase in the presence of VIN3, indicating VIN3 is unlikely to be the cause of VRN2 stability *in vivo*. RT-PCR from total mRNA extracted from +/- estradiol treated seedlings showed that *VIN3* was induced more in lines 1A and 2E, although *VIN3* was still expressed in seedlings not treated with estradiol. RNA levels of *VRN2* and *ACTIN2* are also shown. Coomassie show equal protein loading.

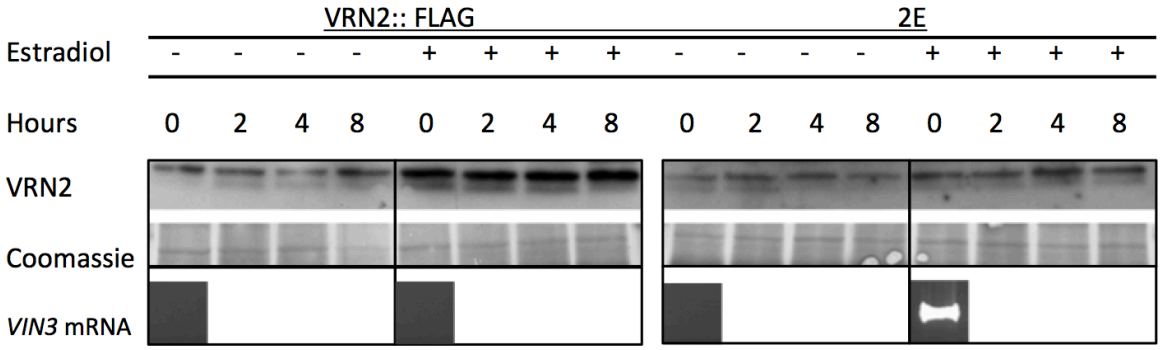

FIGURE 4.8 Ectopic induction of VIN3 does not stabilise VRN2

Western blot of VRN2-FLAG in seedlings expressing VIN3 driven from an estradiol inducible promoter, +/- estradiol, sampled at 0, 2, 4 and 8 h after the addition of cyclohexamide. VRN2-FLAG levels appear constant across the time course. There is more VRN2-FLAG present in estradiol treated control seedlings as well as in inducible VIN3 2E seedlings. RNA levels of *VIN3* at 0 h are also shown. These results suggest VIN3 is not causing the stabilization of VRN2 *in vivo*.

4.4 *vin3* mutant confirmation

As VIN3 was a focus in this project, *vin3* T-DNA mutant seeds were ordered from NASC (SALK_004766). If a role for VIN3 in the stabilization of VRN2 had been demonstrated, then further experiments could have been done using *vin3* mutant plants. These resources could however, still be useful in future experiments to study *vin3* phenotypes in flowering, and possibly in cHIP experiments to see how the mutant affects methylation at *FLC*.

In order to genotype the seedlings, primers were designed to the left border and right border of the T-DNA insert and one from the middle of the insert. PCR confirmed the SALK_004766 T-DNA mutant was homozygous for *vin3* (FIGURE 4.9). Homozygous plants were grown under 2 weeks vernalization and leaf samples taken. Total RNA was extracted and cDNA synthesized. The cDNA analysis using PCR primers from the start and end of the CDS confirms a total gene knockout. The *vin3* mutants have been crossed with MC-VRN2-GUS (in Ler), MC-VRN2-FLAG (in Ler) and *prt6-1* (in Col-0), and seeds have been collected. These were to be used in future experiments to study VRN2 localization and VRN2 stabilization if VIN3 did have an effect on VRN2 stability, with the hypothesis being that if VIN3 stabilized VRN2, then VRN2-FLAG would not accumulate in the cold in the *vin3* mutant. As there was lack of evidence to support the hypothesis that VIN3 shielded the N-terminus of VRN2 (FIGURES 4.3, 4.4, 4.5, 4.6, 4.7, 4.8) this line of work was not continued.

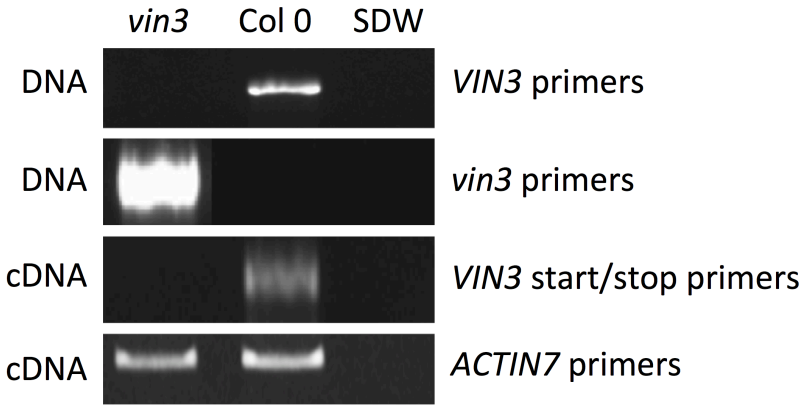

FIGURE 4.9 Confirmation of *vin3* mutant in Col-0

PCR from the left and right border and including the tDNA insert confirms the vin3 mutant using genomic DNA.
Full length PCR from cDNA also confirms the *vin3* total knockout mutant. *ACTIN7* PCR was used as a control.

4.5 Discussion

The data in the previous chapter revealed that the N-end rule pathway restricts VRN2 accumulation under non-vernalizing conditions but VRN2 levels are enhanced during vernalization. The increase in VRN2 levels cannot be explained by changes in *PRT6* expression, which remains unchanged during vernalization (Gibbs unpublished). In this chapter one possible mechanism behind VRN2 accumulation and stabilization was explored. *VIN3* is transcriptionally induced by low temperatures and is known to interact with the VRN2-PRC2 complex and so the hypothesis that VIN3 might protect VRN2 from degradation through shielding the N-degron was conceived. However, VRN2-HA remained unstable during *in vitro* protein degradation assays where *VRN2* and *VIN3* were co-expressed and when VIN3 was synthesized and subsequently mixed with the VRN2 reaction. In the *in vivo* experiment, it was found that ectopic expression of *VIN3* under the control of an estradiol inducible promotor was insufficient to stabilize VRN2-FLAG. Thus, there was no evidence to support the hypothesis that VIN3 prevents VRN2 degradation.

There are other genes that have been found to be up-regulated in the cold and downregulated on return to warm conditions such as ALCOHOL DEHYDROGENASE1 (ADH1) (Jarillo et al., 1993) and PLANT CYSTEINE OXIDASE1 (PCO1) (Gibbs et al., 2018). These genes behave in a similar manner as *VIN3*. Perhaps one of these proteins is responsible for VRN2 N-degron shielding, although there is not yet evidence of them interacting with

VRN2. Some cold-responsive genes are also up regulated during hypoxia (Gibbs et al., 2018). Perhaps VRN2 is stabilized due to shielding by one of the genes induced by hypoxia. Alternatively, as VRN2 is regulated by the gas sensing Cys/Arg N-end rule pathway, it could be stabilized due to the fact there are low oxygen and nitric oxide levels during vernalization, and so the gas-sensing step is prevented, halting VRN2 degradation. A recent investigation supporting this theory has independently tested this hypothesis and evidence suggests that there is a connection between the cold and hypoxia signalling that may explain why VRN2 is stabilized (Gibbs et al., 2018). The mechanism that leads to VRN2 stabilization has yet to be determined in full and further study is needed to verify the link between cold temperatures and the low oxygen signalling pathway.

The *vin3* T-DNA mutant SALK_004766 was confirmed by PCR and RT-PCR and this was crossed with MC-VRN2-GUS and MC-VRN2-FLAG to produce seeds that could be used in future experiments examining the effects of *vin3* plants on VRN2 stability and localization. Whilst this work has not found evidence to support the hypothesis that VIN3 shields the N-degron of VRN2, there still is further work required to see if there is N-degron shielding by an alternative protein, whether hypoxia is the cause of VRN2 stability, whether decreased PCO activity leads to VRN2 stabilization during vernalization (as has recently been proposed by Gibbs et al., (2018), or there is another mechanism we have not yet identified. In the previous chapter VRN2 was confirmed to be the only Su(z)12 homologue in plants to be a substrate of the Cys/Arg N-end rule pathway (Figure 3.4). The final aim of this project is to see

how VRN2 evolved to become part of the N-end rule pathway and this is discussed in the next chapter.

Chapter 5

Investigating how VRN2 evolved as an N-end Rule Pathway Substrate

5.1 Introduction

The PRC2 complex is highly conserved among plants and animals (Hennig and Derkacheva, 2009). Plant Su(z)12-like proteins, VRN2, EMF2 AND FIS2 (Su(z)12-like proteins) associate with the other core protein components to make different PRC2 complexes (FIGURE 1.8) targeting different gene networks. VRN2 is part of the PRC2 complex targeting vegetative development, associating with *SWINGER* (*SWN*), *FERTILIZATION INDEPENDENT ENDOSPERM* (FIE) and *MULTICOPY SUPPRESSOR OF IRA1* (MSI1) proteins (Wood et al., 2006, De Lucia et al., 2008). In this chapter the evolution of VRN2 is discussed, investigating how VRN2 became co-opted to the N-end rule pathway, introducing a novel function for the PRC2 complex. This will enable us to examine how the N-end rule pathway regulation of the VRN2 by the N-end rule pathway has played a part in plant development and evolution through the coupling of VRN2 stability to environmental sensing.

Gene duplications are a major contributor to genome evolution, increasing genetic diversity, potentially having an effect on morphology and physiology and bringing about novel phenotypes (Soltis and Soltis, 2016). Whole genome duplications are common in plants and result in plants with multiple sets of their genomes (polyploids), for example the modern wheat variety *Triticum aestivum* possesses 3 genomes (AABBDD), an allopolyploid (six copies of its genome make this a hexaploid) (Qiu et al., 2017a).The most recent polyploidy event in evolutionary history is specific to Brassicas (Qiu et al., 2017b).

Duplication of a gene can result in divergence of that gene, the ancestral function of the gene is lost or altered and a novel function or regulation is acquired (Moore and Purugganan, 2005). Chen et al. (2009) proposed that the VEF-domain gene family consisting of VRN2, EMF2 and FIS2 has arisen as the result of gene duplication and subsequent diversification of gene sequences leading to the divergence between plants and animals.

The Polycomb Group (PcG) proteins were originally characterized in *Drosophila* and they epigenetically regulate gene expression by forming complexes that repress target genes (Chen et al., 2009). VRN2 (found in plants) is a homologue of Su(z)12, a PcG protein that is found in animals (Butenko and Ohad, 2011). Su(z)12 forms a complex with Extra sex combs (Esc), P55 and Enhancer of zeste (E(z)) to form the PRC2 complex (Kuzmichev et al., 2002, Muller et al., 2002). VRN2 forms the PRC2 complex with SWN (homologous to E(z)) (Chanvivattana et al., 2004), FIE (homologous to ESC) (Ohad et al., 1999) and MSI1 (homologous to p55) (Hennig et al., 2003). In Drosophila there is only one Su(z) 12 but in Arabidopsis there are three homologues; VRN2 (Gendall et al., 2001), EMF2 (Yoshida et al., 2001) and FIS2 (Ohad et al., 1999). VRN2, EMF2 and FIS2 can all form part of a PcG complex but they have all evolved to target different gene networks. As mentioned previously (chapter1.4.4), of the three Su(z)12 homologues found in plants, VRN2 is the only homologue that begins with an MC-terminus and the only one found to be regulated by the Cys/Arg N-end rule pathway.

The N-end rule pathway is found in species other than plants but VRN2, along with ERFVIIs are the only N-end rule substrates found in plants to date ((Licausi et al., 2011, Gibbs et al., 2014b)). The aim of this part of the study was to investigate whether MC-initiating Su(z)12s) (VRN2-like proteins), exist in flowering plants other than Arabidopsis by analysing and aligning Su(z)12-like protein sequences from a range of species. It was previously considered that a VRN2 protein was only found in Brassicaceae (Chen et al., 2009). By doing this analysis, VRN2-like proteins regulated by the N-end rule might be identified in plants other than dicots. Adding more ancient plants such as gymnosperms and mosses to the alignments may also identify when and how VRN2 and VRN2-like MC-initiating Su(z)12 variants evolved. Further, part of the mechanism behind gaining novel N-end rule substrates was investigated by observing if changing the N-terminus of a protein to an MC would bring it under N-end rule regulation. If possible, it may have implications in controlling stress tolerance, flowering and other important pathways in crop plants to improve their vigour and yields.

5.2 Sequence alignments of putative EMF2 and VRN2-like protein sequences from diverse land plants species

VRN2 has been proposed to have evolved following the duplication of an ancient EMF2-like gene, resulting in a new Su(z)12 homologue in the dicots of the Brassicacea family (Chen et al., 2009). It has also been suggested that FIS2 evolved from VRN2 in the same way (Qiu et al., 2017b). EMF2-like protein sequences (orthologous genes evolved from a common ancestral EMF2-like gene) from diverse clades of angiosperms were identified by BLAST searches using *Arabidopsis* VRN2 and EMF2 proteins as a reference. These sequences were then aligned with Clustal Omega and it was observed that many of them have an internal MC amino acid sequence ~20 amino acids downstream of Met1 (FIGURE 5.1A). Due to this observation, EMF2-like and VRN2-like protein sequences from representative land plant clades were aligned in order to investigate more ancient plant species to observe when the MC arose. Here a selection of sequenced plant genomes from spermatophytes (angiosperms and gymnosperms), one from the lycophytes and one from the bryophytes were taken from the NCBI database and aligned using Clustal W software (FIGURE 5.1B). All of the identified EMF2-like proteins have an Nt-cap region present, whilst the Nt-cap region was absent in all of the VRN2-like proteins. Alignments also show conservation of key functional VEF and C2H2 zinc finger domains but only the N-terminus alignment is shown as this was to find the emergence of the N-degron at the Nt. The Nt-MC of *Arabidopsis* VRN2 protein aligns with EMF2 at amino acid 21. This reveals that the VRN2 N-terminus is similar to EMF2 but with the N-

cap removed leaving an exposed MC N-terminus, which suggests a gene duplication and truncation event of an ancient EMF2-like protein lead to the formation of VRN2.

Sequence alignment from diverse clades of the angiosperms revealed VRN2-like proteins throughout flowering plants. The factor used here to determine if something is a VRN2-like protein is the presence of the MC at the N-terminus as well as the similarity of sequences. In non-angiosperms the internal MC was found in EMF2-like proteins in gymnosperms but generally not in other taxa such as *Physcomitrella patens* and *Selaginella moellendorffii*. The internal MC is absent in some extant angiosperm clades, suggesting it is not functionally important in EMF2 but it was important as a precursor for the generation of VRN2. These analyses show that the MC sequence is present in the basal angiosperm *Amborella trochopoda* and reveal that the MC sequence was fixed in ancient EMF2 orthologues before angiosperms emerged, as shown in the gymnosperm *Pinus jeffreyi* and *Ginkgo biloba* sequences. This supports the hypothesis that an ancient EMF2 orthologue could have duplicated and the Nt-cap removed to give the capacity of VRN2-like proteins to be coupled to the N-end rule pathway. Therefore, giving plants the capacity over time to become O_2 and NO sensing organisms via the Cys/Arg N-end rule.

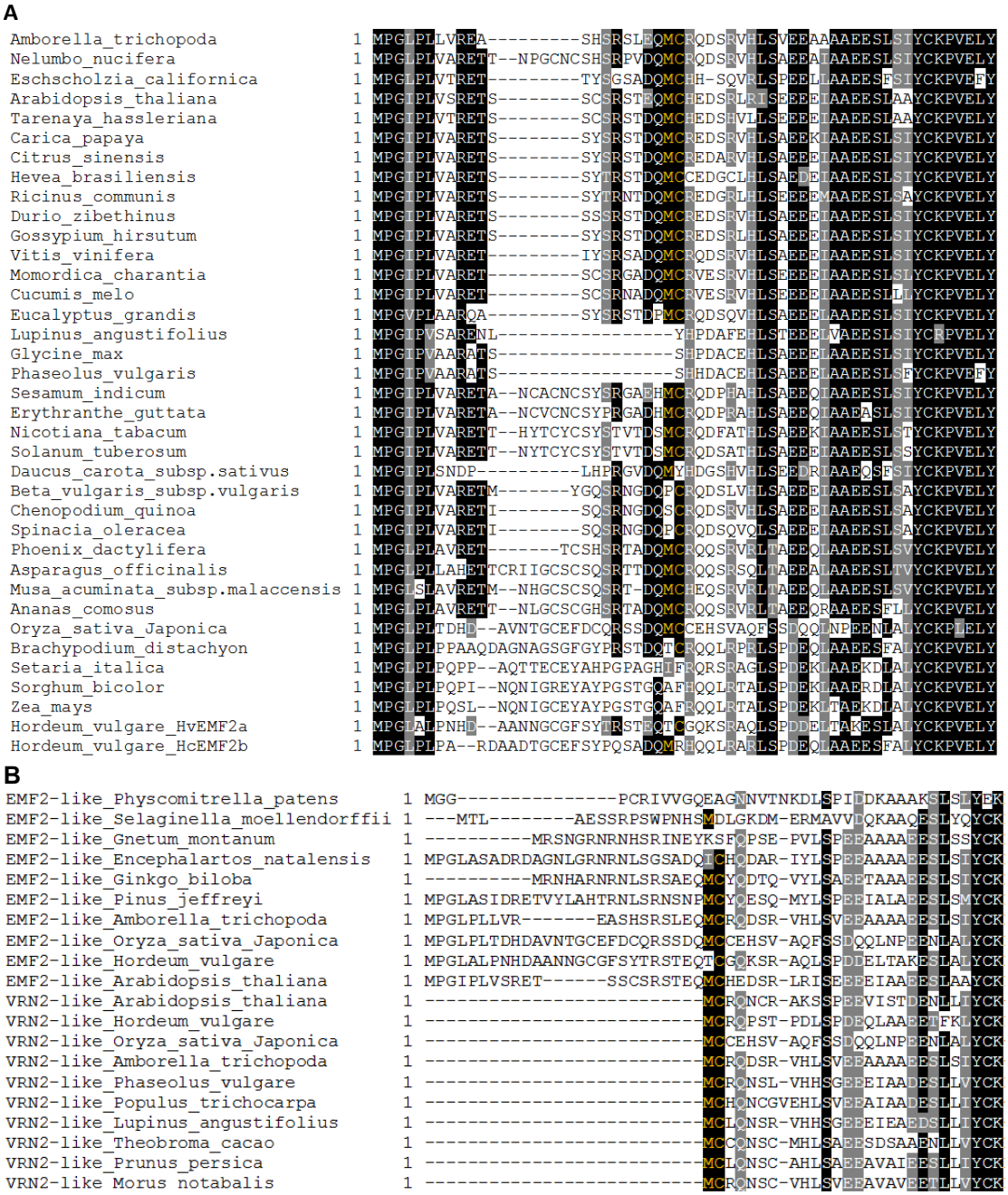

FIGURE 5.1 Alignment of EMF2 orthologous sequences representing diverse clades of flowering plants

A. Sequence alignment of the N-terminus of EMF2 proteins from angiosperms showing the position of the internal MC dipeptide highlighted in yellow.

B. EMF2 and VRN2 orthologous sequences (genes evolved from a common ancestral EMF2-like gene) representing diverse clades of land plants. The VRN2 MC N-terminus aligns with an internal MC in EMF2-like proteins highlighted in yellow.

Black and grey shading denotes identical and similar amino acids respectively. Sequences were obtained from NCBI. Alignments were conducted at Clustal Omega using the default settings. https://www.ebi.ac.uk/Tools/msa/clustalo/

Alignments were then converted to this output using Boxshade 3.21, with fractional sequences that must agree for shading set at 1.

5.3 A VRN2-like protein exists in Barley

Since the Su(z)12 proteins in animals and basal land plants do not initiate MC-, it was decided to investigate how Su(z)12 was coupled to the N-end rule pathway specifically in angiosperms. Recently it has been reported that EMF2 orthologues exist in Medicago of the Fabaceae family (Jaudal et al., 2016) and also in the monocot rice (Yang et al., 2013). Orthologues have also been found in other monocots including wheat and barley (Chen et al., 2009). Barley (*Hordeum vulgare*) is a monocot species that is distantly related to *Arabidopsis* but upon close analysis of the N-terminus of barley EMF2-like proteins, it was revealed to possess a VRN2-like protein, annotated as HvEMF2c, which initiated MC. It was decided to clone HvEMF2c in order to test whether this protein might be regulated in a similar way to Arabidopsis VRN2; i.e. whether a VRN2-like protein in plants other than the Brassicaceae is co-opted to the N-end rule pathway.

Barley cDNA was generated from total RNA extracts and used as a template to amplify the full length HvEMF2c by PCR. The product was then ligated into the pTNT vector and confirmed by restriction digest with Eco-RI-HF and KpnI-HF and by sequencing. An *in vitro* protein degradation assay was performed using MC-HvEMF2c, MA-HvEMF2c and MC-HvEMF2 supplemented with bortezomib. The samples were incubated for 30min and then the CHX and Bortezomib/SDW was added. Samples were taken at 0, 60 and 120min. Western blotting shows that MA-HvEMF2c is stable, highlighting the importance of cysteine as the destabilizing residue present at the Nt. The addition of the 26S proteasome inhibitor bortezomib stabilized MC-HvEMF2c,

suggesting N-end rule regulation. MC-HvEMF2c is degraded over time (FIGURE 5.2) showing a similar pattern to VRN2 degradation (FIGURE 3.4). This supports the hypothesis that Mc-HvEMF2c is a substrate of the N-end rule pathway and VRN2-like MC-initiating proteins exist and are regulated by the N-end rule pathway in plants other than Brassicas. The results confirm *in vitro* that HvEMF2c has a functional MC N-degron that is likely modified post-translationally, causing it to be degraded over time. The fact that MC-HvEMF2c is degraded agrees with the hypothesis that an N-end rule regulated variant of Su(z)12 is conserved in flowering plants. Previously VRN2 was only shown to be a substrate of the N-end rule pathway in dicots but results here show similar regulation in monocots also. Data presented in this chapter suggests that oxygen and nitric oxide sensitive Su(z)12 variants are not only found in Brassicaceae but are present throughout the angiosperms. Hypoxia treatments a nitric oxide scavenger cPTIO studies observing protein stabilization/degradation would confirm this hypothesis further. This result may have importance in increasing yield in crop species, as it gives us insight to how flowering is controlled in cereals.

HvEMF2c may be a functional orthologue of VRN2 as it is also a substrate of the N-end rule pathway, but was likely annotated as HvEMF2c, as the main body of the gene/protein shares more similarity with EMF2. In conclusion, a VRN2-like protein from barley, a monocot species distantly related to *Arabidopsis*, was confirmed *in vitro* to have a functional Cys2 derived N-degron. This suggests that O_2-sensitive Su(z)12 variants are present throughout flowering plants. Future work could study expression of the

HvEMF2c protein in *Arabidopsis* so protein degradation could be observed *in planta* to confirm this as a VRN2-like protein, check functionality and confirm it as a substrate of the N-end rule pathway *in vivo*.

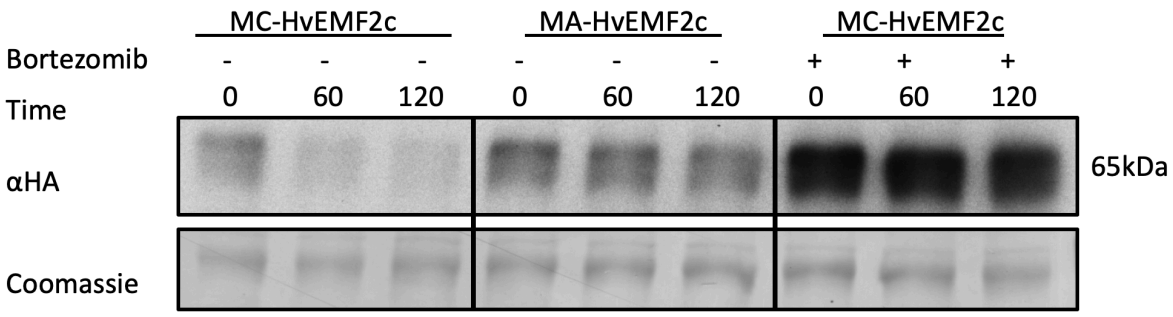

FIGURE 5.2 Barley EMF2c is a substrate of the Cys/Arg N-end rule pathway *in vitro*

Western blot showing an *in vitro* cyloheximide (CHX) chase of WT and mutant (Ala2) variants of the barley VRN2-like protein HvEMF2c (+/- bortezomib; BZ). MC-HvEMF2c-HA is degraded over time but stabilized with the addition of the proteasome inhibitor Bortezomib. MA-HvEMF2c-HA is stable. Coomassie staining shows equal loading.

5.4 Can an EMF2 substrate of the Cys/arg N-end rule pathway be created by altering the amino acid residues at the N-terminus?

N-degrons comprise of a destabilizing Nt-residue, a Lys for ubiquitylation and an N-terminal protein structure that exposes the N-terminus for interaction with other proteins (Gibbs et al., 2014a). EMF2 has a conserved lysine residue towards the N-end at amino acid 47 (FIGURE 5.1) and it shares sequence similarity to VRN2 and so could have a similar tertiary structure leaving the N-terminus accessible. WT EMF2 has proline (an N-end rule stabilizing residue) as the second amino acid at the Nt. By altering MP-EMF2 N-terminus to MC-EMF2 and assessing protein stability, an attempt was made to create a novel Cys/arg N-end rule substrate.

In order to do this *Arabidopsis* cDNA was generated from total RNA extracts. This was used as a template to amplify the full length EMF2 gene by PCR. Primers were used to amplify the WT MP-EMF2 and to amplify an MC-EMF2 PCR product. The amplicons and pTNT vector were digested with Eco-RI and KpnI restriction enzymes and a ligation reaction was conducted for 16 h. Heat shock was used to transform the plasmid into DH5α *E.coli* and colonies were selected on LBA with Ampicillin. Colonies were then grown overnight, DNA extracted and digested with the same enzymes. The digests with the expected band patterns were sequenced and correct constructs were taken forward to the *in vitro* the rabbit reticulocyte lysate protein degradation assays. MC-VRN2-HA, MP-EMF2-HA and MC-EMF2-HA reactions were incubated for

30min and a CHX chase was performed. Bortezomib was added to the MC initiating sample of the gene. Samples were taken at 0, 60 and 120 min.

Western blotting showed that MP-EMF2-HA was stable over time (FIGURE 5.3), suggesting that it is not a substrate of the N-end rule pathway. This was expected because proline is a stabilizing residue of the N-end rule. The Cys mutated second amino acid MC-EMF2-HA also remained stable over time. This attempt to artificially create and N-end rule substrate by altering the N-terminus was unsuccessful, however this does not mean that another protein could not be manipulated in this manner. The way EMF2 protein folds may have shielded the MC terminus or the Lysine may be too far downstream or in the wrong position to allow ubiquitylation by PRT6. Whilst MC-EMF2-HA was degraded over the CHX chase, MC-EMF2-HA was stable with Bortezomib present, as expected, as this inhibits the 26S proteasome. These results suggest that a gene duplication event and a point mutation would not be the only factors in play during the divergence of the VRN2 gene to become co-opted to another regulatory pathway. This leads to the hypothesis that it was a gene duplication and truncation event, exposing the internal MC that has led to VRN2 N-end rule regulation and diverse function. This was investigated in the next section.

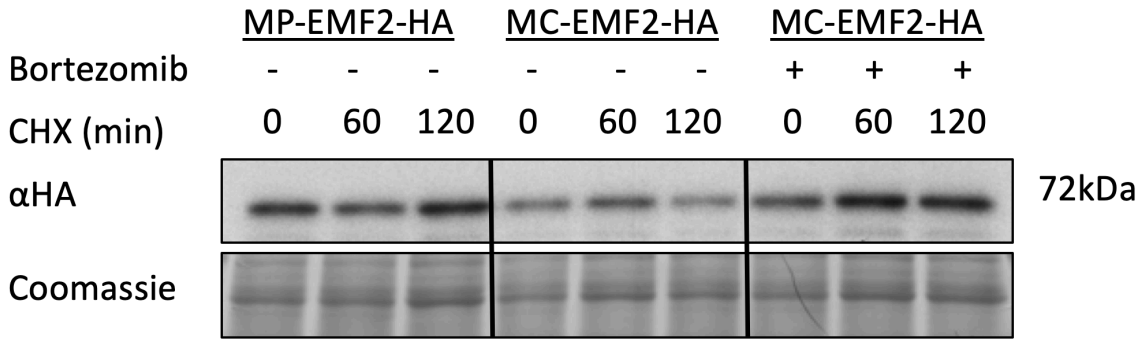

FIGURE 5.3 Can we create substrates of the N-end rule pathway by changing the N-terminus to MC?

Western blot showing an *in vitro* rabbit reticulocyte lysate system cyloheximide (CHX) chase of full-length *Arabidopsis* EMF2-HA (initiating MP) and mutant (Cys2) variant of *Arabidopsis* EMF2 protein (+/- bortezomib; BZ). Wild type MP-EMF2-HA is not a substrate of the Cys/Arg N-end rule pathway because it is stable. A substitution creating an MC N-terminus means the protein is present at slightly lower levels but it remains at the same levels across the time points. Treatment with the proteosome inhibitor bortezomib stabilizes MC-EMF2-HA protein to higher levels. Coomassie staining shows equal loading.

5.5 VRN2 likely evolved from and ancient EMF2-like protein due to a gene duplication and truncation event

The sequence alignments of EMF2 and VRN2 homologous sequences representing diverse clades of land plants (FIGURE 5.1 B), revealed that the internal MC dipeptide was fixed before the angiosperms emerged. The MC thus gave an ancient EMF2-like protein the capacity to become a VRN2-like oxygen and nitric oxide sensing protein, regulated by the Cys/Arg N-end rule pathway, following the loss of the Nt-N-cap sequence. Alignment of VRN2 and EMF2 protein sequences revealed the C2H2 and VEF functional domains are conserved but the Nt-N-cap is lost in VRN2 (FIGURE 1.9 and FIGURE 5.4 A and B). The MC terminus of VRN2 aligns with an internal MC at amino acid 21 of EMF2, downstream of Met1 at the C-terminal end of the Nt-cap. It was hypothesized in this study that there was a duplication event in the genome and a truncation in EMF2 during evolution that lead to the formation of VRN2. Then VRN2 became co-opted to the N-end rule pathway, leading to expansion and divergence in the regulation of genes in the same VEF family. A truncated version of EMF2 was created in this study, the new N-terminus beginning at amino acid 21, hence initiating with MC. The aim was to see if truncated EMF2c is regulated by the N-end rule pathway in the same way as VRN2.

Truncated EMF2 (tEMF2) was amplified from the pTNT vector containing the full-length gene (SECTION 5.4). This was done using primers targeted toward the internal MC starting at amino acid 21 and the end of the gene (FIGURE

5.4 B). These primers were also used to add restriction sites to either end of the tEMF2 amplicon. The truncated EMF2 gene was inserted into the pTNT vector transformed into DH5α *E.coli*. The MC-tEMF2-HA, MA-tEMF2-HA and MC-tEMF2-HA plus bortezomib reactions were incubated in a heat block for 30 minutes, cyclohexamide was added and then samples were taken at 0, 60 and 120 min. Truncated MA-tEMF2-HA was stable, as expected, as this does not have the MC terminus required to be a Cys/Arg N-end rule substrate. Remarkably, truncated (MC-) EMF2 degraded over time and was extremely unstable in vitro via its Nt-Cys2 residue (FIGURE 5.5 A). This supports the hypothesis that truncated EMF2 is a substrate of the N-end rule pathway and that VRN2 evolved from EMF2 via duplication and truncation.

The MC-tEMF2-HA should be stabilized by bortezomib if truncated EMF2 is targeted for degradation by the 26S proteasome via the N-end rule pathway. However, truncated MC-tEMF2-HA was degraded at all time points with bortezomib treatment (FIGURE 5.5 A). The experiment was repeated by performing another *in vitro* protein degradation assay except bortezomib was added from the beginning of the reaction instead of after the 30 min initial incubation and no cyclohexamide was added so protein could still be synthesized in the reaction. Interestingly, the truncated MC-EMF2-HA was stabilized with the bortezomib treatment (FIGURE 5.5 B). This suggests that tEMF2 not only is a substrate of the N-end rule pathway but it is actually degraded faster and has a higher turnover compared with VRN2. The evidence shows that MC-tEMF2-HA degrades faster than 30 min and is extremely unstable relating to its cysteine residue. However, if bortezomib is

added from the start of expression without adding cyclohexamide, this allows the truncated protein to stabilize and accumulate over the time course. The earlier alignments (FIGURE 5.1 B) show that the MC sequence was fixed before the emergence of angiosperms, i.e. in gymnosperms such as (*Pinus jefreyii* and *Ginkgo biloba*). This evidence, along with the evidence *in vitro* that tEMF2 is an N-end rule substrate, supports the hypothesis that VRN2 was likely recruited to the N-end rule pathway by a gene duplication and N-terminal truncation of an ancient EMF2-like protein.

5.4 A)

```
EMF2          1 MPGIPLVSRETSSCSRSTEQMCHEDSRLRISEEEEIAAEESLAAYCKPVELYNI
VRN2          1                     MCRQNCRAKSSPEEVISTDENLLIYCKPVRLYNI
                                    **.. .* . * ** *...* *  ***** ****
```

5.4 B)

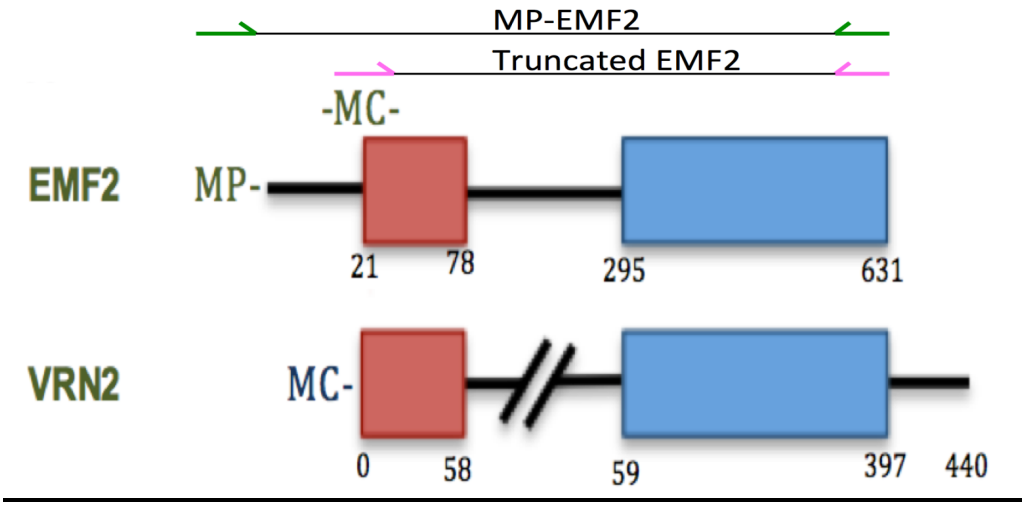

FIGURE 5.4 *Arabidopsis* VRN2 aligns with EMF2

A) Protein alignment from *Arabidopsis* showing that VRN2 aligns with EMF2 at an internal MC at amino acid 21 in EMF2 and the N-terminal MC N-degron of VRN2
B) Schematic showing VRN2 alignment with EMF2 at an internal MC. The EMF2 has an N-terminal cap. The C2H2 (in red) and VEF domain (in blue) are conserved and VRN2 has a C-terminal extension. Green arrows indicate primer position for PCR of full-length MP-EMF2 and Pink arrows are the primer position for truncated EMF2 amplification.

5.5 A)

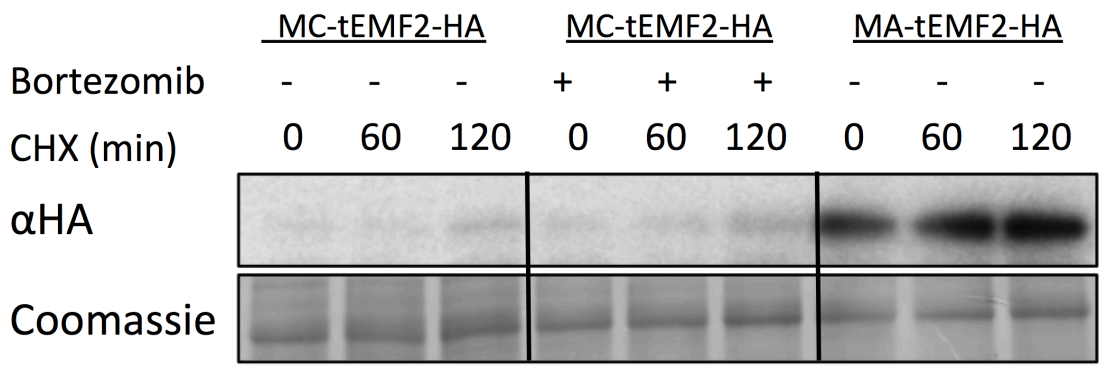

5.5 B)

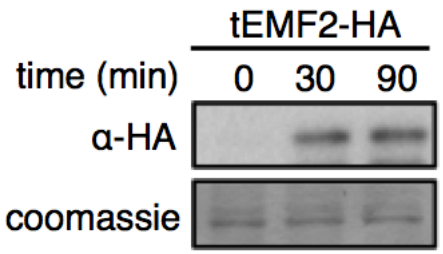

FIGURE 5.5. Truncated EMF2 (tEMF2) is a substrate of the N-end rule pathway *in vitro*

Western blots showing an *in vitro* CHX chase of full-length *Arabidopsis* EMF2-HA (initiating MP-), and WT or mutant (Ala2) tEMF2-HA, +/- BZ.
A) MC-tEMF2-HA is degraded over time and the MA-tEMF2-HA is stable as expected. The bortezomib treatment did not stabilise the MC protein which meant the protein may not be degrade by the 26s proteosome. Coomassie staining shows equal loading.
B) A western blot showing an in vitro protein degradation assay of MC-tEMF2-HA. Bortezomib was added at the beginning of incubation and no cyclohexamide was added. Interestingly here, MC-tEMF2-HA becomes stable over time. These results suggest that tEMF2 is a substrate of the Cys/Arg N-end rule pathway and is actually turned over faster than VRN2. tEMF2-HA is 72kDa.

5.6 Truncated EMF2 is a substrate of the Cys/Arg n-end rule pathway *in vivo*

In the previous section it was shown that tEMF2 was likely a substrate of the N-end rule pathway *in vitro*. In order to test the hypothesis that tEMF2 is a substrate of the Cys/Arg N-end rule pathway *in planta* tEMF2 was first inserted into the pE2c cloning vector to fuse the gene with a HA tag sequence needed for visualization using western blotting. An LR reaction was used to insert tEMF2-HA from pE2c into the pB2GW7 vector (which contains the 35S promotor for overexpressing the gene). Colony PCR and restriction digests were used to check the insert was correct. The tEMF2-HA pB2GW7 construct was then transformed into *Agrobacterium tumefaciens* by electroporation and Col-0 and *prt6-1* plants were transformed with tEMF2-HA pB2GW7 by floral dip. Seeds were collected and grown on ½ MS supplemented with Hygromycin. This was repeated until plants were found to be homozygous for MC-tEMF2-HA (see methods section 2.2.6).

Protein was extracted from 7-day-old seedlings and quantified using a Bradford assay. The western blot showed the tEMF2-HA could only be detected in the *prt6-1* mutants and not in the WT (FIGURE 5.6 A). Steady state levels of tEMF2 were high in the *prt6-1* mutant compared to WT, indicating that tEMF2-HA levels are likely linked to PRT6. There was no significant difference in mRNA levels judged from the *ACTIN7* control PCR. Coomassie staining showed there was equal loading. This result is as expected for N-end rule pathway regulation, since in normal conditions MC-

proteins are degraded by the 26S proteasome and in the *prt6-1* E3 mutant there would be no ubiquitylation and therefore no degradation by the 26S proteasome.

It is known that VRN2 becomes stabilized in the cold during vernalization (Wood et al., 2006). Earlier, cold-induced stabilization of VRN2 was shown to be related to the N-end rule (FIGURE 3.8). Here, tEMF2-HA stability was observed to see if it would become stable when subject to vernalization treatment. To test this hypothesis, seeds from two independent Col-0 lines (labelled 2.7 and 3.2) were grown for 7 days on ½ MS and then subject to 0, 2 or 2+1 weeks vernalization treatment (where 2+1 was 2 weeks vernalization at 5 °C short days, plus 1 wk at 22 °C long days). The results showed close similarity with how VRN2 behaves (FIGURE 5.6 B). Both lines showed an equivalent trend in protein stability levels. In long days at 22 °C MC-tEMF2-HA protein levels were low. With 2 weeks of vernalization the MC-tEMF2-HA protein levels accumulate. Once plants were returned to 22 °C, the protein was less abundant. Coomassie shows equal loading except in line 3.2 where there is more protein loaded at 0 and 2+1 weeks, but this does not have an effect on conclusions drawn from the western blot. *ACTIN7* mRNA transcript levels show consistency between lines.

These results suggest that tEMF2 is regulated in a similar way to VRN2, in response to cold. The *in vitro* outcomes corroborate the *in vitro* results and support a potential mechanism for the evolutionary recruitment of Su(z)12 to the Cys/Arg N-end rule pathway in angiosperms via gene duplication and a

truncation event leading to an exposed MC initiating N-degron in an ancient EMF2-like protein in angiosperms.

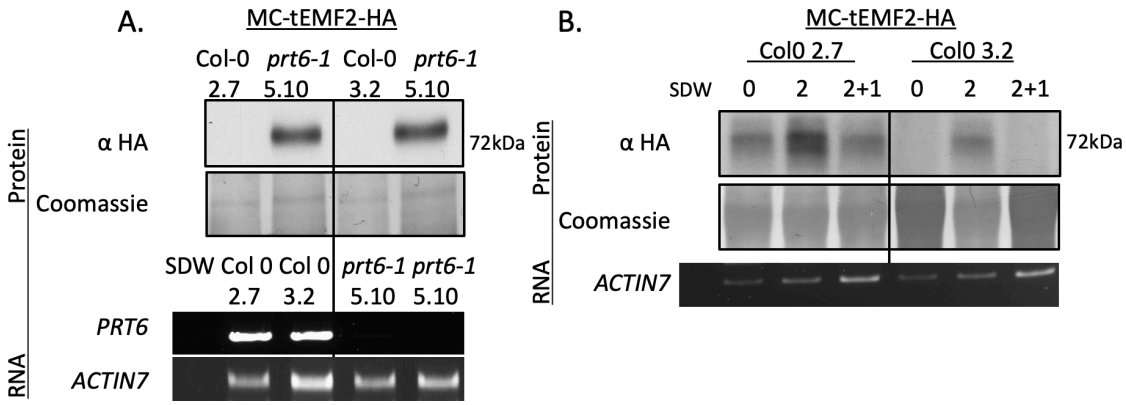

FIGURE 5.6 Truncated EMF2 is a substrate of the Cys/Arg N-end rule pathway *in vivo*

A) Western blot of *in vivo* steady state protein levels of truncated EMF2-HA (MC-tEMF2-HA) in Col-0 vs *prt6*-1. In Col-0 MC-tEMF2-HA is unstable in Col-0 whereas it is stable in the *prt6-1* E3-ligase mutant.
B) Western blot of *in vivo* protein levels of tEMF2 during 0, 2 and 2+1 weeks vernalization. Two independent transgenic lines are shown. MC-tEMF2-HA is stable under cold conditions but is unstable when returned to 22 °C. Coomassie staining shows that protein levels are not due to loading errors.

5.7 Discussion

The sequence alignments (Figure 5.1) revealed that the MC sequence was fixed in ancient EMF2-like proteins before the angiosperms emerged. The internal MC sequence in EMF2-like proteins can be found in other angiosperms such as *Amoborella trichopoda* and in some gymnosperms such as *Pinus jeffreyi* but not in the basal land plants. Until recently it was thought that MC-initiating VRN2-like proteins could only be found in the Brassicaceae family but MC-initiating EMF2-like proteins had been found in some monocots such as rice, wheat and barley (Chen et al., 2009). In this study a VRN2-like protein that has been annotated HvEMF2c in barley was found to be regulated by the N-end rule pathway *in vitro*. This protein behaved as VRN2 does *in vitro* and *in vivo*, as MC-HvEFF2c-HA was found to be unstable in protein degradation assays. These results indicate the VRN2-like proteins exist in plants other than the Brassicaceae. It is likely that the HvEMF2c protein has been mis-annotated and actually represents a barley orthologue of VRN2, however this would need to be tested *in vivo*. In this study an attempt was made to clone the truncated *Pinus jeffreyi* EMF2 into the pTNT vector, as was a gymnosperm that had an MC Su(z)12 homologue, but unfortunately cloning was unsuccessful. Different restriction sites, different competent cells and different growing conditions were tried but the gene inserted backwards. With more time a different pine species could have been used for the experiment or the experiment could have been tried on another gymnosperm species such as *Ginkgo biloba*. It would also be interesting to study the *Amborella trichopoda* EMF2 and examine if this showed similar

results. This would give us more insight into when VRN2 may have evolved from EMF2 because it could show that MC-initiating VRN2-like proteins in gymnosperms are regulated by the Cys/Arg N-end rule (i.e. before the emergence of angiosperms).

Taken together, the evidence in this chapter suggests that the evolution of VRN2 may have occurred when angiosperms emerged, to include monocots and dicots. It could even have occurred before the evolution of the angiosperms and further study could explore the possibility that Su(z)12-like proteins in gymnosperms or basal land plants behave in the same way as VRN2. Two Su(z)12-like genes have been found in rice (*Oryza sativa*) *OsEMF2a* and *OsEMF2b* (Hennig and Derkacheva, 2009, Luo et al., 2009), with OsEMF2b being found as part of the PRC2 complex. A VIN3-like protein OsVIL2 has been shown to directly interact with OsEMF2b and a null mutant of *OsEMF2b* causes late flowering (Yang et al., 2013). In the future it would be interesting to clone the *OsEMF2b* gene, in a similar approach as used for the *HvEMF2c* gene, to detect if OsEMF2b is regulated as VRN2 is, by the Cys/Arg N-end rule pathway. It could be speculated that there are more VRN2-like proteins in monocots that may have been mis-annotated due to sequence alignments appearing similar to EMF2 and not taking into account the Nt. More VRN2-like proteins could be regulated by the N-end rule pathway even if they do not function in exactly the same way due to the *FLC* gene not being present and vernalization not controlling flowering in all cereals. To test the function of the *HvEMF2c* gene in this study it could be put into *Arabidopsis* to see if protein stability is affected *in vivo*, to complement the results *in vitro*.

Further, phenotypic analyses such as flowering time assays could also be done to test *HvEMF2c* function and check if HvEMF2c can complement an *Arabidopsis vrn2* mutant. This could demonstrate it may have a similar function to VRN2 in the vernalization pathway.

The next part of the study showed that not all proteins can be regulated by the N-end rule pathway, even with manipulation to contain potential N-degron sequences (FIGURE 5.3). The full length EMF2 was not degraded over time and changing the WT MP N-terminus of full length EMF2 to an MC N-terminus did not introduce degradation by the 26S proteasome or allow it to become regulated in the same way as VRN2. Factors such as the position of the N-terminus in the tertiary protein structure and other residues downstream of the N-terminus can affect whether a protein can be modified post-translationally in a way to cause regulation by the N-end rule pathway. Interestingly though, the truncating MP-EMF2-HA to MC-tEMF2-HA showed a decrease in protein levels over time *in vitro* and this study provides evidence that not only was there a gene duplication event of EMF2 but there was also a truncation event to bring about the exposed MC N-degron, giving rise to VRN2. *in vivo* tEMF2-HA was stabilized in the *prt6-1* mutant and also stabilized during vernalization. This further supports the hypothesis that there was a duplication and truncation event leading to the evolution of VRN2 from EMF2. It would be interesting to see if the truncated EMF2 can complement the phenotypes of the *vrn2-5* mutants to test the functionality of the truncated EMF2 *in vivo*.

In summary, the work here has uncovered a novel mechanism plants have evolved for perceiving varied environmental conditions and responding with epigenetic changes to control development and flowering in angiosperms. This has been accomplished by the evolution of a gas-sensitive (Gibbs et al., 2018) N-degron in an ancient EMF2-like protein. Coupling of an Su(z)12 –like protein to the Cys/Arg N-end rule pathway has allowed the PRC2 complex to evolve new function in angiosperms via VRN2 and its regulation of flowering after vernalization. This may have facilitated the emergence of flowering as a reproductive strategy, particularly in colder climates, by directly linking PRC2 activity to the perception of the environment, whilst also being a starting point for further diversification of PRC2 function.

Chapter 6

Final Discussion

6.1 VRN2 is an N-end rule substrate

The N-end rule pathway is a specific branch of the UPS that is directed by which amino acid is present at the N-terminus (Gibbs et al., 2014a). It is highly conserved in Eukaryotes, having been studied in yeast (Bachmair et al., 1986), mammals (Davydov and Varshavsky, 2000) and plants (Gibbs et al., 2011, Licausi et al., 2011). There is also a variant of the N-end rule pathway in prokaryotes (Darwin, 2009). Only a few substrates have been identified in plants and prior to the work presented here, the ERFVII transcription factors were the only gas sensing substrates of the Cys/Arg N-end rule pathway found in plants (Gibbs et al., 2011, Licausi et al., 2011, Gibbs et al., 2014a). In this study, evidence shows that the Su(z)12-like PRC2 component, VRN2 is a substrate of the Cys/Arg N-end rule pathway *in vitro* (FIGURE 3.4) and *in vivo* (FIGURE 3.5) and its function is linked to flowering and plant development. The instability of VRN2 is related to its MC destabilizing Nt-residues as demonstrated by a C2A point mutation, which led to constitutive stablilization of VRN2. Stabilization with bortezomib indicated that VRN2 is degraded by the 26S proteasome, further supporting its regulation by the N-end rule pathway. VRN2 was stable in *prt6-1* and *ate1ate2* mutants, which are involved in ubiquitylation and arginylation of Cys/arg N-end rule pathway substrates respectively. Recently, Gibbs et al., (2018) used Methionine amino peptidase (MAP) on short polypeptides to remove the Nt-methionine to show plant cysteine oxidases (PCOs) can directly target cysteine residues at the Nt. They also show that PCO activity was reduced in roots of vernalized seedlings where NO is depleted. In the future, studying MAP activity and PCO

activity could provide more information about the oxygen sensing step of the Cys/Arg N-end rule pathway during vernalization and the regulation of VRN2 and other possible Cys/Arg N-end rule substrates.

6.2 VRN2 localization

Vernalization is the process whereby a plant delays flowering until it has experienced a prolonged period of cold, in order to flower in more favourable conditions in the spring (Song et al., 2012). *FLC* encodes a highly expressed MADS box transcriptional repressor protein, which negatively regulates genes that promote flowering, thus acts as a flowering repressor (Gendall et al., 2001). VRN2 forms part of the VRN2-PRC2 complex, which is a regulator of vernalization by the addition of the repressive H3K27me3 epigenetic mark to *FLC*, causing *FLC* suppression and thus allowing flowering.

Previous studies have found that *FLC* is predominantly expressed in regions of the plant that are mitotically active (i.e. the shoot and root apical meristems) and that these areas are the sites of cold perception where the epigenetic vernalization state occurs (Wellensiek, 1962, Sung and Amasino, 2004a). Greb et al. (2007) show VRN2 to be restricted to the meristems and vasculature and similar observations were made in this study (FIGURE 3.6). Although VRN2 is present in the same location as *FLC*, VRN2 may not always be suppressing *FLC*. VRN2 may be degraded too quickly for *FLC* repression and require the cold for it to be abundant enough to repress *FLC*, and VRN2 could have other functions. The root and shoot meristem are proposed to be

hypoxic parts of the plant (Considine et al., 2017) and so high VRN2 levels in these areas would also be expected, as low oxygen levels would mean cysteine could not be oxidized, thus leading to VRN2 stability. Histochemical staining of VRN2-GUS showed VRN2 stabilization throughout the plant in the *prt6-1* and *ate1ate2* mutants, suggesting that the N-end rule pathway restricts VRN2 to meristematic regions under normal growth conditions (FIGURE 3.6). Western blotting showed VRN2 abundance increased during vernalization, whereas mRNA levels remained unchanged (FIGURE 3.8). Once returned to 22 °C VRN2 was again depleted. Comparison of VRN2-GUS to FLC-GUS localization could indicate if VRN2 stabilization in response to cold is required throughout the plant to effectively silence *FLC*. Observing if VRN2 stabilization correlates with oxygen and NO levels could give more insight into why VRN2 is degraded or stable in certain tissues/cells. Recently, Gibbs, et al., (2018) showed root meristems had low NO levels during vernalization, which could be the reason for VRN2 and ERFVII stability in these regions.

VRN2 has previously been shown to be localized in the nucleus of plant cells (Gendall et al., 2001), and has also been found in the nucleoplasm (Hecker et al., 2015). This study confirmed VRN2 localization in the nucleus of root tips with YFP tag attached to the C-terminus (Figure 3.7). Further, the data here shows there was no difference in VRN2 protein levels observed between the confocal images of the Col-0 and *prt6-1* lines tested, in contrast to the results of VRN2-GUS western blots (FIGURE 3.5). Quantitative analysis of confocal images may confirm if VRN2 levels vary between the WT, *prt6-1* backgrounds. However, further study is needed to confirm VRN2 localization

within cells of different tissues of the plant, as it was unclear from this study whether VRN2 was cytosolic further up the root in other cell types/tissues. Performing western blotting on the cytoplasm and different cell fractions could help to confirm if VRN2 is cytosolic.

It would also be interesting to discover if the localization of VRN2 in the nucleus/cytoplasm is only observed when it is interacting within the VRN2-PCR2 complex or whether VRN2 is visible in these locations when it is not associated with the PRC2. This could explain why VRN2 and FLC are both found in meristematic tissues. *FLC* is not constantly being suppressed by VRN2, so perhaps VRN2 is not always located in the nucleus. Co-immunoprecipitation and bimolecular fluorescence complementation of VRN2 and the PRC2 components would help to uncover if the localization pattern observed is when VRN2 is associated with the PRC2 complex. We know that VRN2 is important for regulation of flowering time by histone methylation of *FLC* (Henderson and Dean, 2004), but there may be other possible targets of VRN2. ChIP-seq analysis could reveal differences in chromatin modifications in our mutant lines. This, along with RNA-seq analysis would reveal if VRN2 has any other DNA methylation targets other than *FLC*.

6.3 VRN2, vernalization and flowering

Flowering time and seed development are of academic and economic interest (Hennig and Derkacheva, 2009). If we can understand how plants use epigenetics (heritable changes in gene expression) to control their development, we may be able to manipulate the vernalization pathway to help

improve crop yields. A T-DNA insertion mutant was identified as a novel *vrn2* mutant allele, here designated *vrn2-5* (FIGURE 3.9). In this study *vrn2-5* was used to produce a *vrn2-5 prt6-1* double mutant in order to perform phenotypic analyses, to try to uncover the functional relevance of VRN2 regulation by the N-end rule pathway. Here, it was shown that VRN2 is not involved in the ABA response during germination (FIGURE 3.10) even though the N-end rule pathway has previously been linked to ABA signalling through PRT6 and ATE1/2 (Holman et al., 2009. Zhang et al., 2018), and through the ERFVIIs (Gibbs et al., 2014b). The results here suggest the cold signalling associated with vernalization does not involve abscisic acid, as in (Liu et al., 2002). *vrn2-5* did however, show a significant decrease in establishment compared to WT at 1μM ABA, suggesting VRN2 may be involved in the ABA response during establishment.

Increased knowledge of vernalization response mechanisms and the effect of VRN2 regulation by the N-end rule pathway on flowering time, could lead to a deeper understanding of how different *Arabidopsis* accessions have evolved and adapted to varying environmental conditions in the wild. In naturally occurring Arabidopsis accessions, the *FRIGIDA* (*FRI*) and *FLOWERING LOCUS C* (*FLC*) genes determine flowering time variation and the requirement for vernalization (Gendall et al., 2001). The naturally occurring *San Felieu2* (*Sf2*) ecotype has a dominant *FRI* allele, meaning they respond to vernalization (Diallo et al., 2010). The *vrn2-5*, *prt6-1* and *vrn2-5 prt6-1* mutants were crossed into a vernalization-requiring Col-0 *FRI*-Sf2 background (Figure 3.12). In the Col-0 *FRI*-Sf2 background, increasing vernalization

length decreased temporal flowering time over all lines (FIGURE 3.13). In *vrn2-5* mutant we would not expect a vernalization response, but these plants decreased flowering time with increased vernalization. This suggested that *vrn2-5* is not a complete knockout and that perhaps there was still some functional protein being produced. The *vrn2-1* mutant line has a mutation that introduces a stop codon into the gene that was shown to reduce the flowering response of late flowering genotypes (i.e. vernalization-requiring plants experienced vernalization but flowered late) (Gendall et al., 2001). Perhaps using this alternative mutant allele in combination with *prt6-1* mutant in future flowering time assays if used as a comparison, would hopefully compliment the results here, as the behavior of these *vrn2-1* mutant lines should be similar to *vrn2-5*. *vrn2* and *vrn2-5 prt6-1* mutants on average flowered later than Col-0 *FRI*-Sf2 and *prt6-1* lines, although there was not a statistically significant difference between flowering times with all treatments. In the absence of vernalization, *vrn2-5 prt6-1* flowered significantly later developmentally than other lines. The results indicated some effects of VRN2 and N-end rule regulation on flowering time, but the flowering time assays need to be repeated with greater numbers of plants before any firm conclusions can be drawn.

It is important to remember that VRN2 and vernalization is not the only pathway that is regulating flowering by repression of *FLC*. The autonomous pathway also represses *FLC* to promote flowering (Sheldon et al., 1999) and late flowering autonomous pathway mutants can be reversed by vernalization (Koornneef et al., 1991). In this study, vernalization treatments were

conducted under short days, whereas the growth conditions after vernalization were under long days. However, the aim was to test the effect vernalization (i.e. the effect of cold) had on flowering time, not the effect of day length. In future, vernalization experiments would be better conducted with consistent day lengths, in both the warm and cold temperatures. This would enable a distinction between possible effects the photoperiod flowering pathway had on flowering time and the effect of vernalization by removing the day length variable. As vernalization is not the only pathway controlling flowering time, the addition of gibberellic acid (GA) to plants as they are growing could also rule out whether the loss of VRN2 function had affected on the GA pathway behind flowering (Mouradov et al., 2002, Moon et al., 2003, Shindo et al., 2006).

This study has shown an effect of cold treatment and *prt6-1 vrn2-5* on flowering time in vernalization-requiring accessions of *Arabidopsis* plants. More specifically, the Col-0 *FRI*-Sf2 introgression line was chosen so only the *VRN2* and *PRT6* genes were altered during crosses with Col-0 and the rest of the genetic background would be the same. However, it would be interesting to look at the effect of *prt6-1* and *vrn2-5* mutations in other vernalization dependent accessions because different accessions have varying stability of *FLC* repression (Shindo et al., 2006). For example, studying Edi-0 and H51 accessions (Nappzinn, 1957) that have active *FRI* alleles, or the Bil-7 background that also respond rapidly to vernalization (Shindo et al., 2006). The genes *FRIGIDA LIKE 1* (*FRL1*) and *FRIGIDA LIKE 2* (*FRL2*) are similar in sequence to *FRIGIDA* but are not functionally redundant, and so are all required for delaying flowering over winter (Michaels et al., 2004). Perhaps

using a background with dominant alleles of all three of these genes may produce more conclusive results. Alternatively, mutants of the autonomous pathway such as *flowering control locus a* (*fca*) or *multicopy suppressor of ira1* (*msi1* also known as *fve*) will produce late flowering plants and these could have been used as alternative late flowering backgrounds in these experiments.

6.4 VRN2 and abiotic stress

6.4.1 Heat stress response

Vicente et al. (2017) showed a role for the N-end rule in heat stress tolerance via the ERFVIIs. Here, the aim was to examine a potential role for VRN2 in heat tolerance, since VRN2 was identified as a new Cys/Arg N-end rule substrate. The experiment was only preliminary and the heat stress methodology needed more refining, as choosing the appropriate heat stress phenotyping assay is important (Yeh et al., 2012). In this experiment it was decided to use the methods of Vicente et al. (2017) so the results could be comparable, however it was difficult to recreate their results. This could be due to details of laboratory environment and differences in the equipment used. At least three replicas were used in each experiment. However, using more repeats and increasing sample size would help obtain more data for statistical analysis to help draw more firm conclusions whether VRN2 has a role in heat tolerance. Seedling survival was measured to score heat stress tolerance in this study, but hypocotyl/root elongation and chlorophyll

accumulation can also be used to test heat stress tolerance and are advantageous because they are quantitative scores (Yeh et al., 2012). Long-term acquired thermotolerance LAT, thermotolerance to moderately high temperatures (TMHT) and gradual acclimation types of heat stress assays could also be carried out in the future because multiple mechanisms and regulation pathways may be involved in each type of thermotolerance.

The accidental observation of *vrn2-5* and *prt6-1 vrn2-5* plants that lead to the heat stress assays was in adult plants (FIGURE 3.14). In the future more studies could involve adult plants in the *vrn2-5* and *prt6-1* single and double lines, as well as in seedlings, as adult plants may have different stress responses compared with seedlings. This preliminary study showed that VRN2 may play a possible role in BT (FIGURE 3.15) but may have a negative effect on heat stress response for SAT (FIGURE 3.16). However, laboratory based assays may not always reflect real heat stress conditions in the natural environment as they are highly complex and involve also water limitation, UV irradiation and light intensity (Yeh et al., 2012).

6.4.2 Salt stress response

Soil salinity has a great effect on plant development (Ma et al., 2015) and it is known that high salt levels delay the onset of flowering in *A. thaliana* (Achard et al., 2006). A potential role for VRN2 in plant responses to salt stress was also investigated since Vicente et al. (2017) had shown a function for the N-end rule pathway via ERFVIIs in this process. In the salt stress assay here, it was observed that *vrn2-5 prt6-1* plants were greener and larger than the other

lines, indicating a possible salt tolerance (FIGURE 3.17). The experiment needs repeating in order to reveal if the tolerance observed in the double mutant is associated with *vrn2-5* tolerance or whether it confirms the results of Vicente et al. (2017) where *prt6-1* was shown to be salt tolerant. This was a preliminary experiment but, in the future, it could be repeated by measuring size and colour of seedlings alongside measuring electrolyte leakage (conductivity) of leaves, in order to produce quantifiable results. Another method would be to grow seedlings on ½ MS containing NaCl of various concentrations, for a period of time and then transferring them to plain media to measure recovery.

Abiotic stress has been linked to reduced nitric oxide levels caused by lowered NITRATE REDUCTASE levels and the ERFVIIs have been found to become stable under salt stress (Vicente et al., 2017). Conserved features of stress signalling across fungi and plants involve calcium, reactive oxygen species (ROS) and NO (Zhu, 2016). The fact that NO is known to be involved in stress responses has an implication for the stability of Cys/Arg N-end rule substrates, as lowered nitric oxide would mean substrates such as VRN2 would become stable. Overexpression of ERFVII N-end rule substrates has been shown to enhance abiotic stress tolerance in several species including *Arabidopsis*, *Oryza* and *Rumex* (Gibbs et al., 2015). Perhaps using a transgenic line over-expressing VRN2, or a VRN2 inducible line, as well as the *vrn2-5* and *prt6-1* single and double mutant lines may yield more insight into VRN2 involvement in stress responses. VRN2 has been found to play a role in promoting hypoxia tolerance (Gibbs et al., 2018). If stress-stabilized

VRN2 could be found to enhance abiotic heat and salt stress tolerance it would provide a further link between the stress-signalling pathway to the N-end rule pathway and chromatin remodelling. Identifying stress sensors in plants and understanding the cross-talk between stress-signalling and developmental signalling pathways remains an important but challenging goal.

6.5 The mechanism behind VRN2 stabilization during vernalization

In chapter 1 (FIGURE3.8) it was determined that VRN2 is stabilized in cold conditions. However, the mechanism behind the switch from VRN2 being degraded, to VRN2 becoming stable during temperature decreases is unknown. The component of oligomeric complex 1 (COG1) which is a subunit of the Golgi complex, was found to be stable in complex as the other proteins of the Golgi complex shielded its Nt, preventing its degradation (Shemorry et al., 2013). It has also shown previously that VIN3 interacts with VRN2 in the PRC2 complex (Wood et al., 2006). It is also known that transcription of *VIN3* is only induced during cold exposure but mRNA is not detectable when returned to warm temperatures (Sung and Amasino, 2004b, Alexandre and Hennig, 2008). It was hypothesized therefore, that VIN3 shields the MC N-terminus of VRN2, preventing its degradation by the N-end rule pathway, causing VRN2 stabilization during vernalization. However, the results here suggest that this is not the case.

With co-expression of VIN3 and VRN2 *in vitro* and co-expression of VRN2 and VIN3 with the addition of cyclohexamide in vitro, VRN2 was still degraded

over time (FIGURE 4.3 and 4.4). VIN3 induction is the most upstream molecular effect of vernalization, (it is expressed before VRN2) and this is consistent with VIN3 having a role in cold acclimation and sensing the duration of cold exposure (Sung and Amasino, 2004b). However, adding pre-synthesised VIN3 to the VRN2 reaction of the *in vitro* assay still did not stabilize VRN2 (FIGURE 4.5). When *VIN3* was induced by estradiol *in vivo*, VRN2 levels were equivalent to those without estradiol treatment (FIGURE 4.6, 4.7). With the addition of cyclohexamide to estradiol treated seedlings sampled over 8 hours VRN2 was still degraded (FIGURE 4.8). For *in vivo* experiment it was not possible to determine whether VIN3 protein was being affected, as it was not cloned with a tag. Instead of this, *VIN3* RNA transcription was shown, however, in the future, VIN3-HA could be cloned with a C-terminal HA tag to allow detection of protein. Constitutive *VIN3* expression was shown to not be a suitable substitute for cold exposure during vernalization, (i.e. the cold is still needed to initiate vernalization), as it does not result in cold-independent early flowering (Sung and Amasino, 2004b). Therefore, estradiol-inducible *VIN3* may not be able to mimic the effect of cold conditions, as there must be factors other than VIN3 that cause VRN2 stabilization.

If shielding of the MC N-terminus does occur, it is likely to be done by another protein or another molecule. The PhD finger domain in VIN3 has been shown to be able to bind with phosphoinositides, which are found in cell membranes (Gozani et al., 2003). Perhaps when VIN3 interacts with VRN2 it brings a phosphoinositide molecule into close proximity, which then could shield the N-

terminus of VRN2, instead of shielding occurring via VIN3 directly. Vernalization triggers a series of histone modifications in *FLC* such as reduced histone acetylation and increased histone K27 and K9 methylation and this involves VIN3, VRN1 and VRN2 (Bastow et al., 2004, Sung et al., 2006b). These modifications recruit LIKE HETEROCHROMATIN PROTEIN1 (LHP1) to ensure epigenetic memory of the repressed state of *FLC* (Mylne et al., 2006, Sung et al., 2006a). *VIN3* is also not the only gene to become up regulated during cold exposure (Gibbs et al., 2018). Perhaps LHP1 or another cold regulated protein may shield the N-terminus of VRN2. Shielding could be via another protein in the PRC2 complex (SWI, FIE or MSI1), as cold could alter the protein structure, meaning that VRN2 is only shielded during vernalization and not in warmer temperatures.

The mechanism behind VRN2 stabiization may not involve Nt-shielding at all. The processes underlying vernalization and flowering are complex and there are a number of possible stabilization mechanisms. ADH1 (a key hypoxia response gene) and PCO1 (one of the enzymes required for cysteine oxidation in the Cys/Arg N-end rule), have also been shown to become up-regulated in the cold but down-regulated upon return to warm conditions (Gibbs et al., 2018). This is an indication of a link between cold conditions and low oxygen and nitric oxide levels during vernalization, which would affect Cys/Arg substrates of the N-end rule pathway such as VRN2. Further work on how hypoxia response genes affect N-end substrate stability during vernalization would provide new insight into plant physiology linking the N-end, abiotic stress and low temperature sensing. However, the question of

how VRN2 transitions from being degraded to becoming stable still needs to be addressed.

6.6 Evolution of an ancient VRN2-like protein allowing neo-functionalization of PRC2 complexes

Su(z)12 is a PgG protein found in animals (Butenko and Ohad, 2011). The Su(z)12 forms a complex with Extra sex combs (Esc), P55 and Enhancer of zeste (E(z)) to form the PRC2 complex (Kuzmichev et al., 2002, Muller et al., 2002). The PRC2 complex is highly conserved among plants and animals (Hennig and Derkacheva, 2009). VRN2, EMF2 AND FIS2 are Su(z)12 homologues but of these, VRN2 is the only Su(z)12 with an MC Nt. Thus, the evolutionary origins of VRN2 and its connection with the N-end rule were explored.

It was observed that the Su(z)12 homologue EMF2 in angiosperms has an internal MC and that MC N-terminus in VRN2-like proteins of diverse clades of land plants align with this internal EMF2 MC (FIGURE 5.1). VRN2 was thought to have evolved in the Brassicaceae (Chen et al., 2009) but in this study a VRN2-like protein in the monocot Barley (annotated HvEMF2c) was shown to degrade over time in an *in vitro* protein degradation assay (FIGURE 5.2). HvEMF2c was shown to be a substrate of the Cys/Arg N-end rule pathway, thus demonstrating that oxygen and nitric oxide sensitive Su(z)12 variants are present throughout the angiosperms (i.e. that VRN2 is not restricted to the Brassicaceae). In the future, Arabidopsis could be

transformed with HvEMF2c-HA, in order to perform a protein degradation assay and confirm HvEMF2c as a Cys/Arg N-end rule substrate *in vivo*. HvEMF2c-HA protein degradation assays could also be done in barley itself. However, as the lifecycle of barley is longer than *Arabidopsis* and the DNA sequences of Barley are less well known, this would need much more time.

Glyma11g13220 in soybean has been found to be a functional homologue of *Arabidopsis* VRN1 and vernalization pathway genes have been conserved during the evolution of this crop species (Lu et al., 2015). It would be intriguing to test whether rice OsEMF2b, which has an MC N-terminus (and therefore proposed to be a VRN2-like protein), is also an N-end rule substrate and also test whether VRN2-like proteins in gymnosperms such as ginkgo or pine are substrates, as the extent to which vernalization mechanisms are conserved among plant species remains to be determined. This study has shown that other vernalization gene homologues such as VRN2-like proteins exist in diverse angiosperm clades (FIGURE 5.1) and could be N-end rule regulated in more species than was first thought as we have now confirmed a VRN2-like protein from barley, a monocot species distantly related to Arabidopsis, is a Cys/Arg N-end rule substrate.

Gene duplications are a major contributor to genome evolution, increasing genetic diversity, having an effect on morphology and physiology and bringing about novel phenotypes (Soltis and Soltis, 2016). It has been suggested that the VEF-domain gene family consisting of VRN2, EMF2 and FIS2 has arisen as the result of gene duplication and subsequent diversification of gene

sequences leading to the divergence between plants and animals (Chen et al., 2009). Thus, the idea of a gene duplication and truncation event, leading to N-end rule regulation of a VRN2-like protein, was explored. N-degrons comprise of a destabilizing Nt-residue, a Lys site for ubiquitylation and an Nt protein structure that exposes the N-terminus on the outside of the protein for interaction with other proteins (Gibbs et al., 2014a). An attempt was made to create a novel Cys/Arg N-end rule substrate by mutating the Nt-MP of *At*EMF2 to an MC. It was shown that the full length *At*EMF2 was not destabilized when mutating its N-terminus to an MC (FIGURE 5.3), which demonstrates that not all proteins can become N-end rule substrates. This also indicates that a gene duplication event and a point mutation would not be the only factor leading to divergence of a gene to become co-opted to another regulatory pathway. Remarkably however, the MC-tEMF2-HA (truncated EMF2) was degraded *in vitro* (FIGURE 5.5) and also stabilized in *prt6-1* and during vernalization treatments *in vivo* (FIGURE 5.6). tEMF2 is an N-end rule substrate, thus supporting the hypothesis VRN2 has evolved from an ancient EMF2-like protein by a duplication and truncation event, exposing the internal MC that has led to VRN2 N-end rule regulation and diverse function.

6.7 Final remarks

Overall, this study has reported that flowering plants have evolved an Su(z)12 variant that is regulated by the oxygen and nitric oxide-sensing Cys/Arg N-end rule pathway. N-end rule regulation of VRN2 restricts VRN2 abundance, ensuring it is only stabilized in specific tissues or in specific conditions such as those experienced during vernalization. The rapid post-translational control of VRN2 by the N-end rule pathway could thereby control PRC2 activity on *FLC* throughout development. VRN2 is functionally distinct from the ERFVIIs yet they are still regulated by the same branch of the N-end rule pathway. This means that plants can respond to factors such as low oxygen, low nitric oxide, low temperatures and stress by the same mechanism (i.e. N-end rule regulation) but with different gene targets. This could mean that there are more N-end rule substrates and further roles of VRN2 yet to be discovered.

VRN2 is stable under vernalization conditions and in meristematic regions of the plants that are thought to be hypoxic but the mechanism of VRN2 the stabilization is still unknown. The regulation of VRN2 by the N-end rule pathway gives a novel connection between PRC2 activity and the perception of the environment in land plants. This has implications for crop improvement: if this mechanism can be manipulated to improve resilience against hypoxic stress such as flooding, or manipulated to allow plants to flower whenever needed, this could increase crop yield.

A novel mechanism for gas sensing in plants was achieved through the evolution of a gas sensitive N-degron in an ancient Su(z)12-like protein, bringing about a new function for the PCR2. Given the role of VRN2 in the regulation and coordination of flowering with seasonal cues, the coupling of this Su(z)12 to the Arg/N-end rule pathway may have facilitated the emergence of seasonal flowering as a reproductive strategy in plants. The work here, has uncovered a novel mechanism through which environmental signals can be perceived and transduced into epigenetic changes to control development and flowering.

Chapter 7

References

Aasland, R., Gibson, T. J. and Stewart, A. F. (1995) 'THE PHD FINGER - IMPLICATIONS FOR CHROMATIN-MEDIATED TRANSCRIPTIONAL REGULATION', *Trends in Biochemical Sciences,* 20(2), pp. 56-59.

Achard, P., Cheng, H., De Grauwe, L., Decat, J., Schoutteten, H., Moritz, T., Van Der Straeten, D., Peng, J. R. and Harberd, N. P. (2006) 'Integration of plant responses to environmentally activated phytohormonal signals', *Science,* 311(5757), pp. 91-94.

Alexandre, C. M. and Hennig, L. (2008) 'FLC or not FLC: the other side of vernalization', *Journal of Experimental Botany,* 59(6), pp. 1127-1135.

An, J. Y., Seo, J. W., Tasaki, T., Lee, M. J., Varshavsky, A. and Kwon, Y. T. (2006) 'Impaired neurogenesis and cardiovascular development in mice lacking the E3 ubiquitin ligases UBR1 and UBR2 of the N-end rule pathway', *Proceedings of the National Academy of Sciences of the United States of America,* 103(16), pp. 6212-6217.

Arnesen, T., Van Damme, P., Polevoda, B., Helsens, K., Evjenth, R., Colaert, N., Varhaug, J. E., Vandekerckhove, J., Lillehaug, J. R., Sherman, F. and Gevaert, K. (2009) 'Proteomics analyses reveal the evolutionary conservation and divergence of N-terminal acetyltransferases from yeast and humans', *Proceedings of the National Academy of Sciences of the United States of America,* 106(20), pp. 8157-8162.

Bachmair, A., Finley, D. and Varshavsky, A. (1986) 'INVIVO HALF-LIFE OF A PROTEIN IS A FUNCTION OF ITS AMINO-TERMINAL RESIDUE', *Science,* 234(4773), pp. 179-186.

Bastow, R., Mylne, J. S., Lister, C., Lippman, Z., Martienssen, R. A. and Dean, C. (2004) 'Vernalization requires epigenetic silencing of FLC by histone methylation', *Nature,* 427(6970), pp. 164-167.

Birve, A., Sengupta, A. K., Beuchle, D., Larsson, J., Kennison, J. A., Rasmuson-Lestander, A. and Muller, J. (2001) 'Su(z)12, a novel Drosophila Polycomb group gene that is conserved in vertebrates and plants', *Development,* 128(17), pp. 3371-3379.

Brower, C. S., Piatkov, K. I. and Varshavsky, A. (2013) 'Neurodegeneration-Associated Protein Fragments as Short-Lived Substrates of the N-End Rule Pathway', *Molecular Cell,* 50(2), pp. 161-171.

Burn, J. E., Bagnall, D. J., Metzger, J. D., Dennis, E. S. and Peacock, W. J. (1993) 'DNA METHYLATION, VERNALIZATION, AND THE INITIATION OF FLOWERING', *Proceedings of the National Academy of Sciences of the United States of America,* 90(1), pp. 287-291.

Butenko, Y. and Ohad, N. (2011) 'Polycomb-group mediated epigenetic mechanisms through plant evolution', *Biochimica Et Biophysica Acta-Gene Regulatory Mechanisms,* 1809(8), pp. 395-406.

Chanvivattana, Y., Bishopp, A., Schubert, D., Stock, C., Moon, Y. H., Sung, Z. R. and Goodrich, J. (2004) 'Interaction of polycomb-group proteins controlling flowering in Arabidopsis', *Development,* 131(21), pp. 5263-5276.

Chen, L. J., Diao, Z. Y., Specht, C. and Sung, Z. R. (2009) 'Molecular Evolution of VEF-Domain-Containing PcG Genes in Plants', *Molecular Plant,* 2(4), pp. 738-754.

Chen, S. J., Wu, X., Wadas, B., Oh, J. H. and Varshavsky, A. (2017) 'An N-end rule pathway that recognizes proline and destroys gluconeogenic enzymes', *Science,* 355(6323).

Choi, J., Hyun, Y., Kang, M. J., Yun, H., Yun, J. Y., Lister, C., Dean, C., Amasino, R. M., Noh, B., Noh, Y. S. and Choi, Y. (2009) 'Resetting and regulation of FLOWERING LOCUS C expression during Arabidopsis reproductive development', *Plant Journal,* 57(5), pp. 918-931.

Ciechanover, A. (1998) 'The ubiquitin-proteasome pathway: on protein death and cell life', *Embo Journal,* 17(24), pp. 7151-7160.

Coego, A., Brizuela, E., Castillejo, P., Ruiz, S., Koncz, C., del Pozo, J. C., Pineiro, M., Jarillo, J. A., Paz-Ares, J., Leon, J. and Consortium, T. (2014) 'The TRANSPLANTA collection of Arabidopsis lines: a resource for functional analysis of transcription factors based on their conditional overexpression', *Plant Journal,* 77(6), pp. 944-953.

Considine, M. J., Diaz-Vivancos, P., Kerchev, P., Signorelli, S., Agudelo-Romero, P., Gibbs, D. J. and Foyer, C. H. (2017) 'Learning To Breathe: Developmental Phase Transitions in Oxygen Status', *Trends in Plant Science,* 22(2), pp. 140-153.

Crevillen, P., Yang, H. C., Cui, X., Greeff, C., Trick, M., Qiu, Q., Cao, X. F. and Dean, C. (2014) 'Epigenetic reprogramming that prevents transgenerational inheritance of the vernalized state', *Nature,* 515(7528), pp. 587-+.

Curtis, M. D. and Grossniklaus, U. (2003) 'A gateway cloning vector set for high-throughput functional analysis of genes in planta', *Plant Physiology,* 133(2), pp. 462-469.

Darwin, K. H. (2009) 'Prokaryotic ubiquitin-like protein (Pup), proteasomes and pathogenesis', *Nature Reviews Microbiology,* 7(7), pp. 485-491.

Davydov, I. V. and Varshavsky, A. (2000) 'RGS4 is arginylated and degraded by the N-end rule pathway in vitro', *Journal of Biological Chemistry,* 275(30), pp. 22931-22941.

De Lucia, F., Crevillen, P., Jones, A. M. E., Greb, T. and Dean, C. (2008) 'A PHD-Polycomb Repressive Complex 2 triggers the epigenetic silencing of FLC during vernalization', *Proceedings of the National Academy of Sciences of the United States of America,* 105(44), pp. 16831-16836.

Derkacheva, M. and Hennig, L. (2014) 'Variations on a theme: Polycomb group proteins in plants', *Journal of Experimental Botany,* 65(10), pp. 2769-2784.

Deshaies, R. (1999) 'Mechanism and regulation of the SCF ubiquitination pathway', *Kidney International,* 56(4), pp. 1186-1187.

Deshaies, R. J. and Joazeiro, C. A. P. (2009) 'RING Domain E3 Ubiquitin Ligases', *Annual Review of Biochemistry Annual Review of Biochemistry*, pp. 399-434.

Diallo, A., Kane, N., Agharbaoui, Z., Badawi, M. and Sarhan, F. (2010) 'Heterologous Expression of Wheat VERNALIZATION 2 (TaVRN2) Gene in Arabidopsis Delays Flowering and Enhances Freezing Tolerance', *Plos One,* 5(1).

Ditzel, M., Wilson, R., Tenev, T., Zachariou, A., Paul, A., Deas, E. and Meier, P. (2003) 'Degradation of DIAP1 by the N-end rule pathway is essential for regulating apoptosis', *Nature Cell Biology,* 5(5), pp. 467-473.

Dougan, D. A., Truscott, K. N. and Zeth, K. (2010) 'The bacterial N-end rule pathway: expect the unexpected', *Molecular Microbiology,* 76(3), pp. 545-558.

Dougan, D. A. and Varshavsky, A. (2018) 'Understanding the Pro/N-end rule pathway', *Nature Chemical Biology,* 14(5), pp. 415-416.

Du, F. Y., Navarro-Garcia, F., Xia, Z. X., Tasaki, T. and Varshavsky, A. (2002) 'Pairs of dipeptides synergistically activate the binding of substrate by ubiquitin ligase through dissociation of its autoinhibitory domain', *Proceedings of the National Academy of Sciences of the United States of America,* 99(22), pp. 14110-14115.

Eisele, F. and Wolf, D. H. (2008) 'Degradation of misfolded protein in the cytoplasm is mediated by the ubiquitin ligase Ubr1', *Febs Letters,* 582(30), pp. 4143-4146.

Fair, K., Anderson, M., Bulanova, E., Mi, H. F., Tropschug, M. and Diaz, M. O. (2001) 'Protein interactions of the MLL PHD fingers modulate MLL target gene regulation in human cells', *Molecular and Cellular Biology,* 21(10), pp. 3589-3597.

Fjellheim, S., Boden, S. and Trevaskis, B. (2014) 'The role of seasonal flowering responses in adaptation of grasses to temperate climates', *Frontiers in Plant Science,* 5.

Frottin, F., Martinez, A., Peynot, P., Mitra, S., Holz, R. C., Giglione, C. and Meinnel, T. (2006) 'The proteomics of N-terminal methionine cleavage', *Molecular & Cellular Proteomics,* 5(12), pp. 2336-2349.

Gallastegui, N. and Groll, M. (2010) 'The 26S proteasome: assembly and function of a destructive machine', *Trends in Biochemical Sciences,* 35(11), pp. 634-642.

Garzon, M., Eifler, K., Faust, A., Scheel, H., Hofmann, K., Koncz, C., Yephremov, A. and Bachmair, A. (2007) 'PRT6/At5g02310 encodes an Arabidopsis ubiquitin ligase of the N-end rule pathway with arginine specificity and is not the CER3 locus', *Febs Letters,* 581(17), pp. 3189-3196.

Gendall, A. R., Levy, Y. Y., Wilson, A. and Dean, C. (2001) 'The VERNALIZATION 2 gene mediates the epigenetic regulation of vernalization in Arabidopsis', *Cell,* 107(4), pp. 525-535.

Gibbs, D. J., Bacardit, J., Bachmair, A. and Holdsworth, M. J. (2014a) 'The eukaryotic N-end rule pathway: conserved mechanisms and diverse functions', *Trends Cell Biol,* 24(10), pp. 603-611.

Gibbs, D. J., Bailey, M., Tedds, H. M. and Holdsworth, M. J. (2016) 'From start to finish: amino-terminal protein modifications as degradation signals in plants', *New Phytologist,* 211(4), pp. 1188-1194.

Gibbs, D. J., Conde, J. V., Berckhan, S., Prasad, G., Mendiondo, G. M. and Holdsworth, M. J. (2015) 'Group VII Ethylene Response Factors Coordinate Oxygen and Nitric Oxide Signal Transduction and Stress Responses in Plants', *Plant Physiology,* 169(1), pp. 23-31.

Gibbs, D. J., Isa, N. M., Movahedi, M., Lozano-Juste, J., Mendiondo, G. M., Berckhan, S., Marin-de la Rosa, N., Conde, J. V., Correia, C. S., Pearce, S. P., Bassel, G. W., Hamali, B., Talloji, P., Tome, D. F. A., Coego, A., Beynon, J., Alabadi, D., Bachmair, A., Leon, J., Gray, J. E., Theodoulou, F. L. and Holdsworth, M. J. (2014b) 'Nitric Oxide Sensing in Plants Is Mediated by Proteolytic Control of Group VII ERF Transcription Factors', *Molecular Cell,* 53(3), pp. 369-379.

Gibbs, D. J., Lee, S. C., Isa, N. M., Gramuglia, S., Fukao, T., Bassel, G. W., Correia, C. S., Corbineau, F., Theodoulou, F. L., Bailey-Serres, J. and Holdsworth, M. J.

(2011) 'Homeostatic response to hypoxia is regulated by the N-end rule pathway in plants', *Nature,* 479(7373), pp. 415-U172.

Gibbs, D. J., Tedds, H. M., Labandera, A. M., Bailey, M., White, M.D., Hartman, S., Sprigg, C., Mogg, S.L., Osbourne, R., Dambire, C., Boeckx, T., Paling, Z., Voesenek, L.A.C.J., Flashman, E. and Holdsworth, M. J. (2018) 'Oxygen dependent protyolysis regulates the stability of angiosperm polycomb repressive 2 subunit VERNALIZATION 2.', *Nature Communications,* 9(5438), pp. 1-11.

Giglione, C., Boularot, A. and Meinnel, T. (2004) 'Protein N-terminal methionine excision', *Cellular and Molecular Life Sciences,* 61(12), pp. 1455-1474.

Gonda, D. K., Bachmair, A., Wunning, I., Tobias, J. W., Lane, W. S. and Varshavsky, A. (1989) 'UNIVERSALITY AND STRUCTURE OF THE N-END RULE', *Journal of Biological Chemistry,* 264(28), pp. 16700-16712.

Gozani, O., Karuman, P., Jones, D. R., Ivanov, D., Cha, J., Lugovskoy, A. A., Baird, C. L., Zhu, H., Field, S. J., Lessnick, S. L., Villasenor, J., Mehrotra, B., Chen, J., Rao, V. R., Brugge, J. S., Ferguson, C. G., Payrastre, B., Myszka, D. G., Cantley, L. C., Wagner, G., Divecha, N., Prestwich, G. D. and Yuan, J. Y. (2003) 'The PHD finger of the chromatin-associated protein ING2 functions as a nuclear phosphoinositide receptor', *Cell,* 114(1), pp. 99-111.

Graciet, E., Mesiti, F. and Wellmer, F. (2010) 'Structure and evolutionary conservation of the plant N-end rule pathway', *Plant Journal,* 61(5), pp. 741-751.

Graciet, E., Walter, F., O'Maoileidigh, D., Pollmann, S., Meyerowitz, E. M., Varshavsky, A. and Wellmer, F. (2009) 'The N-end rule pathway controls multiple functions during Arabidopsis shoot and leaf development', *Proceedings of the National Academy of Sciences of the United States of America,* 106(32), pp. 13618-13623.

Greb, T., Mylne, J. S., Crevillen, P., Geraldo, N., An, H. L., Gendall, A. R. and Dean, C. (2007) 'The PHD finger protein VRN5 functions in the epigenetic silencing of Arabidopsis FLC', *Current Biology,* 17(1), pp. 73-78.

Heck, J. W., Cheung, S. K. and Hampton, R. Y. (2010) 'Cytoplasmic protein quality control degradation mediated by parallel actions of the E3 ubiquitin ligases Ubr1 and San1', *Proceedings of the National Academy of Sciences of the United States of America,* 107(3), pp. 1106-1111.

Hecker, A., Brand, L. H., Peter, S., Simoncello, N., Kilian, J., Harter, K., Gaudin, V. and Wanke, D. (2015) 'The Arabidopsis GAGA-Binding Factor BASIC PENTACYSTEINE6 Recruits the POLYCOMB-REPRESSIVE COMPLEX1 Component LIKE HETEROCHROMATIN PROTEIN1 to GAGA DNA Motifs', *Plant Physiology,* 168(3), pp. 130-141.

Heide, O. M. (1994) 'CONTROL OF FLOWERING AND REPRODUCTION IN TEMPERATE GRASSES', *New Phytologist,* 128(2), pp. 347-362.

Hellmann, H. and Estelle, M. (2002) 'Plant development: Regulation by protein degradation', *Science,* 297(5582), pp. 793-797.

Henderson, I. R. and Dean, C. (2004) 'Control of Arabidopsis flowering: the chill before the bloom', *Development,* 131(16), pp. 3829-3838.

Hennig, L. and Derkacheva, M. (2009) 'Diversity of Polycomb group complexes in plants: same rules, different players?', *Trends in Genetics,* 25(9), pp. 414-423.

Hennig, L., Taranto, P., Walser, M., Schonrock, N. and Gruissem, W. (2003) 'Arabidopsis MSI1 is required for epigenetic maintenance of reproductive development', *Development,* 130(12), pp. 2555-2565.

Hershko, A. and Ciechanover, A. (1998) 'The ubiquitin system', *Annual Review of Biochemistry,* 67, pp. 425-479.

Hicke, L. (2001) 'A new ticket for entry into budding vesicles - Ubiquitin', *Cell,* 106(5), pp. 527-530.

Holman, T. J., Jones, P. D., Russell, L., Medhurst, A., Tomas, S. U., Talloji, P., Marquez, J., Schmuths, H., Tung, S. A., Taylor, I., Footitt, S., Bachmair, A., Theodoulou, F. L. and Holdsworth, M. J. (2009) 'The N-end rule pathway promotes seed germination and establishment through removal of ABA sensitivity in Arabidopsis', *Proceedings of the National Academy of Sciences of the United States of America,* 106(11), pp. 4549-4554.

Hu, R. G., Sheng, J., Qi, X., Xu, Z. M., Takahashi, T. T. and Varshavsky, A. (2005) 'The N-end rule pathway as a nitric oxide sensor controlling the levels of multiple regulators', *Nature,* 437(7061), pp. 981-986.

Hu, R. G., Wang, H. Q., Xia, Z. X. and Varshavsky, A. (2008) 'The N-end rule pathway is a sensor of heme', *Proceedings of the National Academy of Sciences of the United States of America,* 105(1), pp. 76-81.

Hwang, C. S., Shemorry, A. and Varshavsky, A. (2010) 'N-Terminal Acetylation of Cellular Proteins Creates Specific Degradation Signals', *Science,* 327(5968), pp. 973-977.

Ikeuchi, M., Iwase, A., Rymen, B., Harashima, H., Shibata, M., Ohnuma, M., Breuer, C., Morao, A. K., de Lucas, M., De Veylder, L., Goodrich, J., Brady, S. M., Roudier, F. and Sugimoto, K. (2015) 'PRC2 represses dedifferentiation of mature somatic cells in Arabidopsis', *Nature Plants,* 1, pp. 15089.

Jaba, I. M., Zhuang, Z. W., Li, N., Jiang, Y. F., Martin, K. A., Sinusas, A. J., Papademetris, X., Simons, M., Sessa, W. C., Young, L. H. and Tirziu, D. (2013) 'NO triggers RGS4 degradation to coordinate angiogenesis and cardiomyocyte growth', *Journal of Clinical Investigation,* 123(4), pp. 1718-1731.

Jackson, P. K., Eldridge, A. G., Freed, E., Furstenthal, L., Hsu, J. Y., Kaiser, B. K. and Reimann, J. D. R. (2000) 'The lore of the RINGs: substrate recognition and catalysis by ubiquitin ligases', *Trends in Cell Biology,* 10(10), pp. 429-439.

Jarillo, J. A., Leyva, A., Salinas, J. and Martinezzapater, J. M. (1993) 'LOW-TEMPERATURE INDUCES THE ACCUMULATION OF ALCOHOL-DEHYDROGENASE MESSENGER-RNA IN ARABIDOPSIS-THALIANA, A CHILLING-TOLERANT PLANT', *Plant Physiology,* 101(3), pp. 833-837.

Jaudal, M., Zhang, L. L., Che, C., Hurley, D. G., Thomson, G., Wen, J. Q., Mysore, K. S. and Putterill, J. (2016) 'MtVRN2 is a Polycomb VRN2-like gene which represses the transition to flowering in the model legume Medicago truncatula', *Plant Journal,* 86(2), pp. 145-160.

Jiang, D. H., Wang, Y. Q., Wang, Y. Z. and He, Y. H. (2008) 'Repression of FLOWERING LOCUS C and FLOWERING LOCUS T by the Arabidopsis Polycomb Repressive Complex 2 Components', *Plos One,* 3(10).

Johanson, U., West, J., Lister, C., Michaels, S., Amasino, R. and Dean, C. (2000) 'Molecular analysis of FRIGIDA, a major determinant of natural variation in Arabidopsis flowering time', *Science,* 290(5490), pp. 344-347.

Kaelin, W. G. and Ratcliffe, P. J. (2008) 'Oxygen sensing by metazoans: The central role of the HIF hydroxylase pathway', *Molecular Cell,* 30(4), pp. 393-402.

Kellogg, E. A. (2001) 'Evolutionary history of the grasses', *Plant Physiology,* 125(3), pp. 1198-1205.

Kim, H. K., Kim, R. R., Oh, J. H., Cho, H., Varshavsky, A. and Hwang, C. S. (2014) 'The N-Terminal Methionine of Cellular Proteins as a Degradation Signal', *Cell,* 156(1-2), pp. 158-169.

Kim, J. M. and Hwang, C. S. (2014) 'Crosstalk between the Arg/N-end and Ac/N-end rule', *Cell Cycle,* 13(9), pp. 1366-1367.

Kim, S. T., Tasaki, T., Zakrzewska, A., Yoo, Y. D., Sung, K. S., Kim, S. H., Cha-Molstad, H., Hwang, J., Kim, K. A., Kim, B. Y. and Kwon, Y. T. (2013) 'The N-end rule proteolytic system in autophagy', *Autophagy,* 9(7), pp. 1100-1103.

Kim, S. Y. and Michaels, S. D. (2006) 'SUPPRESSOR OFFRI 4 encodes a nuclear-localized protein that is required for delayed flowering in winter-annual Arabidopsis', *Development,* 133(23), pp. 4699-4707.

Komander, D. and Rape, M. (2012) 'The Ubiquitin Code', in Kornberg, R.D. (ed.) *Annual Review of Biochemistry, Vol 81 Annual Review of Biochemistry*, pp. 203-229.

Koncz, C. and Schell, J. (1986) 'THE PROMOTER OF TL-DNA GENE 5 CONTROLS THE TISSUE-SPECIFIC EXPRESSION OF CHIMERIC GENES CARRIED BY A NOVEL TYPE OF AGROBACTERIUM BINARY VECTOR', *Molecular & General Genetics,* 204(3), pp. 383-396.

Koornneef, M., Hanhart, C. J. and Vanderveen, J. H. (1991) 'A GENETIC AND PHYSIOLOGICAL ANALYSIS OF LATE FLOWERING MUTANTS IN ARABIDOPSIS-THALIANA', *Molecular & General Genetics,* 229(1), pp. 57-66.

Korves, T. M., Schmid, K. J., Caicedo, A. L., Mays, C., Stinchcombe, J. R., Purugganan, M. D. and Schmitt, J. (2007) 'Fitness effects associated with the major flowering time gene FRIGIDA in Arabidopsis thaliana in the field', *American Naturalist,* 169(5), pp. E141-E157.

Kosmacz, M., Parlanti, S., Schwarzlander, M., Kragler, F., Licausi, F. and Van Dongen, J. T. (2015) 'The stability and nuclear localization of the transcription factor RAP2.12 are dynamically regulated by oxygen concentration', *Plant Cell and Environment,* 38(6), pp. 1094-1103.

Kuzmichev, A., Nishioka, K., Erdjument-Bromage, H., Tempst, P. and Reinberg, D. (2002) 'Histone methyltransferase activity associated with a human multiprotein complex containing the Enhancer of Zeste protein', *Genes & Development,* 16(22), pp. 2893-2905.

Kwon, Y. T., Kashina, A. S., Davydov, I. V., Hu, R. G., An, J. Y., Seo, J. W., Du, F. and Varshavsky, A. (2002) 'An essential role of N-terminal arginylation in cardiovascular development', *Science,* 297(5578), pp. 96-99.

Lang, A. and Melchers, G. (1947) 'VERNALISATION UND DEVERNALISATION BEI EINER ZWEIJAHRIGEN PFLANZE', *Zeitschrift Fur Naturforschung Section B-a Journal of Chemical Sciences,* 2(11-1), pp. 444-449.

Langer, T. (2000) 'AAA proteases: cellular machines for degrading membrane proteins', *Trends in Biochemical Sciences,* 25(5), pp. 247-251.

Lee, M. J., Kim, D. E., Zakrzewska, A., Yoo, Y. D., Kim, S. H., Kim, S. T., Seo, J. W., Lee, Y. S., Dorn, G. W., Oh, U., Kim, B. Y. and Kwon, Y. T. (2012)

'Characterization of Arginylation Branch of N-end Rule Pathway in G-protein-mediated Proliferation and Signaling of Cardiomyocytes', *Journal of Biological Chemistry,* 287(28), pp. 24043-24052.

Lee, M. J., Tasaki, T., Moroi, K., An, J. Y., Kimura, S., Davydov, I. V. and Kwon, Y. T. (2005) 'RGS4 and RGS5 are in vivo substrates of the N-end rule pathway', *Proceedings of the National Academy of Sciences of the United States of America,* 102(42), pp. 15030-15035.

Levy, Y. Y., Mesnage, S., Mylne, J. S., Gendall, A. R. and Dean, C. (2002) 'Multiple roles of Arabidopsis VRN1 in vernalization and flowering time control', *Science,* 297(5579), pp. 243-246.

Licausi, F. (2011) 'Regulation of the molecular response to oxygen limitations in plants', *New Phytologist,* 190(3), pp. 550-555.

Licausi, F., Kosmacz, M., Weits, D. A., Giuntoli, B., Giorgi, F. M., Voesenek, L., Perata, P. and van Dongen, J. T. (2011) 'Oxygen sensing in plants is mediated by an N-end rule pathway for protein destabilization', *Nature,* 479(7373), pp. 419-U177.

Liu, J. Y., Gilmour, S. J., Thomashow, M. F. and van Nocker, S. (2002) 'Cold signalling associated with vernalization in Arabidopsis thaliana does not involve CBF1 or abscisic acid', *Physiologia Plantarum,* 114(1), pp. 125-134.

Lu, J., Suo, H. C., Yi, R., Ma, Q. B. and Nian, H. (2015) 'Glyma11g13220, a homolog of the vernalization pathway gene VERNALIZATION 1 from soybean Glycine max (L.) Merr. , promotes flowering in Arabidopsis thaliana', *Bmc Plant Biology,* 15.

Luo, M., Bilodeau, P., Koltunow, A., Dennis, E. S., Peacock, W. J. and Chaudhury, A. M. (1999) 'Genes controlling fertilization-independent seed development in Arabidopsis thaliana', *Proceedings of the National Academy of Sciences of the United States of America,* 96(1), pp. 296-301.

Luo, M., Platten, D., Chaudhury, A., Peacock, W. J. and Dennis, E. S. (2009) 'Expression, Imprinting, and Evolution of Rice Homologs of the Polycomb Group Genes', *Molecular Plant,* 2(4), pp. 711-723.

Lupas, A. N. and Koretke, K. K. (2003) 'Bioinformatic analysis of ClpS, a protein module involved in prokaryotic and eukaryotic protein degradation', *Journal of Structural Biology,* 141(1), pp. 77-83.

Ma, X. Y., Qiao, Z., Chen, D. H., Yang, W. G., Zhou, R. J., Zhang, W. and Wang, M. (2015) 'CYCLIN-DEPENDENT KINASE G2 regulates salinity stress response and salt mediated flowering in Arabidopsis thaliana', *Plant Molecular Biology,* 88(3), pp. 287-299.

Main, A. L., Harvey, T. S., Baron, M., Boyd, J. and Campbell, I. D. (1992) 'THE 3-DIMENSIONAL STRUCTURE OF THE 10TH TYPE-III MODULE OF FIBRONECTIN - AN INSIGHT INTO RGD-MEDIATED INTERACTIONS', *Cell,* 71(4), pp. 671-678.

Margueron, R. and Reinberg, D. (2011) 'The Polycomb complex PRC2 and its mark in life', *Nature,* 469(7330), pp. 343-9.

Michaels, S. D. and Amasino, R. M. (1999) 'FLOWERING LOCUS C encodes a novel MADS domain protein that acts as a repressor of flowering', *Plant Cell,* 11(5), pp. 949-956.

Michaels, S. D. and Amasino, R. M. (2000) 'Memories of winter: vernalization and the competence to flower', *Plant Cell and Environment,* 23(11), pp. 1145-1153.

Michaels, S. D., Bezerra, I. C. and Amasino, R. M. (2004) 'FRIGIDA-related genes are required for the winter-annual habit in Arabidopsis', *Proceedings of the National Academy of Sciences of the United States of America,* 101(9), pp. 3281-3285.

Mogk, A., Schmidt, R. and Bukau, B. (2007) 'The N-end rule pathway for regulated proteolysis: prokaryotic and eukaryotic strategies', *Trends in Cell Biology,* 17(4), pp. 165-172.

Moon, J., Suh, S. S., Lee, H., Choi, K. R., Hong, C. B., Paek, N. C., Kim, S. G. and Lee, I. (2003) 'The SOC1 MADS-box gene integrates vernalization and gibberellin signals for flowering in Arabidopsis', *Plant Journal,* 35(5), pp. 613-623.

Moore, R. C. and Purugganan, M. D. (2005) 'The evolutionary dynamics of plant duplicate genes', *Current Opinion in Plant Biology,* 8(2), pp. 122-128.

Mouradov, A., Cremer, F. and Coupland, G. (2002) 'Control of flowering time: Interacting pathways as a basis for diversity', *Plant Cell,* 14, pp. S111-S130.

Mozgova, I., Kohler, C. and Hennig, L. (2015) 'Keeping the gate closed: functions of the polycomb repressive complex PRC2 in development', *Plant Journal,* 83(1), pp. 121-132.

Muller, J., Hart, C. M., Francis, N. J., Vargas, M. L., Sengupta, A., Wild, B., Miller, E. L., O'Connor, M. B., Kingston, R. E. and Simon, J. A. (2002) 'Histone methyltransferase activity of a Drosophila polycomb group repressor complex', *Cell,* 111(2), pp. 197-208.

Mur, L. A. J., Mandon, J., Persijn, S., Cristescu, S. M., Moshkov, I. E., Novikova, G. V., Hall, M. A., Harren, F. J. M., Hebelstrup, K. H. and Gupta, K. J. (2013) 'Nitric oxide in plants: an assessment of the current state of knowledge', *Aob Plants,* 5.

Murashige, T. and Skoog, F. (1962) 'A REVISED MEDIUM FOR RAPID GROWTH AND BIO ASSAYS WITH TOBACCO TISSUE CULTURES', *Physiologia Plantarum,* 15(3), pp. 473-497.

Mylne, J. S., Barrett, L., Tessadori, F., Mesnage, S., Johnson, L., Bernatavichute, Y. V., Jacobsen, S. E., Fransz, P. and Dean, C. (2006) 'LHP1, the Arabidopsis homologue of HETEROCHROMATIN PROTEIN1, is required for epigenetic silencing of FLC', *Proceedings of the National Academy of Sciences of the United States of America,* 103(13), pp. 5012-5017.

Nappzinn, K. (1957) 'UNTERSUCHUNGEN ZUR GENETIK DES KALTEBEDURFNISSES BEI ARABIDOPSIS-THALIANA', *Zeitschrift Fur Induktive Abstammungs Und Vererbungslehre,* 88(2), pp. 253-285.

Ninnis, R. L., Spall, S. K., Talbo, G. H., Truscott, K. N. and Dougan, D. A. (2009) 'Modification of PATase by L/F-transferase generates a ClpS-dependent N-end rule substrate in Escherichia coli', *Embo Journal,* 28(12), pp. 1732-1744.

Nishimura, K., Asakura, Y., Friso, G., Kim, J., Oh, S. H., Rutschow, H., Ponnala, L. and van Wijk, K. J. (2013) 'ClpS1 Is a Conserved Substrate Selector for the Chloroplast Clp Protease System in Arabidopsis', *Plant Cell,* 25(6), pp. 2276-2301.

Ohad, N., Yadegari, R., Margossian, L., Hannon, M., Michaeli, D., Harada, J. J., Goldberg, R. B. and Fischer, R. L. (1999) 'Mutations in FIE, a WD polycomb group gene, allow endosperm development without fertilization', *Plant Cell,* 11(3), pp. 407-415.

Ohama, N., Sato, H., Shinozaki, K. and Yamaguchi-Shinozaki, K. (2017) 'Transcriptional Regulatory Network of Plant Heat Stress Response', *Trends in Plant Science,* 22(1), pp. 53-65.

Peters, J. M. (2002) 'The anaphase-promoting complex: Proteolysis in mitosis and beyond', *Molecular Cell,* 9(5), pp. 931-943.

Petroski, M. D. and Deshaies, R. J. (2005a) 'Function and regulation of Cullin-RING ubiquitin ligases', *Nature Reviews Molecular Cell Biology,* 6(1), pp. 9-20.

Petroski, M. D. and Deshaies, R. J. (2005b) 'Mechanism of lysine 48-linked ubiquitin-chain synthesis by the cullin-RING ubiquitin-ligase complex SCF-Cdc34', *Cell,* 123(6), pp. 1107-1120.

Piatkov, K. I., Brower, C. S. and Varshavsky, A. (2012a) 'The N-end rule pathway counteracts cell death by destroying proapoptotic protein fragments', *Proceedings of the National Academy of Sciences of the United States of America,* 109(27), pp. E1839-E1847.

Piatkov, K. I., Colnaghi, L., Bekes, M., Varshavsky, A. and Huang, T. T. (2012b) 'The Auto-Generated Fragment of the Usp1 Deubiquitylase Is a Physiological Substrate of the N-End Rule Pathway', *Molecular Cell,* 48(6), pp. 926-933.

Piatkov, K. I., Oh, J. H., Liu, Y. and Varshavsky, A. (2014) 'Calpain-generated natural protein fragments as short-lived substrates of the N-end rule pathway', *Proceedings of the National Academy of Sciences of the United States of America,* 111(9), pp. E817-E826.

Pickart, C. M. (2001) 'Mechanisms underlying ubiquitination', *Annual Review of Biochemistry,* 70, pp. 503-533.

Potuschak, T., Stary, S., Schlogelhofer, P., Becker, F., Nejinskaia, V. and Bachmair, A. (1998) 'PRTl of Arabidopsis thaliana encodes a component of the plant N-end rule pathway', *Proceedings of the National Academy of Sciences of the United States of America,* 95(14), pp. 7904-7908.

Qiu, T., Dong, Y. Z., Yu, X. M., Zhao, N. and Yang, Y. F. (2017a) 'Analysis of allopolyploidy-induced rapid genetic and epigenetic changes and their relationship in wheat', *Genetics and Molecular Research,* 16(2).

Qiu, Y. C., Liu, S. L. and Adams, K. L. (2017b) 'Concerted Divergence after Gene Duplication in Polycomb Repressive Complexes', *Plant Physiology,* 174(2), pp. 1192-1204.

Rao, H., Uhlmann, F., Nasmyth, K. and Varshavsky, A. (2001) 'Degradation of a cohesin subunit by the N-end rule pathway is essential for chromosome stability', *Nature,* 410(6831), pp. 955-959.

Reddie, K. G. and Carroll, K. S. (2008) 'Expanding the functional diversity of proteins through cysteine oxidation', *Current Opinion in Chemical Biology,* 12(6), pp. 746-754.

Roszak, P. and Kohler, C. (2011) 'Polycomb group proteins are required to couple seed coat initiation to fertilization', *Proceedings of the National Academy of Sciences of the United States of America,* 108(51), pp. 20826-20831.

Sadanandom, A., Bailey, M., Ewan, R., Lee, J. and Nelis, S. (2012) 'The ubiquitin-proteasome system: central modifier of plant signalling', *New Phytologist,* 196(1), pp. 13-28.

Schmidt, R., Zahn, R., Bukau, B. and Mogk, A. (2009) 'ClpS is the recognition component for Escherichia coli substrates of the N-end rule degradation pathway', *Molecular Microbiology,* 72(2), pp. 506-517.

Schrader, E. K., Harstad, K. G. and Matouschek, A. (2009) 'Targeting proteins for degradation', *Nature Chemical Biology,* 5(11), pp. 815-822.

Schuenemann, V. J., Kralik, S. M., Albrecht, R., Spall, S. K., Truscott, K. N., Dougan, D. A. and Zeth, K. (2009) 'Structural basis of N-end rule substrate recognition in Escherichia coli by the ClpAP adaptor protein ClpS', *Embo Reports,* 10(5), pp. 508-514.

Schwartz, Y. B. and Pirrotta, V. (2013) 'A new world of Polycombs: unexpected partnerships and emerging functions', *Nat Rev Genet,* 14(12), pp. 853-64.

Sheldon, C. C., Burn, J. E., Perez, P. P., Metzger, J., Edwards, J. A., Peacock, W. J. and Dennis, E. S. (1999) 'The FLF MADS box gene: A repressor of flowering in Arabidopsis regulated by vernalization and methylation', *Plant Cell,* 11(3), pp. 445-458.

Sheldon, C. C., Conn, A. B., Dennis, E. S. and Peacock, W. J. (2002) 'Different regulatory regions are required for the vernalization-induced repression of FLOWERING LOCUS C and for the epigenetic maintenance of repression', *Plant Cell,* 14(10), pp. 2527-2537.

Sheldon, C. C., Finnegan, E. J., Rouse, D. T., Tadege, M., Bagnall, D. J., Helliwell, C. A., Peacock, W. J. and Dennis, E. S. (2000) 'The control of flowering by vernalization', *Current Opinion in Plant Biology,* 3(5), pp. 418-422.

Sheldon, C. C., Hills, M. J., Lister, C., Dean, C., Dennis, E. S. and Peacock, W. J. (2008) 'Resetting of FLOWERING LOCUS C expression after epigenetic repression by vernalization', *Proceedings of the National Academy of Sciences of the United States of America,* 105(6), pp. 2214-2219.

Shemorry, A., Hwang, C. S. and Varshavsky, A. (2013) 'Control of Protein Quality and Stoichiometries by N-Terminal Acetylation and the N-End Rule Pathway', *Molecular Cell,* 50(4), pp. 540-551.

Shindo, C., Lister, C., Crevillen, P., Nordborg, M. and Dean, C. (2006) 'Variation in the epigenetic silencing of FLC contributes to natural variation in Arabidopsis vernalization response', *Genes & Development,* 20(22), pp. 3079-3083.

Simon, J. A. and Kingston, R. E. (2009) 'Mechanisms of polycomb gene silencing: knowns and unknowns', *Nat Rev Mol Cell Biol,* 10(10), pp. 697-708.

Soltis, P. S. and Soltis, D. E. (2016) 'Ancient WGD events as drivers of key innovations in angiosperms', *Current Opinion in Plant Biology,* 30, pp. 159-165.

Song, J., Angel, A., Howard, M. and Dean, C. (2012) 'Vernalization - a cold-induced epigenetic switch', *Journal of Cell Science,* 125(16), pp. 3723-3731.

Srikanth, A. and Schmid, M. (2011) 'Regulation of flowering time: all roads lead to Rome', *Cellular and Molecular Life Sciences,* 68(12), pp. 2013-2037.

Sriram, S. M., Kim, B. Y. and Kwon, Y. T. (2011) 'The N-end rule pathway: emerging functions and molecular principles of substrate recognition', *Nature Reviews Molecular Cell Biology,* 12(11), pp. 735-747.

Starheim, K. K., Gevaert, K. and Arnesen, T. (2012) 'Protein N-terminal acetyltransferases: when the start matters', *Trends in Biochemical Sciences,* 37(4), pp. 152-161.

Stary, S., Yin, X. J., Potuschak, T., Schlogelhofer, P., Nizhynska, V. and Bachmair, A. (2003) 'PRT1 of Arabidopsis is a ubiquitin protein ligase of the plant N-end rule pathway with specificity for aromatic amino-terminal residues', *Plant Physiology,* 133(3), pp. 1360-1366.

Sultana, R., Theodoraki, M. A. and Caplan, A. J. (2012) 'UBR1 promotes protein kinase quality control and sensitizes cells to Hsp90 inhibition', *Experimental Cell Research,* 318(1), pp. 53-60.

Sung, S. B. and Amasino, R. M. (2004a) 'Vernalization and epigenetics: how plants remember winter', *Current Opinion in Plant Biology,* 7(1), pp. 4-10.

Sung, S. B. and Amasino, R. M. (2004b) 'Vernalization in Arabidopsis thaliana is mediated by the PHD finger protein VIN3', *Nature,* 427(6970), pp. 159-164.

Sung, S. B., He, Y. H., Eshoo, T. W., Tamada, Y., Johnson, L., Nakahigashi, K., Goto, K., Jacobsen, S. E. and Amasino, R. M. (2006a) 'Epigenetic maintenance of the vernalized state in Arabidopsis thaliana requires LIKE HETEROCHROMATIN PROTEIN 1', *Nature Genetics,* 38(6), pp. 706-710.

Sung, S. B., Schmitz, R. J. and Amasino, R. M. (2006b) 'A PHD finger protein involved in both the vernalization and photoperiod pathways in Arabidopsis', *Genes & Development,* 20(23), pp. 3244-3248.

Takahashi, H., Nozawa, A., Seki, M., Shinozaki, K., Endo, Y. and Sawasaki, T. (2009) 'A simple and high-sensitivity method for analysis of ubiquitination and polyubiquitination based on wheat cell-free protein synthesis', *Bmc Plant Biology,* 9.

Tasaki, T. and Kwon, Y. T. (2007) 'The mammalian N-end rule pathway: new insights into its components and physiological roles', *Trends in Biochemical Sciences,* 32(11), pp. 520-528.

Tasaki, T., Mulder, L. C. F., Iwamatsu, A., Lee, M. J., Davydov, I. V., Varshavsky, A., Muesing, M. and Kwon, Y. T. (2005) 'A family of mammalian E3 ubiquitin ligases that contain the UBR box motif and recognize N-degrons', *Molecular and Cellular Biology,* 25(16), pp. 7120-7136.

Tasaki, T., Sriram, S. M., Park, K. S. and Kwon, Y. T. (2012) 'The N-End Rule Pathway', in Kornberg, R.D. (ed.) *Annual Review of Biochemistry, Vol 81 Annual Review of Biochemistry*, pp. 261-289.

Tasaki, T., Zakrzewska, A., Dudgeon, D. D., Jiang, Y. H., Lazo, J. S. and Kwon, Y. T. (2009) 'The Substrate Recognition Domains of the N-end Rule Pathway', *Journal of Biological Chemistry,* 284(3), pp. 1884-1895.

Tobias, J. W., Shrader, T. E., Rocap, G. and Varshavsky, A. (1991) 'THE N-END RULE IN BACTERIA', *Science,* 254(5036), pp. 1374-1377.

Turner, G. C. and Varshavsky, A. (2000) 'Detecting and measuring cotranslational protein degradation in vivo', *Science,* 289(5487), pp. 2117-2120.

Van Zandt, P. A. and Mopper, S. (2002) 'Delayed and carryover effects of salinity on flowering in Iris hexagona (Iridaceae)', *American Journal of Botany,* 89(11), pp. 1847-1851.

Varshavsky, A. (1996) 'The N-end rule: Functions, mysteries, uses', *Proceedings of the National Academy of Sciences of the United States of America,* 93(22), pp. 12142-12149.

Varshavsky, A. (2005) 'Regulated protein degradation', *Trends in Biochemical Sciences,* 30(6), pp. 283-286.

Varshavsky, A. (2011) 'The N-end rule pathway and regulation by proteolysis', *Protein Science,* 20(8), pp. 1298-1345.

Vicente, J., Mendiondo, G. M., Movahedi, M., Peirats-Llobet, M., Juan, Y. T., Shen, Y. Y., Dambire, C., Smart, K., Rodriguez, P. L., Charng, Y. Y., Gray, J. E. and Holdsworth, M. J. (2017) 'The Cys-Arg/N-End Rule Pathway Is a General Sensor of Abiotic Stress in Flowering Plants', *Current Biology,* 27(20), pp. 3183-+.

Vogtle, F. N., Wortelkamp, S., Zahedi, R. P., Becker, D., Leidhold, C., Gevaert, K., Kellermann, J., Voos, W., Sickmann, A., Pfanner, N. and Meisinger, C. (2009) 'Global Analysis of the Mitochondrial N-Proteome Identifies a Processing Peptidase Critical for Protein Stability', *Cell,* 139(2), pp. 428-439.

Weits, D. A., Giuntoli, B., Kosmacz, M., Parlanti, S., Hubberten, H. M., Riegler, H., Hoefgen, R., Perata, P., van Dongen, J. T. and Licausi, F. (2014) 'Plant cysteine oxidases control the oxygen-dependent branch of the N-end-rule pathway', *Nature Communications,* 5.

Wellensiek, S. J. (1962) 'DIVIDING CELLS AS LOCUS FOR VERNALIZATION', *Nature,* 195(4838), pp. 307-&.

White, M. D., Klecker, M., Hopkinson, R. J., Weits, D. A., Mueller, C., Naumann, C., O'Neill, R., Wickens, J., Yang, J. Y., Brooks-Bartlett, J. C., Garman, E. F., Grossmann, T. N., Dissmeyer, N. and Flashman, E. (2017) 'Plant cysteine oxidases are dioxygenases that directly enable arginyl transferase-catalysed arginylation of N-end rule targets', *Nature Communications,* 8.

Wood, C. C., Robertson, M., Tanner, G., Peacock, W. J., Dennis, E. S. and Helliwell, C. A. (2006) 'The Arabidopsis thaliana vernalization response requires a polycomb-like protein complex that also includes VERNALIZATION INSENSITIVE 3', *Proceedings of the National Academy of Sciences of the United States of America,* 103(39), pp. 14631-14636.

Woods, D. P., McKeown, M. A., Dong, Y. X., Preston, J. C. and Amasino, R. M. (2016) 'Evolution of VRN2/Ghd7-Like Genes in Vernalization-Mediated Repression of Grass Flowering', *Plant Physiology,* 170(4), pp. 2124-2135.

Xu, Z. Z., Payoe, R. and Fahlman, R. P. (2012) 'The C-terminal Proteolytic Fragment of the Breast Cancer Susceptibility Type 1 Protein (BRCA1) Is Degraded by the N-end Rule Pathway', *Journal of Biological Chemistry,* 287(10), pp. 7495-7502.

Yadegari, R., Kinoshita, T., Lotan, O., Cohen, G., Katz, A., Choi, Y., Katz, A., Nakashima, K., Harada, J. J., Goldberg, R. B., Fischer, R. L. and Ohad, N. (2000) 'Mutations in the FIE and MEA genes that encode interacting polycomb proteins cause parent-of-origin effects on seed development by distinct mechanisms', *Plant Cell,* 12(12), pp. 2367-2382.

Yamano, K. and Youle, R. J. (2013) 'PINK1 is degraded through the N-end rule pathway', *Autophagy,* 9(11), pp. 1758-1769.

Yan, O. Y., Kwon, Y. T., An, J. Y., Eller, D., Tsai, S. C., Diaz-Perez, S., Troke, J. J., Teitell, M. A. and Marahrens, Y. (2006) 'Loss of Ubr2, an E3 ubiquitin ligase, leads to chromosome fragility and impaired homologous recombinational repair', *Mutation Research-Fundamental and Molecular Mechanisms of Mutagenesis,* 596(1-2), pp. 64-75.

Yang, J., Lee, S., Hang, R. L., Kim, S. R., Lee, Y. S., Cao, X. F., Amasino, R. and An, G. (2013) 'OsVIL2 functions with PRC2 to induce flowering by repressing OsLFL1 in rice', *Plant Journal,* 73(4), pp. 566-578.

Yeh, C. H., Kaplinsky, N. J., Hu, C. and Charng, Y. Y. (2012) 'Some like it hot, some like it warm: Phenotyping to explore thermotolerance diversity', *Plant Science,* 195, pp. 10-23.

Yoshida, N., Yanai, Y., Chen, L. J., Kato, Y., Hiratsuka, J., Miwa, T., Sung, Z. R. and Takahashi, S. (2001) 'EMBRYONIC FLOWER2, a novel polycomb group protein homolog, mediates shoot development and flowering in Arabidopsis', *Plant Cell,* 13(11), pp. 2471-2481.

Yoshida, S., Ito, M., Callis, J., Nishida, I. and Watanabe, A. (2002) 'A delayed leaf senescence mutant is defective in arginyl-tRNA : protein arginyltransferase, a component of the N-end rule pathway in Arabidopsis', *Plant Journal,* 32(1), pp. 129-137.

Zenker, M., Mayerle, J., Lerch, M. M., Tagariello, A., Zerres, K., Durie, P. R., Beier, M., Hulskamp, G., Guzman, C., Rehder, H., Beemer, F. A., Hamel, B., Vanlieferinghen, P., Gershoni-Baruch, R., Vieira, M. W., Dumic, M., Auslender, R., Gil-da-Silva-Lopes, V. L., Steinlicht, S., Rauh, M., Shalev, S. A., Thiel, C., Winterpacht, A., Kwon, Y. T., Varshavsky, A. and Reis, A. (2005) 'Deficiency of UBR1, a ubiquitin ligase of the N-end rule pathway, causes pancreatic dysfunction, malformations and mental retardation (Johanson-Blizzard syndrome)', *Nature Genetics,* 37(12), pp. 1345-1350.

Zhang, H., Gannon, L., Hassall, K.L., Deery, M., Gibbs, D.J., Holdsworth, M.J., van der Hoorn, R.A.L., Lilley, K.S. and Theodoulou, F.L. (2018) ' Genetic interactions between ABA signalling and the Arg/N-end rule pathway during Arabidopsis seedling establishment.' *Nature SCIENTIFIC REPORTS*, 8 (15192), pp. 1-12 DOI: 10.1111/nph.14909

Zhu, J. K. (2016) 'Abiotic Stress Signaling and Responses in Plants', *Cell,* 167(2), pp. 313-324.

Zimmerman, E. S., Schulman, B. A. and Zheng, N. (2010) 'Structural assembly of cullin-RING ubiquitin ligase complexes', *Current Opinion in Structural Biology,* 20(6), pp. 714-721.

Zuo, J. R., Niu, Q. W. and Chua, N. H. (2000) 'An estrogen receptor-based transactivator XVE mediates highly inducible gene expression in transgenic plants', *Plant Journal,* 24(2), pp. 265-273.